

ISSN: 2349-6495(P) | 2456-1908 (O)



# International Journal of Advanced Engineering Research and Science

(IJAERS)

An Open Access Peer-Reviewed International Journal



Journal DOI: 10.22161/ijaers

Issue DOI: 10.22161/ijaers.121

AI PUBLICATIONS

Vol.- 12 | Issue - 1 | Jan 2025

editor.ijaers@gmail.com | editor@ijaers.com | <https://www.ijaers.com/>

# International Journal of Advanced Engineering Research and Science (IJAERS)

(ISSN: 2349-6495(P)| 2456-1908(O))

DOI: 10.22161/ijaers

Vol-12, Issue-1

January, 2025

*Editor in Chief*

Dr. Swapnesh Taterh

*Chief Executive Editor*

S. Suman Rajest

---

Copyright © 2025 International Journal of Advanced Engineering Research and Science

Publisher

*AI Publication*

Email: [editor.ijaers@gmail.com](mailto:editor.ijaers@gmail.com); [editor@ijaers.com](mailto:editor@ijaers.com)

Web: [www.ijaers.com](http://www.ijaers.com)

## **International Editorial/ Reviewer Board**

### **Editor in Chief**

- **Dr. Swapnesh Taterh (Chief-Editor)**, Amity University, Jaipur, India

### **Chief Executive Editor**

- **S. Suman Rajest**, Vels Institute of Science, Technology & Advanced Studies, India  
chief-executive-editor@ijaers.com

### **Associate Editors**

- **Dr. Ram Karan Singh**, King Khalid University, Guraiger, Abha 62529, Saudi Arabia
- **Dr. Shuai Li**, University of Cambridge, England, Great Britain

### **Editorial Member**

- **Behrouz Takabi**, PhD, Texas A&M University, Texas, USA
- **Dr. Gamal Abd El-Nasser Ahmed Mohamed Said**, Port Training Institute (PTI), Arab Academy For Science, Technology and Maritime Transport, Egypt
- **Dr. Hou, Cheng-I**, Chung Hua University, Hsinchu Taiwan
- **Dr. Ebrahim Nohani**, Islamic Azad University, Dezful, IRAN.
- **Dr. Ahmadad Nabih Zaki Rashed**, Menoufia University, EGYPT
- **Dr. Rabindra Kayastha**, Kathmandu University, Nepal
- **Dr. Dinh Tran Ngoc Huy**, Banking and Finance, HCM, Viet Nam
- **Dr. Engin NAS**, Duzce University, Turkey
- **Dr. A. Heidari**, California South University (CSU), Irvine, California, USA
- **Dr. Uma Choudhary**, Mody University, Lakshmangarh, India
- **Dr. Varun Gupta**, National Informatic Center, Delhi, India
- **Dr. Ahmed Kadhim Hussein**, University of Babylon, Republic of Iraq
- **Dr. Vibhash Yadav**, Rajkiya Engineering College, Banda. UP, India
- **Dr. M. Kannan**, SCSVMV University, Kanchipuram, Tamil Nadu, India
- **José G. Vargas-Hernández**, University of Guadalajara Periférico Norte 799 Edif. G201-7, Núcleo Universitario Los Belenes, Zapopan, Jalisco, 45100, México
- **Dr. Sambit Kumar Mishra**, Gandhi Institute for Education and Technology, Baniatangi, Bhubaneswar, India
- **DR. C. M. Velu**, Datta Kala Group of Institutions, Pune, India
- **Dr. Deependra Pandey**, Amity University, Uttar Pradesh, India
- **Dr. K Ashok Reddy**, MLR Institute of Technology, Dundigal, Hyderabad, India
- **Dr. S.R.Boselin Prabhu**, SVS College of Engineering, Coimbatore, India
- **N. Balakumar**, Tamilnadu College of Engineering, Karumathampatti, Coimbatore, India
- **R. Poorvadevi**, SCSVMV University, Enathur, Kanchipuram, Tamil Nadu, India
- **Dr. Subha Ganguly**, Arawali Veterinary College, Sikar, India
- **Dr. P. Murali Krishna Prasad**, GVP College of Engineering for Women, Visakhapatnam, Andhra Pradesh, India
- **Anshul Singhal**, Bio Instrumentation Lab, MIT, USA
- **Mr. Lusekelo Kibona**, Ruaha Catholic University, Iringa, Tanzania
- **Sina Mahdavi**, Urmia Graduate Institute, Urmia, Iran
- **Dr. N. S. Mohan**, Manipal Institute of Technology, Manipal, India
- **Dr. Zafer Omer Ozdemir**, University of Health Sciences, Haydarpassa, Uskudar, Istanbul, TURKIYE
- **Bingxu Wang**, 2721 Patrick Henry St Apt 510, Auburn Hills, Michigan, United States

- **Dr. Jayashree Patil-Dake**, KPB Hinduja College of Commerce, Mumbai, India
- **Dr. Neel Kamal Purohit**, S.S. Jain Subodh P.G. College, Rambagh, Jaipur, India
- **Mohd Muntjir**, Taif University, Kingdom of Saudi Arabia
- **Xian Ming Meng**, China Automotive Technology & Research Center No.68, East Xianfeng Road, Dongli District, Tianjin, China
- **Herlandi de Souza Andrade**, FATEC Guaratingueta, State Center for Technological Education Paula Souza - CEETEPS
- **Dr. Payal Chadha**, University of Maryland University College Europe, Kuwait
- **Ahmed Moustafa Abd El-hamid Elmahalawy**, Menoufia University, Al Minufya, Egypt
- **Prof. Mark H. Rummeli**, University & Head of the characterisation center, Soochow Institute for Energy Materials Innovations (SIEMES), Suzhou, Jiangsu Province, China
- **Dr. Eman Yaser Daraghmi**, Ptuk, Tulkarm, Palestine
- **Holmes Rajagukguk**, State University of Medan, Lecturer in Sisingamangaraja University North Tapanuli, Indonesia
- **Dr. Menderes KAM**, Dr. Engin PAK Cumayeri Vocational School, DÜZCE UNIVERSITY (University in Turkey), Turkey
- **Dr. Jatin Goyal**, Punjabi University, Patiala, Punjab, India | International Collaborator of GEITEC / UNIR / CNPq, Brazil
- **Ahmet İPEKÇİ**, Dr. Engin PAK Cumayeri Vocational School, DÜZCE UNIVERSITY, Turkey
- **Baarimah Abdullah Omar**, Universiti Malaysia Pahang (UMP), Gambang, 26300, Malaysia
- **Sabri UZUNER**, Dr. Engin PAK Cumayeri Vocational School Cumayeri/Duzce/Turkey
- **Ümit AĞBULUT**, Düzce University, Turkey
- **Dr. Mustafa ÖZKAN**, Trakya University, Edirne/ TURKEY
- **Dr. Indrani Bhattacharyya**, Dr. B.C. Roy College of Pharmacy and Allied Health Sciences, Durgapur, West Bengal, India
- **Egnon Kouakou**, Nutrition/Health at University Felix Houphouet Boigny Abidjan, Ivory Coast
- **Dr. Suat SARIDEMİR**, Düzce University, Faculty of Technology, Turkey
- **Dr. Manvinder Singh Pahwa**, Director, Alumni Relations at Manipal University Jaipur, India
- **Omid Habibzadeh Bigdarvish**, University of Texas at Arlington, Texas, USA
- **Professor Dr. Ho Soon Min**, INTI International University, Jln BBN 12/1, Bandar, Baru Nilai, 71800 Negeri Sembilan, Malaysia
- **Ahmed Mohammed Morsy Hassan**, South Egypt Cancer Institute, Assiut University, Assiut, Egypt
- **Xian Ming Meng (Ph.D)**, China Automotive Technology & Research Center, No.68, East Xianfeng Road, Tianjin, China
- **Ömer Erkan**, Konuralp Campus, Düzce-Turkey
- **Dr. Yousef Daradkeh**, Prince Sattam bin Abdulaziz University) PSAU), KSA
- **Peter JO**, IPB University, Indonesia
- **Nazmi Liana Binti Azmi**, Raja Perempuan Zainab II Hospital, 15586 Kota Bharu, Kelantan, Malaysia
- **Mr. Sagar Jamle**, Oriental University, Indore, India
- **Professor Grazione de Souza**, Applied Mathematics, Rio de Janeiro State University, Brazil
- **Kim Edward S. Santos**, Nueva Ecija University of Science and Technology, Philippines.

**Vol-12, Issue-1, January 2025**  
*(10.22161/ijaers.121)*

**Detail with DOI (CrossRef)**

**Combined effects of ultrasound power and DO on nitrogen removal in a low-intensity ultrasound (LIU)-assisted sequencing batch biofilm reactor**

Onwuagbu Chukwubieke Chiemelie, Dr. Xin Zhou, Okeke Ikechukwu Shadrack, Paul Afreh

 DOI: [10.22161/ijaers.121.1](https://doi.org/10.22161/ijaers.121.1)

Page No: 01-15

**Application of Humic Acid and Mulch Dose on Corn (*Zea mays L*) Yield**

Bama Wida Pratama, Luluk Sulistiyo Budi, Indah Rekyani Puspitawati

 DOI: [10.22161/ijaers.121.2](https://doi.org/10.22161/ijaers.121.2)

Page No: 16-26

**New Weighted Taylor Series for Water Wave Energy Loss and Littoral Current Analysis**

Syawaluddin Hutahaeen

 DOI: [10.22161/ijaers.121.3](https://doi.org/10.22161/ijaers.121.3)

Page No: 27-39

**Implementation of the K-Means Clustering Algorithm to Determine the Promotion Strategy of Institut Agama Kristen Negeri Tarutung**

Frainskoy Rio Naibaho, Bambang TJ Hutagalung, Ridsen Anakampun

 DOI: [10.22161/ijaers.121.4](https://doi.org/10.22161/ijaers.121.4)

Page No: 40-48

**Dengue Hospitalizations in the state of Pará over the last decade: An ecological study**

Vando Delgado de Souza Santos, Bianca Abreu Pantoja, Matheus Bassalo Aflalo, Ana Luísa Damasceno Rodrigues, Eduardo de Pinho Domingues, Henrique Fayad Pinheiro, Fábio Costa de Vasconcelos, William Robert Souza, Marcos Gabriel Barbosa Castello Branco, Maria Gabriela da Rocha Florêncio, Dara Estrela Santos Esteves, Valnilson Dias Reis, Ana Olívia Semblano Monteiro, Alcilene Monteiro Lima, Marivaldo de Moraes e Silva, Beatriz Colares Coelho de Souza, Francisco Miguel da Silva Freitas, Larissa Araújo Queiroz, Társis da Silva Sousa, Carlos Vinicius Carrera do Nascimento, Leonardo Barbosa Duarte, Brenda do Socorro Preuss Cardoso, Verena Sousa Reis, Kaylana de Silva Leite, Rayza Gregório Lima, Ayla Luiza Preuss Erbes, Sebastiana Brandão da Costa, Isis Bruna Vasques Carvalho, Rafaella Casanova Ataíde dos Santos, Diego Romani da Costa, Nicole Morais Dillon, Filipe Santos da Silva, Ayanne Castro de Miranda, Eduardo Alberto Rodrigues Tiago

 DOI: [10.22161/ijaers.121.5](https://doi.org/10.22161/ijaers.121.5)

Page No: 49-54



adsorbendum biodegradation (Zhang et al., 2022). However, these methods also face challenges such as inadequate nitrogen removal, high power consumption, and poor environmental adaptability, which leads to noncompliant discharge effluent with stringent regulations and sustainability strategies (Qu et al., 2019). Thus, more research and instruction of these and other new procedures is needed to get over these limits and to guarantee the productive and maintainable treatment.

Sequencing batch biofilm reactors (SBBRs) can simultaneously remove nitrogenous chemicals by intrinsic nitrification and denitrification as the system operates in a fill-and-draw manner (Iaconi et al., 2002; Prendergast, 2005). Key factors that influence SBBR functionality and are widely studied for the enhancement of nitrogen removal efficiency are hydraulic retention time, aeration flow, and biofilm density (Ding et al., 2011; Wang et al., 2015; Xiang et al., 2016). Gains in treatment efficiency and cost reduction have been achieved through the application of intelligent control systems and the use of fibrous carriers for biofilm adhesion (Ding et al., 2011; Yuan, 2014). Despite SBBRs showing tolerance to different salinities (She et al., 2016), handling recalcitrant chemicals and lowering nitrous oxide emissions remain issues (Chen et al., 2021; Xiang et al., 2016). The integration of advanced oxidation techniques, such as ultrasonic irradiation, holds promise for further enhancing nitrogen removal efficiency.

Ultrasound, which consists of sound waves above 20 kHz, has been known to possess remarkable directional and penetrative capacity (Zhang et al., 2022). Ultrasonication is an eco-friendly method for sludge treatment that enhances biological activity and pollutant extraction from wastewater (Tyagi et al., 2014). It promotes gas, liquid, and oxygen transport (Chisti, 2003) while reducing mass transfer resistance through local turbulence (Rokhina et al., 2009). This process increases cell membrane permeability and accelerates metabolism and growth. When calibrated correctly, ultrasonic intensity can create beneficial ruptures in cell walls without irreversible damage (Sinisterra, 1992). Low-intensity ultrasound modifies cell membrane structures, decreasing the viscosity of phosphodiester bilayers and improving enzyme activity (Lin & Wu, 2002). It destabilizes the extracellular polymeric substance (EPS) matrix, boosting EPS concentration and protein synthesis while enhancing cell permeability. This facilitates the release of intracellular enzymes, improving treatment efficiency, although excessive intensity may lead to cell damage and reduced viability (Liu et al., 2003).

Ultrasonication generates shear stresses from cavitation bubbles, which improve enzyme-substrate interactions and

accelerate enzymatic processes. When applied appropriately, low-intensity ultrasound can promote cell growth and enhance enzyme activity. Conversely, prolonged exposure risks damaging cells and potentially leading to cell death. Research indicates that ultrasonic treatment effectively reduces chemical oxygen demand (COD) and ammonium nitrogen ( $\text{NH}_4^+\text{-N}$ ) levels in wastewater (Tian et al., 2021). For instance, ultrasonic recirculation has been successfully employed to process excess sludge, meeting established effluent standards. Hong-Cui (2012) reported that initial ultrasonic pretreatment of 8-hydroxyquinoline wastewater achieved a 40.4% reduction in CODcr.

A two-stage aerobic biochemical treatment achieved a 99.4% elimination of total Chemical Oxygen Demand (CODcr). Low-intensity ultrasound improved COD removal of low-temperature SBR sewage treatment, being the most effective intensity 0.27 W/L after 20 min. For  $\text{NH}_4^+\text{-N}$  removal, exposure to ultrasound for 15 min was ideal, demonstrating the necessity of striking the right balance between power density and power duration (Ding et al., 2011). Ultrasound enhances COD and nitrogen removal rates (Wünsch, 2004; Zhang et al., 2011) and promotes cell proliferation and enzyme activity (Biradar et al., 2010; Liu et al., 2007) when used with biological treatments. The present study dealt with the coupling technology of ultrasonic irradiation and Sequencing Batch Biofilm Reactors (SBBRs) established in previous studies to enhance nitrogen removal via biofilm destruction and microbial activity.

This research investigates Submerged Biological Biofilm Reactors (SBBRs) exhibited with ultrasonic irradiation for the preservation of the environment. Through a three-phase experimental design, it examines the effect of high-power ultrasound on biological denitrification, structures of extracellular polymers and microbial community under various carbon-to-nitrogen (C/N) ratios and ammonia concentration levels. The study aims to optimize conditions for maximum nitrogen removal and the cultivation of beneficial microbial communities.

## II. MATERIALS AND METHODS

### 2.1 SBBR running device

Figure 1 shows the experimental running device and reactor schematic. Four parallel reactors, each with a 500 ml working volume filled 50% with PU (Polyurethane) as a biofilm carrier, were tested. Reactor 1 served as the control (no ultrasound), while reactors 2, 3, and 4 received different ultrasonic powers. Aeration was supplied via an air compression pump connected to an aeration disk at the bottom, regulated by a mass flow meter for DO control.

Temperature was maintained at  $30 \pm 2^\circ\text{C}$  using a water bath system.

The SBBR reactors operated in cycles: influent, aeration (11.5 h), sedimentation (20 min), and discharging (5 min) (Figure 2), with a water discharge ratio of 2/3 and cycle durations of 24 or 48 hours based on phase characteristics.

Ultrasonic irradiation was applied for 10 min during aeration. After filling, reactors R1, R2, and R3 were placed in the ultrasound chamber with the rod penetrating the water to a depth of 20 mm. Parameters like power and irradiation time were adjustable post-irradiation.



Fig.1: Experimental device

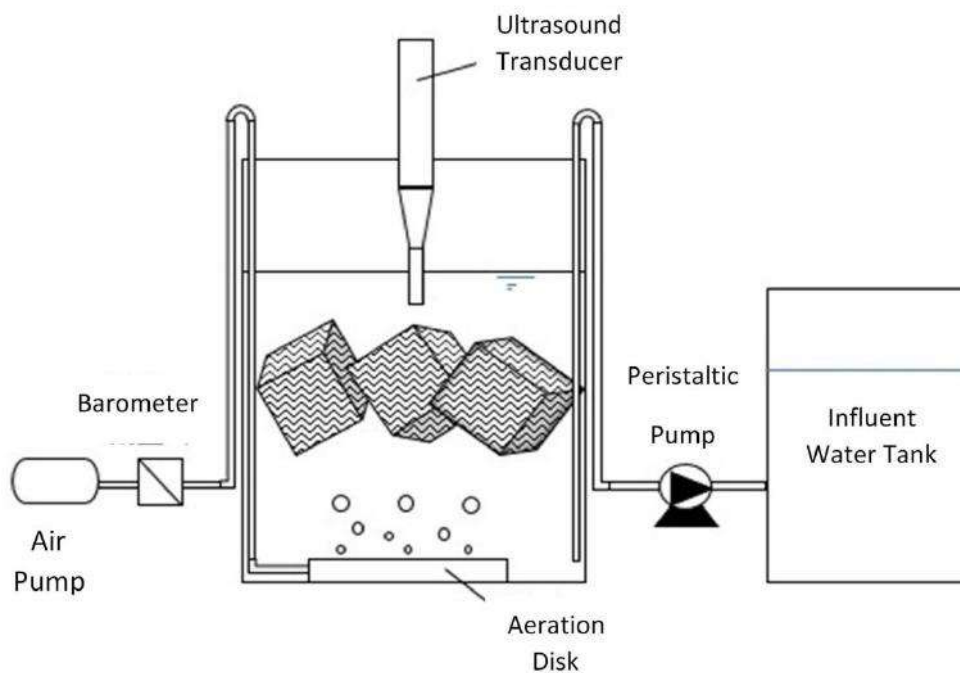


Fig.2: SBBR scheme

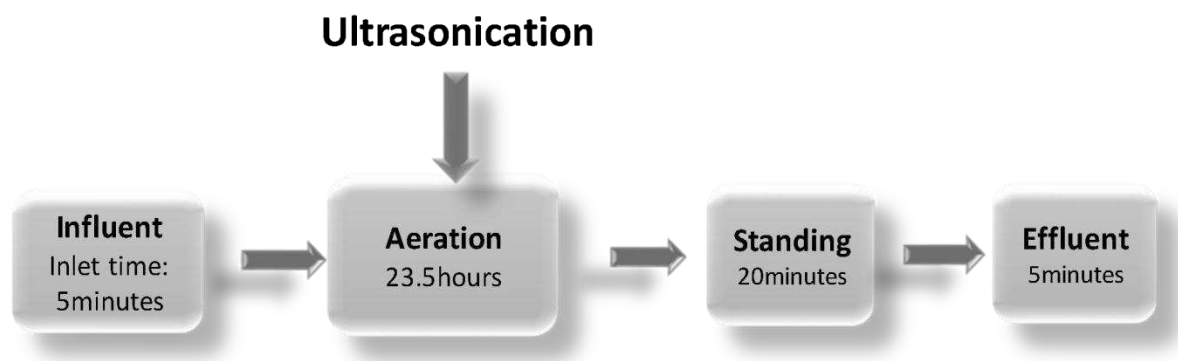


Fig.3: Operating steps

**2.1.1 Running phases**

Our studies, as outlined in Table 1, had three distinct running stages. The initial phase was conducted with varying influent ammonia concentrations between 200 and

400 mg/L. The second phase was conducted with varying C/N ratios, whereas the third phase was executed under conditions of elevated influent ammonia concentrations and high-power ultrasonication.

Table 1: Details of the Running phases

Running Phase	Influent Ammonia (mg/L)	C/N Ratio	Ultrasound Power (W)	Irradiation time (Min)	Water Discharging Ratio	Cycle Duration
P1	200/300/400	3	0/180	0/10	3/5	24H
P2	300	2.5/1.5/2.5/3.5	0/180/180/180	0/10/10/10	3/5	24H
P3	400/600/800/1000	2	0/180/360/540	0/10/10/10	3/5	48H

**2.2 Sludge inoculation and influent water**

The feed sludge for this experiment was sourced from the SBR aeration tank of a wastewater treatment plant in Shanxi Province. After 24 hours of aeration to restore its activity, the sludge was mixed with water and PU biofilm filler for domestication, with conditions continuously monitored. Three uniform biofilm fillers were used in each of the four reactors.

Municipal water, along with glucose, NH<sub>4</sub>Cl, and KH<sub>2</sub>PO<sub>4</sub>, supplied carbon, ammonia, and phosphorus while maintaining an N/P ratio of 5:1. NaHCO<sub>3</sub> was added to keep the reactors basic, and a nutrient solution provided essential trace elements. Anhydrous glucose served as the carbon source due to its availability.

Table 2: Details of trace elements

Trace Elements	CoCl <sub>2</sub> 6H <sub>2</sub> O	MnSO <sub>4</sub>	H <sub>3</sub> BO <sub>4</sub>	NiCl <sub>2</sub> 6H <sub>2</sub> O	ZnSO <sub>4</sub> 7H <sub>2</sub> O	FeCl <sub>3</sub>	CuSO <sub>4</sub>
Contents	0.15	0.12	0.15	0.19	0.12	1.5	0.03

**2.3 Analysis and Calculation Methods**

**2.3.1 Analysis**

The effluent NH<sub>4</sub><sup>+</sup>-N, NO<sub>2</sub><sup>-</sup>-N, NO<sub>3</sub><sup>-</sup>-N concentrations, and COD concentrations were all investigated and monitored based on the standards techniques. The measurements of DO concentrations and pH in the reactors were performed using a DO meter (Model 550A,

YSI, USA) and a Ph meter (Mettler TOLEDO FE20-Kit), respectively.

**2.3.2 Calculations**

2.3.2.1 The Ammonium Loading Rate (ALR) of influent was calculated by:

$$\text{NAR} = \frac{[\text{NH}_4^+ - \text{N}]_{\text{inf}}}{[\text{NO}_2^- - \text{N}]_{\text{eff}}}$$

2.3.2.2 The Nitrite Accumulation Ratio (NAR) was calculated by formula (F1) (Yingyay et al., 2014)

$$\text{NAR} = \frac{[\text{NO}_2^- - \text{N}]_{\text{eff}}}{[\text{NO}_2^- - \text{N}]_{\text{eff}} + [\text{NO}_3^- - \text{N}]_{\text{eff}}}$$

2.3.2.3 The Free Ammonia (FA) was calculated by the formula (F2) (Ford et al., 1980):

$$\text{FA} = \frac{17}{14} \times \frac{[\text{NH}_4^+ - \text{N}]_{\text{inf}} \times 10^{ph}}{\exp[6334/(273 + T)] + 10^{ph}}$$

2.3.3 EPS Analysis

During the experiment, biofilm Extracellular Polymer Analysis was performed. The biofilms on the filler are subjected to different steps, extracting three parts of extracellular polymers from biofilms: Soluble EPS, Loosely Bound EPS, and Tightly Bound EPS.

2.3.4 Microbial Analysis

Microbial biodiversity was analyzed using high-speed sequencing tests, calculating several indices: ACE, Chao, Shannon, Simpson, and Coverage. The ACE and Chao indices assess community abundance, while the Shannon and Simpson indices measure community diversity. A lower Shannon index indicates less diversity and a higher Simpson index also reflects lower diversity. The calculation formulas for these indices are F3, F4, F5, and F6.

$$S_{chao1} = S_{obs} + \frac{n_1(n_1-1)}{2(n_2+1)} \quad (F3)$$

$$S_{ACE} = \begin{cases} S_{abund} + \frac{S_{rare}}{C_{ACE}} + \frac{n_1}{C_{ACE}} \hat{Y}_{ACE}^2, \text{ for } \hat{Y}_{ACE} < 0.80 \\ S_{abund} + \frac{S_{rare}}{C_{ACE}} + \frac{n_1}{C_{ACE}} \hat{Y}_{ACE}^2, \text{ for } \hat{Y}_{ACE} \geq 0.80 \end{cases} \quad (F4)$$

$$H = -\sum_{i=1}^{abund} \left[ \frac{S_{rare} \cdot i(i-1)n_i}{C_{ACE} N_{rare}(N_{rare}-1)} \right] \ln \left[ \frac{S_{rare} \cdot i(i-1)n_i}{C_{ACE} N_{rare}(N_{rare}-1)} \right] + \left[ \hat{Y}_{ACE}^2 \left\{ 1 + \frac{N_{rare}(1-C_{rare}) \sum_{i=1}^{abund} i(i-1)n_i}{N_{rare}(N_{rare}-C_{ACE})} \right\} \right] \ln \left[ \hat{Y}_{ACE}^2 \left\{ 1 + \frac{N_{rare}(1-C_{rare}) \sum_{i=1}^{abund} i(i-1)n_i}{N_{rare}(N_{rare}-C_{ACE})} \right\} \right] \quad (F5)$$

$$D_h = \frac{1}{H} \quad (F6)$$

III. RESULTS AND DISCUSSION

3.1 Effects of ultrasonication on nitrogen removal in SBBR systems

The ultrasonic irradiation technique involves inserting a transducer rod into a submerged biofilm reactor (SBBR) solution at a depth of 20 mm, with a polyurethane biofilm filler occupying 50% of the reactor's volume. Ultrasonic power levels were set at 0 W, 180 W, 270 W, and 360 W for reactors R1, R2, R3, and R4, respectively, while testing various dissolved oxygen (DO) concentrations.

The influent consisted of ammonia nitrogen at 50 mg/L and chemical oxygen demand (COD) at 100 mg/L, with a water-changing ratio of 2/3, a cycle duration of 12 hours, and an irradiation time of 10 minutes. Initial DO was 3.5 mg/L, leading to low ammonia nitrogen and total nitrogen (TN) removal rates but high effluent nitrate concentrations. Increasing ultrasonic power decreased nitrate levels, while higher DO levels enhanced nitrification.

Lowering DO to 2.5 mg/L and then to 2 mg/L stabilized the ammonium load, regardless of power levels. In sonicated reactors, effluent ammonia nitrogen initially rose but then declined over time. The TN removal rate peaked at 270 W in reactor R1, indicating that optimizing DO content and power input is crucial for reducing ammonium loads in wastewater treatment systems.

Starting from cycle 30, the dissolved oxygen (DO) concentration was reduced to 1.5 mg/L, resulting in a steady decline in effluent nitrate concentrations across all four reactors. Initially, the total nitrogen (TN) removal rate dropped significantly but later increased, with the highest rates found in reactors R1 (0 W) and R2 (180 W). Increasing the DO to 2 mg/L led to gradual improvements in ammonia nitrogen and TN removal rates in reactors R2 and R3. By cycle 51, reactor R2 achieved a 99.4% removal rate for ammonia nitrogen and 91.7% for TN. Lowering the DO back to 1.5 mg/L caused decreases in R1 and R4, while reactors R2 and R3 showed increases, with R3 reaching a 99.1% ammonia nitrogen removal rate. Ultrasonic irradiation enhanced ammonia-oxidizing bacteria (AOB) activity and suppressed nitrite-oxidizing bacteria (NOB) activity, particularly under high concentrations and low temperatures. Optimal conditions for removal were established at 180 W of ultrasonic power, 10 minutes of irradiation, and a DO of 2 mg/L.

By cycle 6, the nitrite accumulation rates in reactors R0 and R1 rose to 45% and 49%, respectively, increasing to over 73% by cycle 15 with ultrasonic treatment. In the third stage, at an ammonia concentration of 300 mg/L, the nitrite accumulation rate in the R1 sonicated reactor peaked at 94.4%. The average nitrite accumulation rate

was 39.02% in the R0 control reactor compared to 82.99% in R1, with R1 consistently outperforming R0 at various ammonia concentrations. The high nitrite accumulation and low nitrate levels resulted from incomplete nitrification and insufficient nitrite conversion. The TN removal rate increased during startup, with notable efficiencies of 93.59% in R0 and 99.07% in R1 at 200 mg/L influent ammonia. Ultrasonic irradiation also enhanced assimilable organic carbon (AOC) activity under high ammonia levels, with the effects being more significant under challenging conditions.

The nitrogen removal performance in both reactors was notable, with the sonicated reactor outperforming the control reactor. During the startup phase, the highest total nitrogen (TN) removal rates were 85.42% for the control reactor (R0) and 84.21% for the sonicated reactor (R1).

After seven cycles, the TN removal rates were 75.45% for R0, 71% for R1, 64.16% for R2, and 61.75% for R3. Gradual increases in ammonia concentration benefit TN removal; however, excessive ammonia can harm microorganisms. A rise in ammonia nitrogen may enhance the effect of ultrasound on ammonia-oxidizing bacteria (AOB).

Figure 4 indicates that nitrogen transformation processes, such as nitrification and denitrification, are influenced by dissolved oxygen (DO) concentrations and power levels, highlighting the importance of optimizing these parameters for efficient nitrogen removal in wastewater treatment. Additionally, microbial populations involved in nitrogen cycling are sensitive to oxygen availability and other environmental factors, which can be adjusted to achieve lower ammonium and nitrate levels.

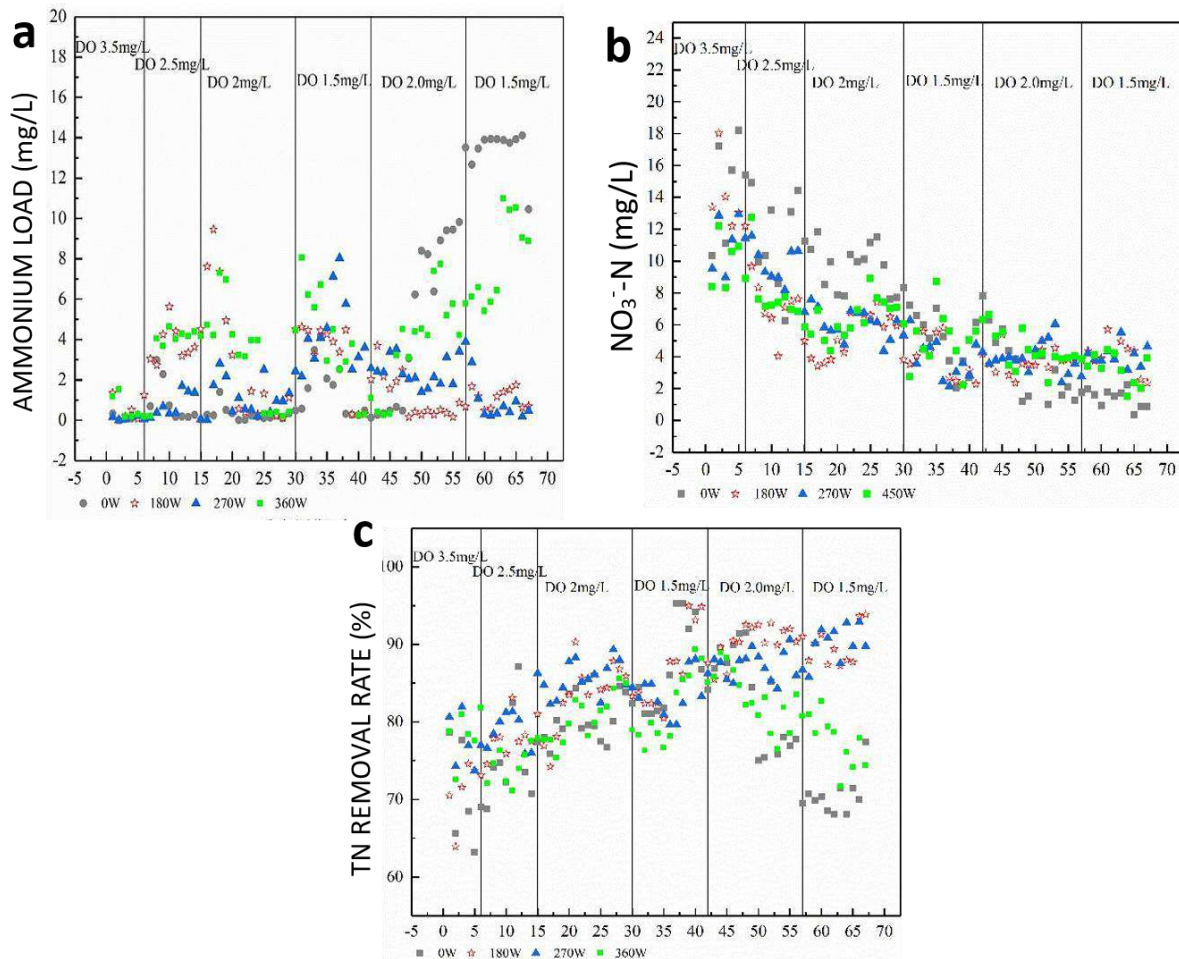


Fig.4 (a) Effluent  $\text{NH}_4^+\text{-N}$  concentration; (b) Effluent  $\text{NO}_3^-\text{-N}$  concentrations; (c) TN removal rate.

### 3.2. Effects of ultrasound on extracellular polymer Substances (EPSs)

Extracellular Polymer Substance (EPS) as an organic substance secreted by microorganisms consists of carbohydrates, proteins, nucleic acids, and humic acids.

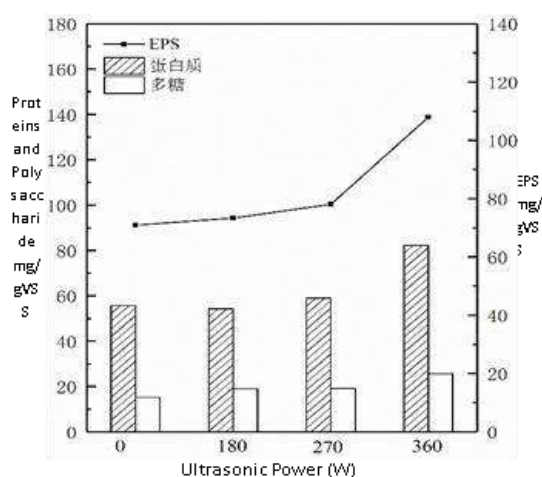
Microbial survival, adhesion, and aggregation (Xiao et al., 2010; Ding et al., 2011). EPS is divided into soluble EPS (S-EPS), loose EPS (LB-EPS) and compact EPS (TB-EPS) (Sheng et al., 2010). LB-EPS and TB-EPS facilitate adhesion and aggregation, where TB-EPS possesses

potent flocculating capacities (Malamis & Andreadakis, 2009). Extracellular polymeric substance (EPS) constitutes a significant part of the biofilm formed, is involved in all aspects of biofilm biological activity, and consists of proteins and polysaccharides (Sponza, 2003) in ultrasound-enhanced (SBBR) sequencing batch biofilm reactor (SBBR) systems.

This study examined the impact of 180W ultrasonic energy on EPS during biological nitrogen removal in SBBR systems. EPS was isolated from biofilms developed in two reactors, and differences comparing control and sonicated reactor EPS contents were performed. The concentrations of S-EPS, LB-EPS, and TB-EPS in the P1 stage of the experiments were demonstrated in Table 2.

Table 1: EPS concentration of Biofilm

Reactor	EPS CONCENTRATION (mg/gVSS)					
	S-EPS		LB-EPS		TB-EPS	
	PN	PS	PN	PS	PN	PS
<b>R1</b>	14.48	5.22	21.23	3.65	19.95	6.34
<b>R2</b>	10.62	2.19	20.31	1.82	23.34	15.02
<b>R3</b>	9.61	2.63	22.96	4.19	26.38	12.26
<b>R4</b>	17.70	7.96	29.22	5.00	35.36	12.69



Change of EPS and its components (DO= 2.0 mg/L)

Influence of influent ammonia, carbon-to-nitrogen (C/N) ratio and water changing rate on the EPS (extracellular polymeric substance) content of biofilms in 4-stage period of P1 phase (Fig. 5) This higher EPS content in sonicated reactor (R2) compared to control reactor (R1) could be associated with increased metabolite secretion which is beneficial for Anammox activity (Duan et al., 2011). Ultrasonic treatment enhances extracellular polymeric substances (EPS) production under high ammonia conditions, suggesting that the biofilm structure was potentially damaged, and microorganisms needed to produce more EPS to protect themselves (Wang et al., 2010; Gao et al., 2017).

In R1, the S-EPS content was 48.8 mg/g VSS, while in R2, it was 49.7 mg/g VSS. Protein content was 16.77 mg/g VSS for R1 and 29.87 mg/g VSS for R2, showing R2 had more protein. R2's LB-EPS was 57.3 mg/g VSS versus 36.36 mg/g VSS for R1, supplying nutrients for anaerobic ammonia-oxidizing bacteria (Gao et al., 2017). The TB-EPS content was also higher in R2 at 73.09 mg/g VSS compared to 53.55 mg/g VSS in R1. Overall, R1 had higher polysaccharide content, while R2 had superior protein content. A decrease in EPS may suggest better living conditions for anaerobic ammonia-oxidizing bacteria (Jin, 2013).

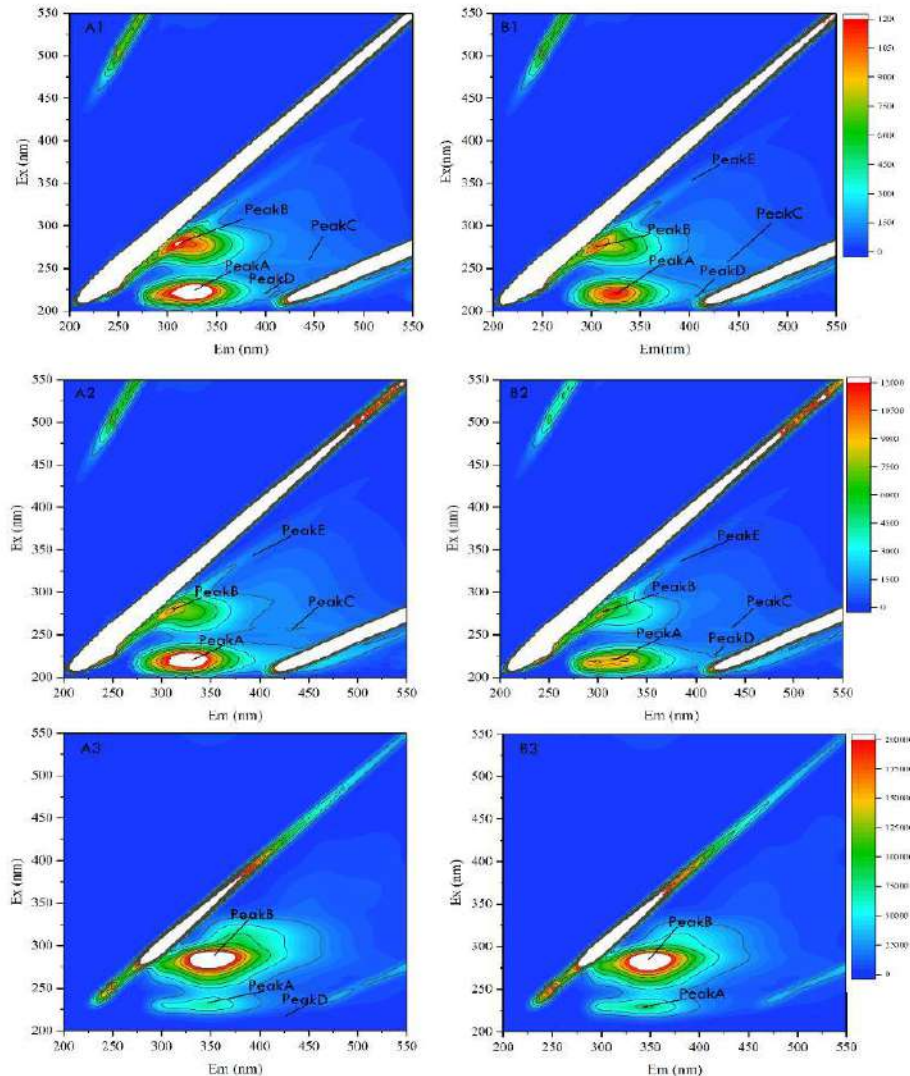


Fig.6: 3D-EEM fluorescence spectra of EPS in R1 and R4 (A1, A2, A3. present S-EPS, LB-EPS and TB-EPS at R1/ B1, B2, B3 present S-EPS, LB-EPS and TB-EPS at R4)

### 3.3. Ultrasonic power effects under different C/N ratios (1.5, 2.5, 3.5) on Microbial community

High-speed sequencing technology was used to analyze the microbial communities in wastewater treatment systems employing sonicated biofilm batch reactors (SBBR) with high-power ultrasound at 180W. The analysis, covering 98% of the biofilms, revealed that as the carbon-to-nitrogen (C/N) ratio increased, the Shannon index rose from 3.72 to 4.79, while the Simpson index increased from 0.03 to 0.04. The ACE and Chao1 index

values for the reactors varied, with the R4 reactor having the highest Chao1 index.

At a C/N ratio of 3.5, the ACE and Chao1 indices peaked in the R3 reactor, indicating enhanced microbial richness. The microbial distribution varied significantly across reactors, mainly comprising Proteobacteria, Bacteroidetes, Planctomycetes, Acidobacteria, Candidatus Saccharibacteria, Chloroflexi, and Ignavibacteriae. Proteobacteria decreased with higher C/N ratios, particularly in the R1 control reactor compared to the sonicated R2 reactor at a C/N ratio of 2.5. In contrast,

Bacteroidetes and Candidatus Saccharibacteria increased at higher C/N ratios in the sonicated reactors, peaking at 3.5.

The study also examined the effects of varying ultrasonic powers on biofilm microbial communities. Analysis at the P1 stage showed that major genera included Ferruginibacter, Paracoccus, Simplicispira, Dokdonella, and Saccharibacteria. Proportions of Candidatus Kuenenia in reactors R1, R2, R3, and R4 were 3.08%, 1.19%, 0.35%, and 0.35%, respectively. The proportion of Ferruginibacter rose with increasing C/N ratios, while Paracoccus denitrificans, known for nitrogen loss, decreased alongside the increasing C/N ratio. In sonicated reactors, Simplicispira and Dokdonella proportions rose with higher C/N ratios, while Paracoccus denitrificans, Candidatus Kuenenia, and Nitrospira proportions declined as the C/N ratio increased.

Ammonia-oxidizing bacteria (AOB) in the four reactors were primarily Nitrosomonas, with proportions of 0.61%, 0.46%, 0.07%, and 0.26% in R1 (C/N = 2.5), R2 (C/N = 1.5), R3 (C/N = 2.5), and R4 (C/N = 3.5), respectively. The highest proportion of Nitro-Spira, a denitrifying gram-negative bacterium, was found in the R0 reactor. This indicates that the combination of the C/N ratio and high ultrasound action may inhibit AOB and nitrite-oxidizing bacteria (NOB) growth. The nitrite-removing microorganisms include AOB, NOB, denitrifying bacteria (DB), heterotrophic bacteria (HB), and anaerobic ammonia-oxidizing bacteria (AnAOB). DB utilizes nitrites and nitrates as electron acceptors to produce nitrogen.

Figure 7 shows that as the C/N ratio increased from 1.5 to 3.5, significant shifts in microbial community abundance occurred. AOB and NOB were low in number while denitrifying bacteria were abundant. ANAMMOX was also present, with Candidatus Kuenenia making up a significant portion.

### 3.3.1 Functional Bacteria

Heterotrophic nitrifying-aerobic denitrifying bacteria and facultative denitrifying bacteria coexisted in the reactors,

in which most denitrifying bacteria belonged to Thermomonas, Luteimonas and Hydrogenophaga. As a Gram-negative aerobic bacterium capable of dissimilatory NO<sub>2</sub>-N reduction to N<sub>2</sub>O (Young et al., 2007), Luteimonas was involved in 5.15% of the bacterial population in reactor R4, 3.72% in control reactor, and appeared in least abundance in reactor R2. Autotrophic denitrifying hydrogen-dependent bacteria, like Hydrogenophaga, were present in all reactors, with their concentration peaking at 180W (19.50%). The control reactor predominantly composed of Azospira (Tan & Hurek, 2003), accounting for 2.13% of the total bacterial population. In addition, abundant recovery of anaerobic ammonia-oxidizing bacteria, Candidatus Kuenenia, was been identified (Wang et al., 2018).

Studies have shown that the ability of Candidatus Kuenenia to improve the competitive advantage of Anammox bacteria in sludge when subjected to ultrasound technology, leading to better ammonia removal efficiency of Anammox reactors during high nitrogen loading conditions. The proportions of Candidatus Kuenenia in reactors R1, R2, R3, and R4 were 3.08%, 1.19%, 0.35%, and 0.35%, respectively. Candidatus Kuenenia growth is inhibited at high ultrasonic power and/or at a high C/N ratio, affecting nitrogen removal. Denitrifiers were the most abundant microbial populations in the reactors (29.54%-48.5%), with higher C/N ratios resulting in a more abundant community. The control reactor R1, ANAMMOX bacteria showed the maximum activity, where almost at 2.5 level.

This ratio favors the enhanced growth of denitrifying bacteria, helping in the quick conversion of nitrate into ammonium and increasing the ammonia nitrogen amount. Besides that, an increase in Lysobacter and Ferruginibacter population at an increased ultrasonic power significantly influences other functional microbial groups. Conclusion In this respect, a higher C/N value is advantageous due to its stimulation for denitrifying bacteria.

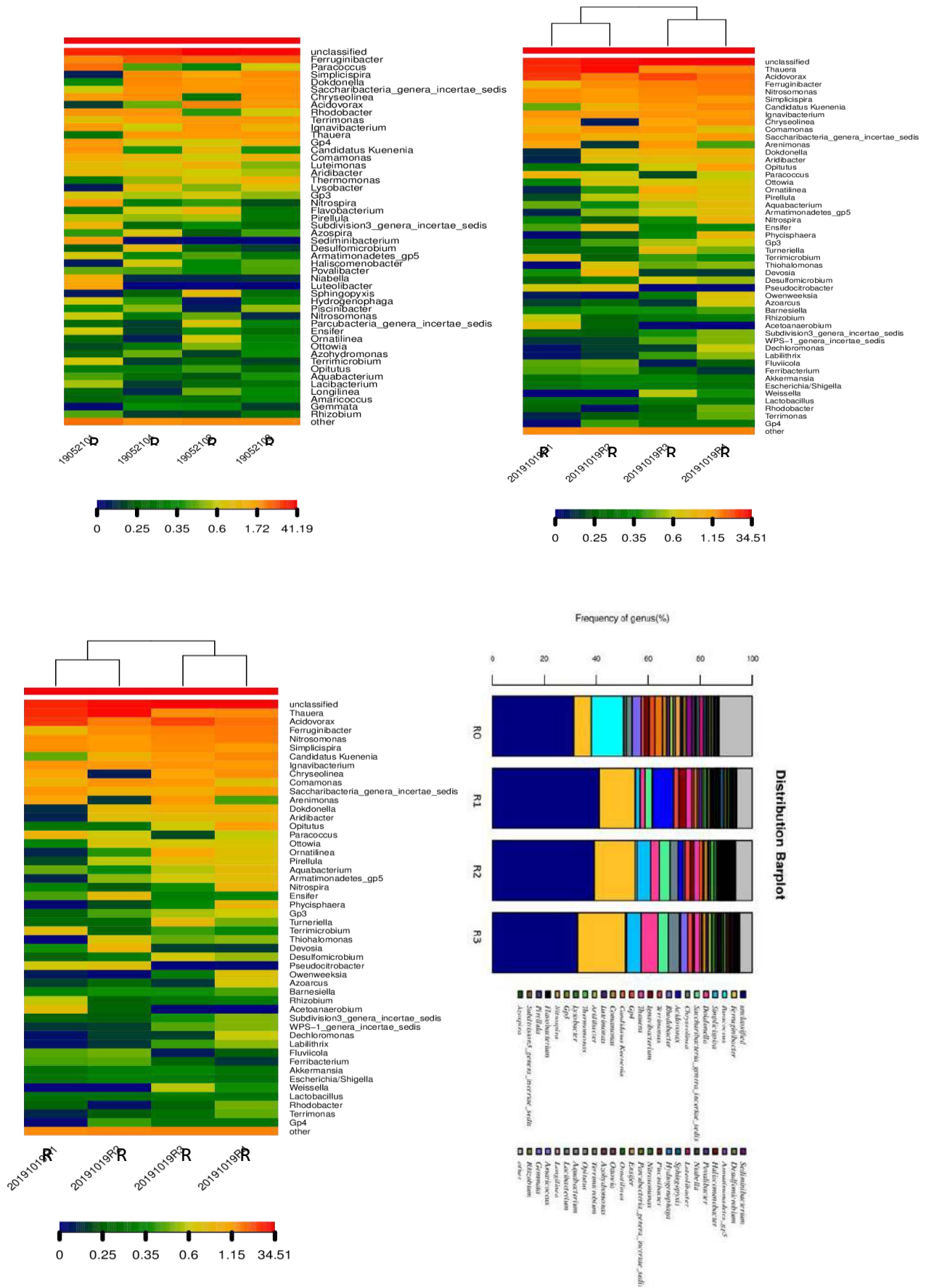


Fig.7: Microbial Community at Genus level and Distribution Barplot

The biodiversity of microorganisms in the Submerged Biofilm Batch Reactor (SBBR) was analyzed under

various levels of ultrasound power. Significant differences in microbial composition were found across

the four reactors, mainly consisting of *Proteobacteria*, *Bacteroidetes*, *Planctomycetes*, *Chloroflexi*, *Ignavibacteriae*, and *Verrucomicrobia*.

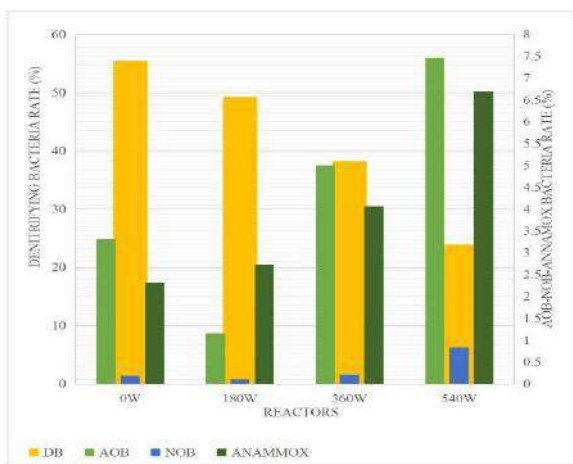
At the genus level, the communities were categorized into ammonia-oxidizing bacteria (AOB), nitrite-oxidizing bacteria (NOB), denitrifying bacteria (DB), heterotrophic bacteria (HB), and anaerobic ammonia-oxidizing bacteria (ANAMMOX). The AOB were primarily *Nitrosomonas*, with the highest proportion (7.47%) observed in the R3 reactor at 540W. *Nitrospira* dominated the NOB, also peaking in the R3 reactor. *Thauera* was the most abundant denitrifying bacteria across all reactors, and *Acidovorax* was also present. Increased ultrasound power led to notable changes in microbial abundance. *Paracoccus* showed the highest proportions in the control reactor, while *Candidatus Kuenenia*, a resilient ANAMMOX bacterium, exhibited greater resistance to ultrasound effects. The result demonstrates that high ultrasonic power can boost the development and multiplication of *Candidatus Kuenenia's* bacteria and raise the nitrogen removal performance of the ANAMMOX reactor under high nitrogen load working circumstances. The maximum concentration of *Acidovorax* was obtained in the control reactor. Foladori et al 2007, found that Gram-positive bacteria have a 10-15 times stronger cell wall than Gram-negative bacteria, rendering them more vulnerable to ultrasonic

effects. According to Xie et al., the 2008 study observed that the species with larger cell walls may assist in the gradual enrichment of these bacteria in the reactor when ultrasound is applied.

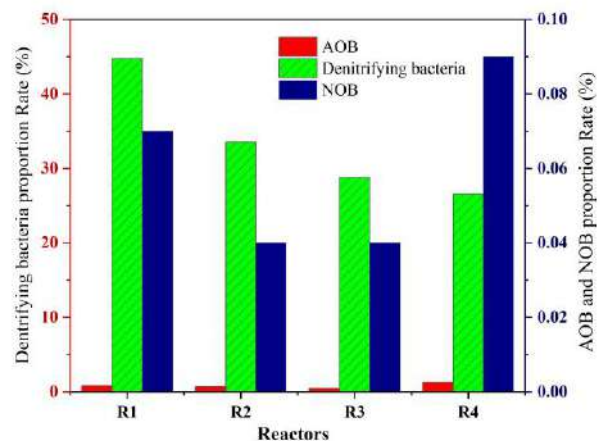
The study analyzed relative abundances of aerobic bacteria (AOB) non-obese bacteria (NOB) and nitrite bacteria (ANAMMOX) in a sonicated reactor system. Due to the increment of the ultrasonic power, the value of AOB level also increased, maximizing in the R3 reactor at 540 W. However, NOB bacteria were normally found in low amounts, where the proportions of NOB were the highest in the R2 and R3 reactors at 360 W and 540 W, respectively. NOB can be inhibited under anaerobic conditions.

ANAMMOX bacteria, in particular, responded positively in proportion to increasing ultrasonic power, with the control reactor (R0) showing the lowest proportion and the highest proportion seen in the R3 reactor at 540 W. While the DB fraction was found to decrease as a consequence of ultrasound inhibiting DB, NOB quantities increased as ultrasonic power increased.

This resulted in promoting the growth of AOB, NOB, and ANAMMOX bacteria by 360 W and 540 W of high-power ultrasound, while inhibitory effects were observed on the growth of DB.



A



B

Fig.8: (A) Denitrifying Bacteria Rate (B) Denitrifying Bacteria Proportion Rate (%)

#### IV. CONCLUSION

The research proved that ultrasonic treatment is beneficial for nitrogen removal in SBBR systems by improving the effectiveness of nitrifying and denitrifying bacteria. Applying ultrasonic powers of 180 W and 270 W under specific dissolved oxygen conditions achieved ammonia

nitrogen and total nitrogen removal rates of up to 99.4% and 91.7%, respectively. Moderate ultrasonic power improved microbial activity and the structure of the biofilm, resulting in better nitrogen removal without causing significant cellular damage.

In contrast, higher ultrasonic powers increased the production of extracellular polymeric substances (EPS), which helped protect microorganisms and maintain biofilm stability under stress; however, excessive power did not yield further improvements in nitrogen removal efficiency. The study also emphasized the interaction between dissolved oxygen concentration and ultrasonic power in shaping nitrogen transformation processes, underscoring the importance of optimal combinations of these factors for maximizing treatment efficiency. The heightened EPS production observed in ultrasonically treated reactors indicates a protective response that promotes biofilm formation and resilience.

#### DECLARATION OF COMPETING INTEREST

The authors declare that they have no known competing financial interests or personal relationships that could have appeared to influence the work reported in this paper.

#### DATA AVAILABILITY

Data will be made available on request.

#### ACKNOWLEDGEMENTS

This work was supported by the National Natural Science Foundation of China (NO. 21607111), Fundamental Research Program of Shanxi Province (NO. 20210302123198), the Opening Project of National Engineering Laboratory for Advanced Municipal Wastewater Treatment and Reuse Technology and State Key Laboratory of Pollution Control, Resource Reuse Foundation, Tongji University (NO. PCRRF18011) and Innovation Project for Graduate Students of Shanxi Province (NO. RC1900001671).

#### REFERENCES

- [1] B. Patrik Arnz, 2001. Nutrient Removal from Municipal Wastewater in Sequencing Batch Biofilm Reactors: Wasserg UTE, Munich.
- [2] F. J. Erik R.Coats, 2011. Post-anoxic denitrification driven by PHA and glycogen within enhanced biological phosphorus removal: *Bioresource Technology Volume 102, Issue 2*, pp. Pages 1019-1027.
- [3] Y. W. X. Y. H. X. H. T. S. S. X. T. B. W. S. Shi, 2011. Aerobic granulation for nitrogen removal via nitrite in a sequencing batch reactor and the emission of nitrous oxide: *Bioresources Technology*, vol. 102, p. 2536–2541.
- [4] J. R. M. H. M. Prendergast, 2005. The efficiency of a sequencing batch reactor (SBBR) in organic carbon and phosphorus removal: *Journal of Environmental Science and Health, Part A: Toxic/Hazardous Substances and Environmental Engineering*, vol. 40, n° %18, pp. 1619-1626.
- [5] C. Di Iaconi, A. Lopez, R. Ramadori, A. Di Pinto et R. Passino, 2004. Combined chemical and biological degradation of tannery wastewater by a periodic submerged filter (SBBR): *Water Ressources*, vol. 36, pp. 2205-2214.
- [6] N. G. A. & N. V. Majid, 2015. Ultrasonication and food technology: A review *Cogent Food & Agriculture* , vol. 1, n° % 11, p. 1071022.
- [7] S.-L. L. A. R. D. Vinay Kumar Tyagi, 2014. Ultrasonic Treatment of Waste Sludge: A Review on Mechanisms and Applications: *Critical Reviews in Environmental Science and Technology*, vol. 44, n° % 111, pp. 1220-1288,
- [8] H. Liu, 2007. Low intensity ultrasound stimulates biological activity of aerobic activated sludge: *Frontiers of Environmental Science & Engineering in China*.
- [9] P. M. S. S. A.B.Pandit, 2010. Excess cell mass as an internal carbon source for biological denitrification," *Bioresource Technology*, vol. 101, no. Issue 6, pp. 1787-1791.
- [10] Mahvi, A., 2009. Application of Ultrasonic Technology for Water and Wastewater Treatment: *Iranian J Publ Health*, vol. 1, p. 17.
- [11] Raj B, Rajendran V, Palanichamy P, 2004. Science and technology of ultrasonics: UK.
- [12] Lutz, H. T., 2016. Basics of Ultrasound: chez *Manual of diagnostic Ultrasound in Infectious Tropical Diseases*, p. 167.
- [13] Zhang G, Zhang P, Gao J, Chen Y., 2008. Using acoustic cavitation to improve the bioactivity of activated sludge: *Bioresource technology*, vol. 99, n° % 15, pp. 1497502.
- [14] Chua SY, Adul Latif P, Ibrahim Sh., 2010. Effect of Ultrasonic Irradiation On Landfill Leachate: *Proceedings of Postgraduate Qolloquium Semester 1 2009/2010*.
- [15] Thangavadivel K, Megharaj M, Mudhoo A, Naidu R., 2012. Degradation of organic pollutants using ultrasound. *Handbook on application of ultrasound: sonochemistry for sustainability. CRC Press, Taylor & Francis Group*.
- [16] Sinisterra., 1992. Application of ultrasound to biotechnology an overview: *Ultrasonics*, vol. 30(3), pp. 180-5.
- [17] Chisti Y., 2003. Sonobioreactors: using ultrasound for enhanced microbial productivity: *Trends in biotechnology*, p. 21(2): 89.
- [18] P. V. J. Rokhina EV, 2009. Low-frequency ultrasound in biotechnology: state of the art: *Trends in biotechnology*, vol. 27(5), pp. 298-306.
- [19] Y. A. W. B. C. S. A. Liu Y Y, 2003. Influence of ultrasonic stimulation on the growth and proliferation of *Oryza sativa* Nipponbare callus cells. *Colloids and Surfaces B: Biointerfaces*, vol. 27, p. 287– 293.
- [20] Lin L D WJY. , 2002. Enhancement of shikonin production in single- and two-phase suspension cultures of *Lithospermum erythrorhizon* cells using low-energy ultrasound: *Biotechnology and Bioengineering*, vol. 78(1), pp. 81-8.

- [21] Yu G-H, He P-J, Shao L-M, Zhu Y-S., 2008. Extracellular proteins, polysaccharides and enzymes impact on sludge aerobic digestion after ultrasonic pretreatment: *Water Research*, vol. 42(8-9), pp. 1925-34.
- [22] Yang fei., 2007. Experimental study on low intensity ultrasonic enhanced biological treatment of sewage: chongqing.
- [23] Yan Yixin, Liu Hong., 2006. Optimal selection of ultrasonic irradiation cycle in low intensity ultrasonic enhanced biological treatment of wastewater: *Environmental science*, vol. 27(5), p. 898.
- [24] Tang Xin, Qiao Sen, Zhou Qeng., 2017. Effects of low intensity ultrasound on the activity of short-range nitrification sludge: *Journal of safety and environment*, vol. 01, pp. 267-72.
- [25] Liu Y, Yoshikoshi A, Wang B, Sakanishi A., 2003. Influence of ultrasonic stimulation on the growth and proliferation of *Oryza sativa* Nipponbare callus cells: Colloids and Surfaces. *Bio interfaces*, vol. 27(4), pp. 287-93.
- [26] Zheng M, Liu Y C, Xin J, ...2015. Ultrasonic Treatment Enhanced Ammoniaoxidizing Bacterial (AOB) Activity for Nitrification Process. *Environmental Science & Technology*, vol. 50 (2), pp. 864-871.
- [27] Zheng M, Liu Y C, Xu K N., 2013. Use of low frequency and density ultrasound to stimulate partial nitrification and simultaneous nitrification and denitrification. *Bioresource technology*, pp. 146: 537-542.
- [28] Zhang R, Jin R, Liu G, Zhou J, Li CL., 2011. Study on nitrogen removal performance of sequencing batch reactor enhanced by low intensity ultrasound. *Bioresource technology*, vol. 102(10), pp. 5717-21.
- [29] Liu H, He Y-h, Quan X-c, Yan Y-x, Kong X-h, Lia A-j., 2005. Enhancement of organic pollutant biodegradation by ultrasound irradiation in a biological activated carbon membrane reactor. *Process Biochemistry*, vol. 9, pp. 3002-7.
- [30] Tan Jiangyue, Xu Zhiqiang., 2013. Study on treatment of coking wastewater by SBR method with low intensity ultrasound. *Environmental science and technology*, vol. 11, pp. 117-20 29.
- [31] H. L. Xie B, 2010. Enhancement of Biological Nitrogen Removal from Wastewater by Low Intensity Ultrasound. *Water Air & Soil Pollution*, Vols. %1 sur %2211(1-4), pp. 157-163.
- [32] Yan Yixin, Liu hong., 2006. Optimal selection of ratio of ultrasonic irradiation sludge in low intensity ultrasonic enhanced wastewater biological treatment. *Environmental science*, vol. 27, p. 908.
- [33] L. G. S. H. Z. Q. P. Tan Jingjing, 2015. Effect of ultrasonic cytolysis on denitrification and dephosphorization system: *Municipal technology*, vol. 05, p. 122.
- [34] Y. Z.-Y. I. H.-C. Li zhan-chen, 2012. Experimental study on degradation of 8-hydroxyquinoline wastewater by ultrasonic-biochemical method. *Sichuan environment*, vol. 31 (2), pp. 11-5, 2012.
- [35] C. Y. J. W. Z. Z. J. Ding chi, 2014. Study on ultrasonic parameter optimization in SMBR treatment with low intensity ultrasonic. *Environmental science and management*, vol. 39 (5), pp. 88-91.
- [36] C. H. Z. J. J. Y. L. Q. J. R. Yu JJ, 2013. Enhancement of ANAMMOX activity by low intensity ultrasound irradiation at ambient temperature. *Bioresource technology*, vol. 142, pp. 693-6, 2013.
- [37] Yu T, Qi R, Li D, Zhang Y, Yang M., 2010. Nitrifier characteristics in submerged membrane bioreactors under different sludge retention times. *Water Research*, vol. 44, n° %19, pp. 23-30.
- [38] Jin R, Liu G, Li C, Xu R, Li H, Zhang L, et al., 2013. Effects of carbon-nitrogen ratio on nitrogen removal in a sequencing batch reactor enhanced with low-intensity ultrasound. *Bioresource technology*, vol. 148:1, pp. 28-34.
- [39] Tang Xin., 2015. Treatment of ammonia nitrogen wastewater by single stage autotrophic nitrogen removal process promoted by low intensity ultrasound. *Dalian university of technology, Dalian*.
- [40] Xie B, Wang L, Liu H., 2008. Using low intensity ultrasound to improve the efficiency of biological phosphorus removal. *Ultrasonics sonochemistry*, , vol. 15(5), pp. 775-81.
- [41] Li Na, Xie Beizhen, Liu Hong., 2010. Treatment effect of A2 / O process enhanced by low intensity ultrasound. *Proceedings of 2010 China renewable energy technology development conference. Beijing*, pp. 2781-4.
- [42] Wünsch B, Heine W, Neis U., 2002. Combating bulking sludge with ultrasound.
- [43] Yang shaoqiang, Xie Beizhen, Liu Hong., 2007. Low intensity ultrasonic enhanced aerobic digestion of expanded sludge. *Water and drainage*, vol. 33 (s1), pp. 50-3.
- [44] Yingyan Y, Ping L, Jinhua W, 2014. N<sub>2</sub>O emission in short-cut simultaneous nitrification and denitrification process: dynamic emission characteristics and succession of ammonia-oxidizing bacteria. *Water Science & Technology*, vol. 69, n° %112, pp. 2541-2547.
- [45] Ford D L, Churchwell R L, Kachtick J W., 1980. Comprehensive Analysis of Nitrification of Chemical Processing Wastewaters. *Journal*, vol. 52, n° %1(11), pp. 2726-2746.
- [46] Hong L, Xin Y Y., 2008. Enhancement Effect of Low Intensity Ultrasound on Biological Wastewater Treatment System in Low Temperature and Design of Application on Biological Wastewater Treatment. *Environmental Science*, vol. 29(3), pp. 721725.
- [47] Xiao-Meng L, Guo-Ping S, Hong-Wei L., 2010. Contribution of extracellular polymeric substances (EPS) to the sludge aggregation. *Environmental Science & Technology*, vol. 44(11), pp. 4355-4360.
- [48] Ding D, Feng C, Jin Y, et al., 2011. Domestic sewage treatment in a sequencing batch biofilm reactor (SBBR) with an intelligent controlling system. *Desalination*, vol. 276(1), pp. 260-265.
- [49] Sheng G P, Yu H Q, Li X Y., 2010. Extracellular polymeric substances (EPS) of microbial aggregates in biological wastewater treatment systems: A review. *Biotechnology Advances*, vol. 28(6), pp. 882-894.

- [50] Malamis S, Andreadakis A., 2009. Fractionation of proteins and carbohydrates of extracellular polymeric substances in a membrane bioreactor system. *Bioresource technology*, vol. 100(13), pp. 3350-3357.
- [51] Sponza D T., 2003. Investigation of extracellular polymer substances (EPS) and physicochemical properties of different activated sludge flocs under steady-state conditions. *Enzyme & Microbial Technology*, vol. 32(3), pp. 375-385.
- [52] Duan X, Zhou J, Qiao S, et al., 2011. Application of low intensity ultrasound to enhance the activity of anammox microbial consortium for nitrogen removal. *ioresource technology*, vol. 102(5), pp. 4290-4293.
- [53] Wang F, Ji M, Lu S., 2010. Influence of Ultrasonic Disintegration on the Dewaterability of Waste Activated Sludge. *Environmental Progress*, vol. 25(3), pp. 257-260.
- [54] Gao X, Xu H, Chen W et al., 2017. Influence of extracellular polymeric substances (EPS) treated by combined ultrasound pretreatment and chemical re-flocculation on water treatment sludge settling performance. *Chemosphere*, vol. 170, pp. 196-206.
- [55] Jin R C, Ma C, Yu J J., 2013. Performance of an Anammox UASB reactor at high load and low ambient temperature. *Chemical Engineering Journal*. vol. 232(10), pp. 17-25.
- [56] S. Fudala-Ksiazek, A. Luczkiewicz, K. Fitobor, and K. Olanczuk-Neyman, 2014. Nitrogen removal via the nitrite pathway during wastewater co-treatment with ammonia-rich landfill leachates in a sequencing batch reactor. *Environmental Science and Pollution Research International*, vol. 21, n° % 112, p. 7307–7318.
- [57] Zhou Y, Oehmen A, Lim M, Vadivelu V., 2011. The role of nitrite and free nitrous acid (FNA) in wastewater treatment plants.,» *Water Ressources*, vol. 45, n° % 115, pp. 4672-82.
- [58] Wood PM., 1986. Nitrification as a bacterial energy source. *Special Publications of the Society for General Microbiology*, vol. 20, pp. 39-62.
- [59] Li Z, Chang Q, Li S, 2017. Impact of sulfadiazine on performance and microbial community of a sequencing batch biofilm reactor treating synthetic mariculture wastewater. *Bioresource technology*, vol. 235(3), pp. 122-130.
- [60] Yuan L, Huang Z, Ruan W, et al., 2015. ANAMMOX performance, granulation, and microbial response under COD disturbance. *Journal of Chemical Technology & Biotechnology*, vol. 90(1), pp. 139-148.
- [61] Barbara Baumann, Mario Snozzi, Alexander J. B. Zehnder, Jan Roelof Van Der Meer, 1996. Dynamics of Denitrification Activity of Paracoccus denitrificans in Continuous Culture during Aerobic-Anaerobic Changes. *Journal of Bacteriology*, vol. 178, n° % 115.
- [62] Stouthamer A H, Boer A P N D, Oost J V D, et al., 1997. Emerging principles of inorganic nitrogen metabolism in Paracoccus denitrificans and related bacteria. *Antonie Van Leeuwenhoek*, Vols. % 1 sur % 271(1-2), pp. 33-41.
- [63] Neef A, Zaglauer A, Meier H, et al., 1996. Population analysis in a denitrifying sand filter: conventional and in situ identification of Paracoccus spp. in methanol-fed biofilms, *Appl Environ Microbiol*, vol. 62(12), pp. 4329-4339.
- [64] Koerner, H., 1993. Anaerobic expression of nitric oxide reductase from denitrifying Pseudomonas stutzeri. *Arch. Microbiol.*, vol. 159, p. 410–416.
- [65] Koerner, H., and W. G. Zumft., 1989. Expression of denitrification enzymes in response to the dissolved oxygen level and respiratory substrate in continuous culture of Pseudomonas stutzeri. *Appl. Environ. Microbiol.*, vol. 55, p. 1670–1676.
- [66] Mcilroy S J, Starnawska A, Starnawski P, et al., 2016. Identification of active denitrifiers in full-scale nutrient removal wastewater treatment systems. *Environmental Microbiology*, vol. 18(1), pp. 50-64.
- [67] Shih-Yi S, Nian-Tsz C, Arun A B, et al., 2010. Terrimonas aquatica sp. nov., isolated from a freshwater spring. *International Journal of Systematic & Evolutionary Microbiology*, vol. 60(12), pp. 2705-2709.
- [68] Gonzalez-Silva B M, Jonassen K R, Bakke I., 2016. Nitrification at different salinities: Biofilm community composition and physiological plasticity. *Water Research*, n° % 195: 48, 2016.
- [69] Nielsen M, Bollmann A, Sliemers O., 2010. Kinetics, diffusional limitation and microscale distribution of chemistry and organisms in a CANON reactor. *Fems Microbiology Ecology*, vol. 51(2), pp. 247-256.
- [70] Weidong W, Weiyue L, Di W, et al., 2019. Differentiation of nitrogen and microbial community in the littoral and limnetic sediments of a large shallow eutrophic lake (Chaohu Lake, China). *Journal of Soils and Sediments*, vol. 19, p. 1005–1016.
- [71] Qin Y., Han B., Cao Y. and Wang T., 2017. Impact of substrate concentration on anammox-UBF reactors start-up. *Bioresource Technology*, vol. 239, p. 422–429.
- [72] Wang T, Zhang D, Sun Y., 2002. Using low frequency and intensity ultrasound to enhance start-up and operation performance of Anammox process inoculated with the conventional sludge. *Ultrasonics Sonochemistry*, pp. 42: 283-292.
- [73] Nogaro G, Burgin A J., 2014. Influence of bioturbation on denitrification and dissimilatory nitrate reduction to ammonium (DNRA) in freshwater sediments. *Biogeochemistry*, vol. 120, n° % 1(1-3), pp. 279-294.
- [74] Foladori P, Laura B, Gianni A, et al., 2007. Effects of sonication on bacteria viability in wastewater treatment plants evaluated by flow cytometry—Fecal indicators, wastewater and activated sludge. *Water Research*, vol. 41(1), pp. 235-243.
- [75] Mehdi Hajsardar, Seyed Mehdi Borghei, Amir Hessam Hassani, Afshin Takdastan, 2015. Optimization of wastewater partial nitrification in Sequencing Batch Biofilm Reactor (SBBR) at fixed do level. *Journal of Biodiversity and Environmental Sciences (JBES)*, vol. 7, pp. 2222-304.
- [76] Patrik Arnz, 2001. Biological Nutrient Removal from Municipal Wastewater in Sequencing Batch Biofilm Reactors. *Wasserg UTE, Munich*.

- [77] Erik R.Coats, AlexanderMockos Frank, J.Loge, 2011. Post-anoxic denitrification driven by PHA and glycogen within enhanced biological phosphorus removal. *Bioresource Technology Volume 102, Issue 2*, pp. Pages 1019-1027.
- [78] Shi, Y.J., Wang, X.H., Yu, H.B., Xie, H.J., Teng, S.X., Sun, X.F., Tian, B.H., et al., 2011. Aerobic granulation for nitrogen removal via nitrite in a sequencing batch reactor and the emission of nitrous oxide, *Bioresources Technology*, vol. 102, p. 2536–2541.
- [79] Majid, I., Nayik, G. A., and Nanda, V., 2015. Ultrasonication and food technology: A review. *Cogent Food & Agriculture*, vol. 1, n° %11, p. 1071022.
- [80] Vinay Kumar Tyagi, Shang-Lien Lo,Lise Appels, Raf Dewil, 2014. Ultrasonic Treatment of Waste Sludge: A Review on Mechanisms and Applications. *Critical Reviews in Environmental Science and Technology*, vol. 44, n° %111, pp. 1220-1288.
- [81] Liu, Hong, 2007. Low intensity ultrasound stimulates biological activity of aerobic activated sludge. *Frontiers of Environmental Science & Engineering in China*.
- [82] Pandit A.B., Prashant M.Biradar S.B.Roy S.F.D'Souza, 2010. Excess Cell Mass As An Internal Carbon Source for Biological Denitrification. *Bioresource Technology*, vol. 101, no. Issue 6, pp. 1787-1791.
- [83] Xiao-Meng L, Guo-Ping S, Hong-Wei L, et al., 2010. Contribution of extracellular polymeric substances (EPS) to the sludge aggregation. *Environmental Science & Technology*, vol. (11), n° %144, pp. 4355-4360.
- [84] Ding D, Feng C, Jin Y, et al., 2011. Domestic sewage treatment in a sequencing batch biofilm reactor (SBBR) with an intelligent controlling system. *Desalination*, vol. 276(1), pp. 260-265.
- [85] Prendergast, J., Rodgers, M., Healy, M.G., 2005. The efficiency of a sequencing batch reactor (SBBR) in organic carbon and phosphorus removal. *Journal of Environmental Science and Health, Part A: Toxic/Hazardous Substances and Environmental Engineering*, vol. 40, n° %18, pp. 1619-1626.
- [86] B. A. S. O. Nielsen M, 2010. Kinetics, diffusional limitation and microscale distribution of chemistry and organisms in a CANON reactor. *Fems Microbiology Ecology*, pp. 51(2): 247-256.
- [87] Gonzalez-Silva B M, Jonassen K R, Bakke I., 2016. Nitrification at different salinities: Biofilm community composition and physiological plasticity. *Water Research*, p. 95: 48.
- [88] S. I. MaintinguerI, I. K. SakamotoII; M. A. T. AdornoII; M. B. A. VarescheII, 2013. Evaluation of the microbial diversity of denitrifying bacteria in batch reactor. *Brazilian Journal of Chemical Engineering*, vol. 30, n° %13.
- [89] Purkhold U., PommereningRo'ser A, Juretschko S., Schmid M. C., Koops H. P., and Wagner M., 2000. Phylogeny of all recognized species of ammonia oxidizers based on comparative 16S rRNA and amoAsequence analysis: implications for molecular diversity surveys *Applied and Environmental Microbiology*, vol. 66, p. 5368–5382.
- [90] Yan J, Hu Y Y., 2009. Partial nitrification to nitrite for treating ammonium-rich organic wastewater by immobilized biomass system. *Bioresource technology*, vol. 99(8), p. 2341-2347.
- [91] Chen H, Liu S, Yang F, et al., 2009. The development of simultaneous partial nitrification, ANAMMOX and denitrification (SNAD) process in a single reactor for nitrogen removal 2009. *Bioresource technology*, vol. 99(4), pp. 1548-1554.

# Application of Humic Acid and Mulch Dose on Corn (*Zea mays* L) Yield

Bama Wida Pratama<sup>1</sup>, Luluk Sulistiyo Budi<sup>2</sup>, Indah Rekyani Puspitawati<sup>3</sup>

<sup>1</sup>Department of Agrotechnology, Merdeka University, Madiun, Indonesia  
[masbamapratama11@gmail.com](mailto:masbamapratama11@gmail.com)

<sup>2</sup>Department of Agrotechnology, Merdeka University, Madiun, Indonesia  
[luluksb@unmer-madiun.ac.id](mailto:luluksb@unmer-madiun.ac.id)

<sup>3</sup>Department of Agrotechnology, Merdeka University, Madiun, Indonesia  
[indahrekyani@gmail.com](mailto:indahrekyani@gmail.com)

Received: 09 Dec 2024,

Receive in revised form: 11 Jan 2025,

Accepted: 17 Jan 2025,

Available online: 22 Jan 2025

©2025 The Author(s). Published by AI  
Publication. This is an open-access article  
under the CC BY license  
(<https://creativecommons.org/licenses/by/4.0/>).

**Keywords**— *Humic acid, mulching, corn growth, crop yield, Randomized Block Design.*

**Abstract**—*This research aims to determine whether there is an interaction between the use of humic acid and mulching on the growth and production of corn plants, the effect of humic acid on the growth and production of corn plants and the effect of the use of mulch or mulching on the growth and production of corn plants. This study used a Randomized Block Design (RAK) with 3 replications in Giripurno Village, Kawedanan District, Magetan Regency. The first factor studied was humic acid (A) consisting of 3 treatments, namely doses of 0 Kg / Hectare, 10 Kg / Hectare, 20 Kg / Hectare and the second factor was mulch (M) consisting of 3 treatments, namely without mulch, plastic mulch, straw mulch. The parameters observed included plant height, stem diameter, number of cobs, weight of wet cobs with husks, weight of wet corn cobs without husks, weight of 1000 grains, number of rows, number of seeds, dry weight without husks, weight of dry husked corn, number of leaves, leaf area. There is interaction with plants on the parameters of yield, namely the weight of wet cobs with husks, weight of 1000 grains, and number of rows because the nutrients in humic acid can provide benefits to the yield of corn plants. The absence of interaction on the parameters of plant height 53 HST, stem diameter, number of cobs, weight of wet cobs without husks, number of seeds, dry weight of whole cobs, weight of dry kernels, number of leaves, leaf area is caused by insufficient dosage and short sample observation time.*

## I. INTRODUCTION

Corn (*Zea mays* L) is one of the important food crops that has high economic value and is popular with the community. Corn has soft textured seeds, making it very popular as a food and snack ingredient. In Indonesia, corn farming is one of the potential agricultural sectors. However, despite its great potential, corn productivity in the region is still not optimal.

Corn is placed in the following taxonomy: Kingdom: Plantae, Division: Spermatophyta, Subdivision: Angiospermae, Class: Monocotyledone, Order:

Graminae, Family: Graminaceae, Genus: *Zea*, and Species: *Zea mays*L

Gajung has three types of roots: seminal roots, aerial roots, and adventitious roots. Seminal roots originate from the radicle and embryo; aerial roots originate from two or more nodes below the soil surface; and adventitious roots are also known as prop roots. Corn plant varieties, soil fertility, and groundwater conditions affect root development. The stems of corn plants are cylindrical with many segments and nodes and have no branches ranging between 150 and 250 cm and are

covered by alternating leaf sheaths from each node. Hybrid corn variety seeds are superior seeds.

Hybrid corn seeds have many advantages, such as disease resistance, faster harvest time, and better quality and quantity of production. Hybrid corn seeds can also produce twin corn cobs, which produce twice the yield. Because hybrid corn seeds do not have the superior properties of the parent, they can only be planted for one planting season.

Around 220 hectares of agricultural land planted with corn in Giripurno Village, according to field data. (Yoni, 2023), the intensification pattern of farmers in Giripurno Village on average cultivates existing agricultural land using chemical fertilizers and pesticides to increase agricultural yields. However, agriculture in Giripurno Village has never implemented soil cultivation using humic acid soil conditioners and mulching on corn plants.

To increase agricultural production, especially in the cultivation of food crops, mulch is one approach. Mulch is a material that covers the soil to prevent water loss through evaporation and weed growth.

Mulch protects the soil surface from erosion and rain exposure and maintains soil moisture, structure, and fertility. In addition, mulch inhibits weed growth. (Nadia, 2020). The use of mulch, which is a surface cover for beds or mounds, is very important because it provides benefits including reducing the rate of evaporation from the soil surface, which saves water use, reduces changes in soil temperature, and reduces the costs and energy required for weed control. In the use of mulching on agricultural land, synthetic mulch and natural mulch can be distinguished. Synthetic, for example, PE plastic mulch made from polyethylene.

Humic acid is a good material to complement inorganic fertilizers. It is very important to pay attention to the dosage of humic acid because it can affect the nutrient content and growth of corn plants. According to Firda's research (2016), humic acid contains 40-80% C elements, 2-4% N elements, 1-2% S elements, and 0-0.3% P elements. Based on research by Hermanto et al. (2013) compared with other doses, the use of humic acid as a fertilizer supplement with a dose of 20 kg/ha showed a better response to plant growth, supported by increased nutrient availability and nutrient uptake.

Currently, humic acid has been used as a fertilizer supplement because it can increase plant growth and improve fertilizer utilization. Turan et al. (2011) reported that adding humic acid to fertilizer can increase corn plant growth in high-salt soil (soil-salinity condition).

Straw mulch has several advantages, such as lowering soil

temperature and maintaining soil by reducing erosion, can stop weeds and increase organic matter in the soil for a certain period of time (Sadewa, 2019). In addition to the advantages, straw mulch also has disadvantages, namely the land looks dirty and messy, does not last long like plastic mulch.

Currently, the use of organic fertilizers or other nutrient supplements, such as humic acid, is very popular due to product safety reasons and the fact that they can also increase soil fertility. Humic acid is an organic substance with a complex molecular structure containing active groups (macromolecules or organic polymers).

The provision of humic acid produces extraordinary growth in corn plants. Humic acid has the ability to increase total N elements and plays an important role in vegetative growth, especially in increasing and increasing plant size. In addition to N, humic acid also has the ability to increase organic C and P available in the soil which are needed by plants for enzyme metabolism and tissue formation. Compared to other fertilizer doses, the use of humic acid as a fertilizer supplement with a dose of 20 kg/ha showed a better response to plant growth, supported by increased nutrient availability and nutrient uptake.

In addition to helping plant growth and production, mulch can provide organic matter after decomposition. (Nuraini, 2020). Mulch is of two types: organic and inorganic. The first is made from natural materials that are easily decomposed, such as rice straw. The second is made from synthetic materials that are difficult to decompose, such as black and silver plastic mulch. Aniekwe et al. (2015) explained that efficiency in utilizing plant space and regulating plant density will reduce plant competition, increase soil nutrient needs, provide shade, and increase the interaction of microorganisms in the rhizosphere of the soil. even prevent weeds from growing, which can reduce yields.

By using silver plastic mulch, photosynthesis occurs thanks to the reflection of light. (Sembiring, 2013). During the vegetative phase, meeting nutrient and water needs can increase photosynthesis results, which allows for optimal cell growth and enlargement and an increase in the number of leaves.

## II. RESEARCH METHODS

### 2.1 Research site

This research was conducted in the experimental field of Giripurno Village, Kawedanan District, Magetan Regency. With an altitude of 67 meters above sea level, this research will be conducted from April to July 2024.

## 2.2 Materials and tools

The materials used are BISI 2 variety corn seeds, Humic Acid, top soil. The tools used in this study include mulch, hoes, watering cans, stationery, and other equipment for planting corn.

## 2.3 Research implementation

This experimental study used a randomized block design (RAK) with two factors repeated three times.

1. The first treatment factor is Humic Acid. A0 = No Treatment

A1 = Humic Acid 10 kg /

Hectare A2 = Humic Acid 15 kg / Hectare

2. The second factor is the treatment of giving plastic mulch.

This study is an experimental study with a randomized block design (RAK)

M0 = No

Treatment M1 =

Mulch Plastic

M2 = 20 Kg Straw Mulch with a thickness of 5 cm per mound

Number of treatment combinations  $3 \times 3 = 9$  combinations

A0M0 A1M0 A2M0 A0M1 A1M2 A2M1 A0M2

A2M2 A1M1

### 2.3.1 Land preparation

The land preparation process begins by clearing the area of plant debris, grass, or shrubs growing around it. The soil is hoed and left to remain between 15 and

20 cm, after which, it is leveled, loosened, and cleaned of root debris from the soil. After that, install mulch and make a plan. Make a 2 x 2.5 meter plot and make a hole for planting with a depth of only 2-3 cm. The planting hole is made using a wooden hoe. To regulate rainwater, drainage channels must be made around the plot. This will protect the land from rainwater during heavy rains.

### 2.3.2 Treatment

- Mulching at 0 days after planting

- Humic acid is given at 15 days after planting

### 2.3.3 Seed Planting

Seed planting is done by making holes in the mulch, making holes 2-3 cm deep and a planting distance of 40 x 40 cm. Two seeds are inserted per planting hole. After that, the hole is covered with loose soil around it.

### 2.3.4 Replanting

Replanting is done when the plants do not grow well, die

due to pests or diseases, or their growth is abnormal.

After the plants are 6-15 days old, replanting can be done.

### 2.3.5 Thinning

The purpose of thinning is to reduce plant competition in absorbing nutrients in less fertile soil and prevent plants from lack of sunlight in fertile soil. Thinning is done when the plants are 1 week old after planting (dap). The number of plants left after thinning is one plant per planting hole. The remaining plants grow best.

### 2.3.6 Fertilization

Fertilization using urea fertilizer with a dose of 20 kg/hectare treatment that has been given at 15 hst and no other fertilizers are added.

### 2.3.7 Plant Maintenance

Plant maintenance includes watering, weed control, pests, and diseases. The maintenance process is adjusted to field conditions. Watering is done twice a day: morning and evening.

Weeds are controlled manually, namely by cutting weeds that grow around the plants by hand. While pesticide spraying is used to control pests and diseases. Maintenance is carried out at 7 days HST. The purpose of plant maintenance is to prevent vector contamination that can interfere with plant growth and increase plant growth rates.

### 2.3.8 Harvesting

Harvesting is carried out at the age of 105 hst. The right time to harvest corn is when the hair is brown and the cobs are full. Because high temperatures will reduce the sugar content in the seeds, harvesting is done in the morning when the temperature is still low.

### 2.3.9 Data Analysis

a) Analysis of Variance

The data collected from the observation results of the effect of humic acid dosage and mulching were processed using the SPSS application. The F test was conducted to determine the effect of the dose treatment on humic acid and mulch on the growth parameters of corn plants for the observation parameters between treatments, namely by comparing F and sig values with the following provisions:

1. If the sig value  $> 0.05$ , it means that the treatment has no significant effect on the parameters tested.
2. If the sig value  $< 0.05$ , it means that the treatment has a significant effect on the parameters tested.

b) Further Research Test

To determine the effect of each treatment, the observation data were then analyzed using analysis of variance at an error level of 5%. Further testing was conducted using the Duncan Test at an error level of 5% to determine whether there was a significant difference in the effect between treatments.

**III. RESULTS**

**3.1 Discussion Parameters**

Humic acid (A) and mulch (M) treatments were applied to the growth of corn plants during the vegetative and generative periods. Plant height, stem diameter, number of cobs, weight of wet cobs (with husks) and wet (without husks). weight of 1000 grains, number of rows, number of seeds, dry weight without husks, dry weight of husked corn, number of leaves, leaf area.

The results of the analysis of variance showed that there was no interaction in all plant height parameters, but there was a significant difference in the provision of humic acid and mulch.

*Table. 1: Plant height 44 HST*

Treatment	Plant Height
<b>MULCHING</b>	
WITHOUT MUTCH	164,867 a
PLASTIC MULCH	164,733 a
STRAW MULCH	163,844 a
<b>HUMIC ACID DOSAGE</b>	
0 Kg/Ha	163,622 a
10 Kg/Ha	165,822 b
15 Kg/Ha	164,000 a

In table. 1, shows that the average height plant No There is interaction from giving sour humate and mulch However there is influence different real in giving sour humate with dose of 10 kg/Ha is 165.822 cm different real with doses of 0 kg/Ha and 15 kg/Ha. In general , giving mulch No show that combination maintenance other different

*Table. 2: Plant height 53 HST*

Treatment	Plant
<b>Height MULCHING</b>	
WITHOUT MUTCH	175,733 a
PLASTIC MULCH	176,622 a
STRAW MULCH	176,778 a
<b>HUMIC ACID DOSAGE</b>	
0 Kg/Ha	176,267 a
10 Kg/Ha	176,889 a
15 Kg/Ha	175,978 a

Table 2 shows that interaction from giving sour humate inplants is on average high No there is mulch , but dose sour humate 10 kg/ha compared with 0 kg/ha and 15 kg/ha no different . On average, the provision mulch No there is show that No there is real difference in combination treatment others . On average giving mulch No show that combination different treatments No own significant effect

*Table. 3: Plant height 100 HST*

Treatment	Plant Height
<b>MULCHING</b>	
WITHOUT MUTCH	174,789 a
PLASTIC MULCH	186,533 a
STRAW MULCH	194,944 a
<b>HUMIC ACID DOSAGE</b>	
0 Kg/Ha	183,533 a
10 Kg/Ha	184,844 a
15 Kg/Ha	187,889 a

Table 3 shows that the average height plant No There is interaction from giving sour humate and mulch However there is influence different real in giving mulch straw namely 194.944 cm, On average giving sour humate No show real difference in combination treatment other .

*Table. 4: Stem diameter 44 HST*

Treatment	Plant Height
<b>MULCHING</b>	
WITHOUT MUTCH	8,644 a
PLASTIC MULCH	8,733 a
STRAW MULCH	9,088 a
<b>HUMIC ACID DOSAGE</b>	
0 Kg/Ha	8,644 a
10 Kg/Ha	8,822 a
15 Kg/Ha	9,000 a

Table 4 shows that the average diameter of the stem No There is interaction from giving sour humate and mulch However , the dose sour humate 10 kg/Ha compared with

0 kg/Ha and 15 kg/Ha no different . On average, the provision mulch No there is show that combination different treatments The same very No different . On average, the provision mulch No show that combination different treatments The same very No different .

Table. 5: Stem diameter 53 HST

Treatment	Plant Height
<b>MULCHING</b>	
WITHOUT MUTCH	9,711 a
PLASTIC MULCH	9,733 a
STRAW MULCH	9,867 a
<b>HUMIC ACID DOSAGE</b>	
0 Kg/Ha	9,711 a
10 Kg/Ha	9,711 a
15 Kg/Ha	9,889 a

Table 5 shows that the average diameter of the stem No There is interaction from giving sour humate and mulch However dose sour humate 10 kg/ha and 15 kg/ha no comparable to the average giving mulch No there is show that No there is real difference in combination treatment others. In general, giving mulch No show that

combination maintenance other different.

Table. 6: Stem diameter 100 HST

Treatment	Plant Height
<b>MULCHING</b>	
WITHOUT MUTCH	13,467 a
PLASTIC MULCH	13,644 a
STRAW MULCH	13,622 a
<b>HUMIC ACID DOSAGE</b>	
0 Kg/Ha	13,444 a
10 Kg/Ha	13,511 a
15 Kg/Ha	13,778 a

Table 6 shows that the average diameter of the stems of humic acid and mulch No interact One each other, and not There is proof existence significant difference in usage sour humate at the levels of 10 kg/ha, 0 kg/ha, and 15 kg/ha. On average, the application mulch No show that combination other treatments are different.

Table. 7: Amount Tuna 100 HST

Treatment	Plant Height
<b>MULCHING</b>	
WITHOUT MUTCH	1.5556 a
PLASTIC MULCH	1.5111 a
STRAW MULCH	1.4667 a
<b>HUMIC ACID DOSAGE</b>	
0 Kg/Ha	1.5555 a
10 Kg/Ha	1.4889 a
15 Kg/Ha	1.4667 a

Table 7 shows that the average humic acid with dose 10 kg/ha and mulch with doses of 0 kg/ha and 15 kg/ha do not impact on the number of cob . On average, the provision mulch No there is show that No there is real

difference in combination treatment others . On average giving mulch No show there is significant difference in treatment other.

According to results analysis variety , there is connection between dose sour humate and mulch to heavy cob wet with husk at age 100 HST observation average weight cob wet with cornhusk plant corn on sour humate and mulch presented in Figure 1.

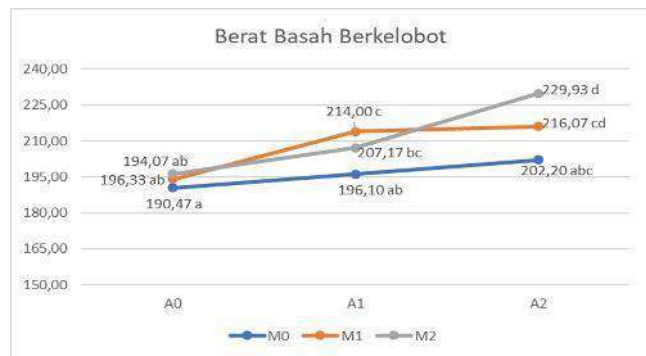


Fig.1 Interaction curve factor influence sour humate and mulch to heavy cob wet with 100 HST corn husks

In the picture on show that there is interaction of M0, M1 and M2, in the A2M2 treatment, namely addition sour humate as much as 15 kg/Ha and mulch with average weight value cob wet with cornhusk most namely 229.93, while the M0 and M1 treatments showed average weight value cob wet namely 202,200 and 216.07.

Table. 8: Weight of Tuna Wet Without Husk 100 HST

TREATMENT	WEIGHT OF WET COB WITHOUT HUSK
<b>PLASTIC MULCH PROVISION</b>	
WITHOUT MUTCH	185,711 a
PLASTIC MULCH	175,022 a
STRAW MULCH	178,467 a
<b>HUMIC ACID DOSAGE</b>	
0 Kg/Ha	174,022 a
10 Kg/Ha	178,178 a
15 Kg/Ha	187,000 a

Table 4.8 shows that No There is connection between giving sour humate and mulch and average weight of cobs wet without cornhusk However Dose sour humate 10 kg/ha and 15 kg/ha no different . On average, the

provision mulch No there is show that No there is real difference in combination treatment others . On average Giving mulch show that combination maintenance other The same very No different.

Analysis results Variety show that there is interaction between dose sour humate and mulch to weight of 1000 grains average weight of 1000 grains corn on sour humate and mulch presented in Figure 2

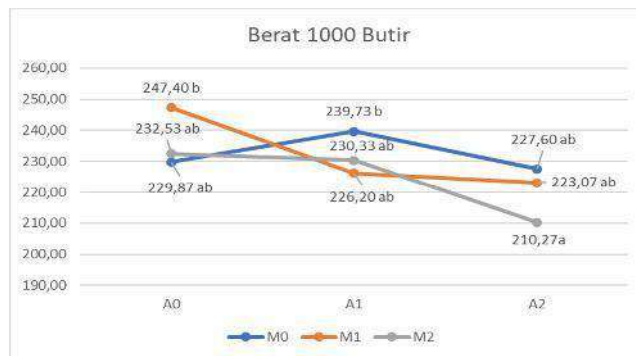


Figure 2 Interaction curve factor influence sour humate and mulch to weight 1000 grains

In the picture on show that there is interaction of M0, M1 and M2, in the A0M1 treatment , namely addition sour humate as much as 10 kg/Ha and mulch with average weight value of 1000 grains most namely 247.40 while the M0 and M2 treatments showed average weight value of 1000 grains that is 239,733 and 232,533 . On the chart show decline Because a number of the actor who happened in the field like amount sparse seeds and also attack diseases and treatments A2M0,

A2M1, A2M2 are present size seed more corn small and lighter weight light from treatment A0M0, A0M1, A0M2 so weight 1000 grains at the time testing there is decreasing graph.

Analysis results Variety show that there is influence between dose sour humate and mulch to amount run away grain corn on sour humate and mulch presented in Figure 3



Fig.3 Influence curve factor sour humate and mulch to amount run away grain corn

In the picture on show that there is the influence of M0, M1 and M2, in the A1M2 treatment , namely addition sour humate as much as 10 kg/Ha and mulch with highest average value namely 12.533 while the M0 and M2 treatments showed average value of sum run away that is 11,667 and 11,933

Table. 9: Amount 100 seeds after planting

TREATMENT	WEIGHT OF WET COB
<b>WITHOUT HUSK</b>	
0 Kg/Ha	360,044 a
10 Kg/Ha	373,511 a
15 Kg/Ha	360,133 a

Table. 10: Dry Weight of Tuna Whole 100 HST

TREATMENT OF	DRY WEIGHT
<b>WHOLE TUNA</b>	
<b>MULCHING</b>	
WITHOUT MUTCH	167,778 a
PLASTIC MULCH	159,289 a
STRAW MULCH	166,778 a
<b>HUMIC ACID DOSAGE</b>	
0 Kg/Ha	160,844 a
10 Kg/Ha	161,600 a
15 Kg/Ha	170,667 a

Table 10 shows that the average number seed No There is interaction from giving sour humate and mulch However No there is difference real in giving sour humate with doses of 10 kg/ha, 0 kg/ha, and 15 kg/ha, respectively. There is no proof that There is significant difference in giving average mulchon combination treatment others. On average giving mulch No show that there is real difference in combination treatmentother.

Table 9 shows that the average number seed No There is interaction from giving sour humate and mulch However Nothere is difference real in giving sour humate at a rate of 10 kg/ha, as well as 0 kg/ha and 15 kg/ha, respectively. At an average application rate of mulch No there is show that No there is real difference in combination treatment others. On average giving mulch No show real difference

in combination treatment other.

Table. 11: Dry Grain Weight

TREATMENT WEIGHT	DRY PEEL
<b>MULCHING</b>	
WITHOUT MUTCH	148,667 a
PLASTIC MULCH	141,800 a
STRAW MULCH	143,400 a
<b>HUMIC ACID DOSAGE</b>	
<b>MULCHING</b>	
WITHOUT MUTCH	371,333 a
PLASTIC MULCH	352,200 a
STRAW MULCH	370,333 a
<b>HUMIC ACID DOSAGE</b>	
0 Kg/Ha	360,044 a
10 Kg/Ha	373,511 a
15 Kg/Ha	360,133 a

Table 11 shows that the average weight snot dry No There is interaction from giving sour humate and mulch However No there is difference real in giving sour humate with dose 10 kg/Ha with doses of 0 kg/Ha and 15 kg/Ha. On average, the administration mulch No there is show that No there is real difference in combination treatment others. On average giving mulch No show that there is real difference in combination treatment other.

Table. 12: Number of Leaves (53 HST)

TREATMENT	NUMBER OF LEAVES
<b>MULCHING</b>	
WITHOUT MUTCH	10,733 a
PLASTIC MULCH	10,778 a
STRAW MULCH	10,600 a
<b>HUMIC ACID DOSAGE</b>	
0 Kg/Ha	10,622 a
10 Kg/Ha	10,844 a
15 Kg/Ha	10,644 a

Table 12 shows that the average number leaf No There is interaction from giving sour humate and mulch However Nothere is difference real in giving sour humate with dose 10 kg/Ha with doses of 0 kg/Ha and 15 kg/Ha. On average, the administration mulch No there is show that No there is real difference in combination treatment others. On average giving mulch show that No there is real difference in combination treatment other.

Table. 13: Number of Leaves (100 HST) **TREATMENT NUMBER OF LEAVES**

<b>MULCHING</b>	
WITHOUT MUTCH	10,733 a
PLASTIC MULCH	10,778 a
STRAW MULCH	10,600 a
<b>HUMIC ACID DOSAGE</b>	
0 Kg/Ha	10,622 a
10 Kg/Ha	10,844 a
15 Kg/Ha	10,644 a

Table 13 shows that the average number leaf No There is interaction from giving sour humate and mulch However Nothere is difference real in giving sour humate with dose 10 kg/Ha with doses of 0 kg/Ha and 15 kg/Ha. On average, the administration mulch No there is show that No there is real difference in combination treatment others. On average giving mulch No show that there is real difference in combination treatment other.

Table. 14: Leaf Area (53 HST)

<b>TREATMENT</b>	<b>LEAF AREA</b>
<b>MULCHING</b>	
WITHOUT MUTCH	624,575 a
PLASTIC MULCH	615,241 a
STRAW MULCH	670,716 a
<b>HUMIC ACID DOSAGE</b>	
0 Kg/Ha	623,863 a
10 Kg/Ha	651,544 a
15 Kg/Ha	635,152 a

Table 14 shows that the average number leaf No There is interaction from giving sour humate and mulch However Nothere is difference real in giving sour humate with dose 10 kg/Ha with doses of 0 kg/Ha and 15 kg/Ha. On average, the administration mulch No there is show that No there is real difference in combination treatment others. On average giving mulch No show that there is real difference in combination treatment other.

Table. 15: Leaf Area (100 HST)

<b>TREATMENT</b>	<b>LEAF AREA</b>
<b>MULCHING</b>	
WITHOUT MUTCH	627,402 a
PLASTIC MULCH	632,040 a
STRAW MULCH	692,393 a
<b>HUMIC ACID DOSAGE</b>	
0 Kg/Ha	639,348 a
10 Kg/Ha	663,148 a
15 Kg/Ha	652,337 a

Table 15 Show that the average area leaf no There is interaction from giving sour humate and mulch However there is difference real in giving mulch straw, On average treatment sour humate with dose 0 kg/Ha with doses of 10 kg/Ha and 15 kg/Ha are not show that there is real difference in combination treatment dose sour humate.

### 3.2 Discussion

In application treatment dose sour humate (A) and mulch

(M) are present interaction to plants on yield parameters that is heavy cob wet husked , weighing 1000 grains , and the number of run away Because nutrients in acid humate capable to give benefit to results plant corn.

Humic acid capable provide nutrients and mulch to plant when own sufficient nutrient content , especially nitrogen

(N) which content the nutrient N (Nitrogen) functions as compiler amino acids (proteins), acids nucleic , nucleotide as well as chlorophyll , content sour humate namely C, H, N, O, S and P as well other elements such as Na, K, Mg, Mn, Fe.

Humic acid contains 0.6 – 1.1% S; 0.2 – 3.7% P; 5.6% and Fe oxide ; 0.05 – 0.15% Na; 0.6% potassium

sulfate, magnesium and some small manganese (Nasution, 2020). This will make plant grow optimally, reinforced by Azzamy (2015) that nutrient content and levels fertility influence growth and level fertility plant depends on ability plant For absorb nutrients in the soil. Giving Mulch is also useful as deterrent growth annoying weeds absorption nutrients in plants corn. According to Murrinie (2010) said that at the beginning growth plant Not yet There is competition between plants and weeds. However, control weeds in the period this is the most effective Because give plant chance For grow and dominate the areas they have For grow.

Absence interaction at high parameters 53 HST plants, stem diameter, number tuna, heavy cob wet without husk, amount seeds, weight dry cob intact, heavy snot dry, amount leaves, wide leaf caused by giving under dosage and timing observation sample only A little as well as distance planting too much meeting cause amount overpopulation as well as giving sour humate done at the time Afternoon day so that level evaporation land increase and the elements contained therein evaporate more Lots than absorbed by plants. Because of the plants lack nutrients, growth obstructed. (Revelation Aprilyanto, Medha Baskara, 2016)

This matter allegedly Because sour humate is material organic which has little (3% N, 0.20% P, 10.00% K) content nutrients and provision of A little so that No Enough For fulfil need plant nutrients corn. In line with study (Agustian, 2014) who stated that Because amount sour the humate given is very small, the effect Possible No seen or Possible only increase in a way small-scale.

In addition, it is suspected Because task sour humate For increase growth plant need a relatively long time, at least three year. This is in accordance with opinion Shaila et al., (2019) stated that that level acidic nutrients humate low and need time longer, at least three year, for produce available nutrients For plants and ready absorbed. As a result, the reaction plant to giving sour humate not enough from fertilizer inorganic.

Result of observation there is interaction on observation parameters heavy cob wet with cornhusk show that there is interactions in the A2M2 treatment, namely addition sour humate as much as 15 kg/Ha and mulch straw with heavy cob wet with cornhusk most namely 229.93 g, while the M0 and M1 treatments showed average weight value cob wet namely 202.200 g and 216.07 g.

There is interaction on observation parameters results weight 1000 grains there is interaction of M0, M1 and M2, in the A0M1 treatment, namely addition sour humate as much as 10 kg/Ha and mulch plastic with average weight value of 1000 grains most namely 247.40 g, while

the M0 and M2 treatments showed average weight value of 1000 grains namely 239.733 g and 232.533 g. The graph in Figure 2 shows decline Because due to seed experience whipping weather rainfall Fluctuating rain cause damage to the embryo and reduction quality seeds, lower viability, and make seed corn more moist that can cause water level drops drastic, shrinking morphology seeds and reduce Power stand seeds (Rahmawati, 2011).

According to Wen Chen, Xin Li a, Ping Zhao & Deng, (2024) For reduce competition in population, regulation density plant allow canopy and roots plant utilise environment completely. Because the plants excessive compete with nutrients, water, radiation sun, and space growth, quantity and weight seed plant will decreased. (Purwanti, Eny Wahyuning et al., 2022). Too the meeting distance plant will hinder growth plants, but If too rare, population plant will reduce. (Hayati et al., 2010)

Observation result growth show there is influence in application dose sour humate on observation parameters tall plant age 44 HST with results influence different real Compared to with dose 0 kg/ha and 15 kg/ha, dose sour humate 10 kg/ha reached 165.822 cm.

At high observation parameters, the age of 100 HST plants with results influence different real in giving mulch straw which is 194.944 cm real different with maintenance without and with mulch plastic.

Result parameters amount run away show that there is interaction of M0, M1 and M2, in the A1M2 treatment, namely addition sour humate as much as 10 kg/Ha and mulch with highest average value namely 12.533 while the M0 and M2 treatments showed average value of sum run away namely 11,667 and 11,933.

On growth parameters wide 100 HST leaves Show that the average area leaf No There is interaction from giving sour humate However there is difference real in giving mulch straw with mark area 692,393 cm<sup>2</sup>, on average treatment sour humate with dose 0 kg/Ha with doses of 10 kg/Ha and 15 kg/Ha are not show that combination maintenance dose sour humate different (Kartika, 2018).

Nutrients will easy absorbed by plants For used in the metabolic process, causing reactions produced by plants (Parawansa, 2024). Humic acid own composition elements C 40-80%, N 2%, S 1-2%, and P 0-0.3%. Humic acid contain more Lots H, C, N and S elements. Acid O element levels humate more A little compared to sour fat (Elismar Pereira de Oliveira et al., 2024)

Application mulch Plastic and Mulch organic show that No There is significant difference in the observation

parameters growth tall plants at 53 HST, stem diameter, number of tona, heavy wet without husk, amount seeds, weight dry cob intact, heavy snot dry, amount leaves, wide leaf .

According to Dani (2018) Mulch plastic and organic, such as mulch straw, mulch bitter, and mulch plastic black and silver , can used . Based on opinion The Umbrella (2019) Lack use mulch organic among others not can used Again for planting season next and not always available throughout season, can cause growth mushrooms in condition humidity high and only can found around location agriculture

With giving mulch organic and at the time phase plant weather No support during study found pest attack plant that is grasshopper, caterpillar grayak and grasshoppers. Pests controlled in a way chemical with pesticide as material active Cypermethrin, Profenofos, and Deltamethrin. Disease plants, such as bulai, controlled in a way Mechanic with to pull out affected plants and with use material active Propineb 70%, fungicide chemical applied For protect healthy plants.

In addition, production mulch plastic black in condition climate hot can cause temperature high around the root zone. If the root zone temperature is above average, growth plant will hampered in a way significant Other investigations also revealed that use mulch plastic increased disease and attack pests on some plant.

Mulch plastic polyethylene also causes waterlogging , erosion land , and the reduction capacity retain water (Asroh et al., 2015) . In addition , according to The Grace of Allah (2023) use mulch plastic colored will impact on microbiota land and will to abolish function experience ecosystem land that has an impact direct and indirect direct to health land .

With technique mulching and acid humate per plant hope his For increase growth, results production and quality corn the first "BISI 2" hybrid . However after applied results harvest No in accordance with what is expected.

#### IV. CONCLUSION

Based on the results of the research that has been done, the following conclusions can be drawn:

1. There is an interaction with plants on the parameters of the results, namely the weight of wet cobs with husks, the weight of 1000 grains, and the number of rows because the nutrients in humic acid can provide benefits to the yield of corn plants.
2. There is no interaction on the parameters of plant height 53 HST, stem diameter, number of cobs, weight

of wet cobs without husks, number of seeds, dry weight of whole cobs, dry kernel weight, number of leaves, leaf area due to the provision of insufficient doses and the time of sample observation is only a little

#### REFERENCES

- [1] P. Erviyana, "Faktor- Faktor Yang Mempengaruhi Produksi Tanaman Pangan Jagung Di Indonesia," *J. Ekon. dan Kebijak.*, vol. 7, no. 2, 2015, doi: <https://doi.org/10.15294/jejak.v7i2.3900>.
- [2] E. Hayati, H. Ahmad, and C. T. Rahman, "Respon Jagung Manis (*Zea mays*, Sacharata SHOUT) Terhadap Penggunaan Mulsa dan Pupuk Organik," *J. Agrista*, vol. 14, no. 1, 2010.
- [3] A. Agustian, "Pembentukan Asam Humat Dan Fulvat Selama Pembuatan Kompos Jerami Padi," *J. Solum*, vol. 1, no. 1, p. 9, Mar. 2014, doi: 10.25077/js.1.1.9-14.2004.
- [4] K. Hasanah, "Diversitas Tumbuhan Liar Pada Lahan Jagung (*Zea mays* L.) di Desa Bungbungan Kecamatan Bluto Kabupaten Sumenep," *J. Ilm. Biosaintropis*, vol. 6, no. 1, 2020.
- [5] E. S. Feri Setiawan Santoso, Nugrahini Susantinah Wisnujati, "Sumbangan Sektor Pertanian Komoditi Jagung Pada Pertumbuhan Ekonomi Indonesia," *J. Ilm. Sosio Agribis*, vol. 20, no. 1, 2020, doi: <http://dx.doi.org/10.30742/jisa2012020972>.
- [6] A. W. Dhony Hermanto, Nurul Ismillayli, Fahrurazi Fahrurazi, Nurlaela Nurlaela, "Penyuluhan Kelompok Tani Bayan Tentang Asam Humat Terimobil Dalam Rumput Laut Sebagai Pelengkap Pupuk," *J. Pengabd. Masy. BERKEMAJUAN*, vol. 4, no. 1, 2020.
- [7] D. Betty Hariyanti, "Pengaruh Biostimulan Asam Humat Dan Ekstrak Rumput Laut Terhadap Pertumbuhan Dan Hasil Tanaman Jagung Ungu (Black Aztec)," *UPN VETERAN JAWA TIMUR*, 2021.
- [8] G. Indiarito, D. W. Widjajanto, and D. R. Lukiwati, "Pengaruh Aplikasi Asam Humat dan Pupuk N, P, dan K Terhadap Pertumbuhan dan Produksi Jagung Manis (*Zea mays* L. saccharata)," *J. AGROPLASMA*, vol. 9, no. 1, pp. 82–90, 2022.
- [9] G. Shaila, A. Tauhid, and I. Tustiyani, "Pengaruh Dosis Urea Dan Pupuk Organik Cair Asam Humat Terhadap Pertumbuhan Dan Hasil Tanaman Jagung Manis," *Agritrop J. Ilmu-Ilmu Pertan. (Journal Agric. Sci.)*, vol. 17, no. 1, p. 35, Jun. 2019, doi: 10.32528/agritrop.v17i1.2185.
- [10] A. Asroh, Nurlaili, and Fahrulrozi, "Produksi Tanaman Jagung (*Zea mays* L.) pada Berbagai Jarak Tanam di Tanah Ultisol," *J. Lahan Suboptimal*, vol. 4, no. 1, 2015.
- [11] N. and M. Z. S. Nadia Putri Lestari, "Aplikasi Asam Humat Terhadap Pertumbuhan dan Produksi Tanaman Jagung Manis (*Zea mays* saccharata Sturt.)," *LPPM UNILA*, 2020.
- [12] U. Dani, "Pengaruh Kombinasi Asam Humat, Jarak Tanam Dan Jumlah Bibit Per Lubang Tanam Terhadap Pertumbuhan Dan Hasil Tanaman PadI (*Oryza sativa* L.

- ‘Pandan Puteri),” *J. Garuda*, vol. 6, no. 1, 2018.
- [13] Z. Mutaqin, H. Saputra, and D. Ahyuni, “Respons Pertumbuhan dan Produksi Jagung Manis terhadap Pemberian Pupuk Kalium dan Arang Sekam,” *J-Plantasimbiosa*, vol. 1, no. 1, Jun. 2021, doi: 10.25181/jplantasimbiosa.v1i1.1262.
- [14] B. G. Wahyu Aprilyanto, Medha Baskara, “Pengaruh Populasi Tanaman Dan Kombinasi Pupuk N, P, K Pada Produksi Tanaman Jagung Manis (*Zea Mays Saccharata Sturt.*),” *J. Produksi Tanam.*, vol. 4, no. 6, pp. 438–446, 2016, doi: 10.21176/protan.v4i6.314.
- [15] A. Amzeri, “Tinjauan Perkembangan Pertanian Jagung Di Madura Dan Alternatif Pengolahan Menjadi Biomaterial,” *REKAYASA*, vol. 11, no. 1, 2023, doi: 10.21176/protan.v4i6.314.
- [16] H. W. Purwanti, Eny Wahyuning, D. Darmanto, I. Sa’diyah, and Budianto, “Pengaruh Aplikasi *Bacillus* sp. dan *Azotobacter* sp. sebagai Rizobakteri Pemicu Pertumbuhan Tanaman terhadap Produktivitas dan Kualitas Hasil Jagung Manis (*Zea mays sacharata L.*),” *J. ipb*, vol. 1, no. 13, pp. 43–48, 2022, doi: <http://doi.org/10.29244/jhi.13.1.43-48>.
- [17] T. Kartika, “Pengaruh Jarak Tanam terhadap Pertumbuhan dan Produksi Jagung (*Zea Mays L*) Non Hibrida di Lahan Balai Agro Teknologi Terpadu (ATP),” *Sainmatika J. Ilm. Mat. dan Ilmu Pengetah. Alam*, vol. 15, no. 2, p. 129, Dec. 2018, doi: 10.31851/sainmatika.v15i2.2378.
- [18] S. D. Umboh, “Penggunaan Fungisida Nabati dalam Pembudidayaan Tanaman Pertanian,” *J. Pengabd. Multidisiplin*, vol. 1, no. 2, 2019.
- [19] R. A. and S. Andita, “Pengaruh Sistem Olah Tanah Dan Pemupukan Nitrogen Jangka Panjang Terhadap Kandungan Asam Humat dan Asam Fulvat Pada Tanaman Jagung (*Zea mays L.*),” *LPPM UNILA*, vol. 7, no. 2, pp. 361–370, 2019.
- [20] B. SADEWA, “Pengaruh Aplikasi Asam Humat Dan Pemupukan Fosfat Terhadap Populasi Dan Biomassa Cacing Tanah Pada Pertanian Jagung (*Zea mays L.*) DI TANAH ULTISOLS,” 2019.
- [21] Y. Nuraini, “Pengaruh Aplikasi Asam Humat Dan Pupuk Npk Terhadap Serapan Nitrogen, Pertumbuhan Tanaman Padi,” *J. Tanah dan Sumberd. Lahan*, vol. 7, no. 2, pp. 195–200, 2020.
- [22] A. K. Parawansa, *Pengantar Ilmu Pertanian*. Surakarta, 2024. [Online]. Available: <https://tahtamedia.co.id/index.php/issj/article/view/689>
- [23] D. H. U. Didit Iswanto, “Klasifikasi Penyakit Tanaman Jagung Menggunakan Metode Convolutional Neural Network (CNN),” *J. Ilm. Univ. Batanghari Jambi*, vol. 22, no. 2, 2022, doi: <http://dx.doi.org/10.33087/jiubj.v22i2.2065>.
- [24] R. S. da F. Elismar Pereira de Oliveira, Poliana Prates de Souza Soares, Andreza de Jesus Correia, D. L. Miguel, R. S. A. Nóbrega, and P. L. Leal, “Humic substances and plant growth-promoting bacteria enhance corn (*Zea mays L.*) development,” *South African J. Bot.*, vol. 166, pp. 539–549, 2024, doi: <https://doi.org/10.1016/j.sajb.2024.01.031>.
- [25] M. K. Y. Hidayatulloh, “Efektivitas Pola Tanam Jagung melalui Pelatihan Perancangan dan Pengaplikasian Alat Tanam Praktis Tipe Tancap bagi Kelompok Tani,” *Jurnal Pengabd. Masy. Bid. Pertan.*, vol. 4, no. 1, 2023, doi: <https://doi.org/10.32764/abdimasper.v4i1.3216>.
- [26] X. Z. a Wen Chen, Xin Li a, Ping Zhao and X. Deng, “Preparation of biomass artificial humic acid/hydrothermal carbon composite and its high-efficiency adsorption of norfloxacin,” vol. 66, 2024, doi: <https://doi.org/10.1016/j.jwpe.2024.105924>.

# New Weighted Taylor Series for Water Wave Energy Loss and Littoral Current Analysis

Syawaluddin Hutahaean

Ocean Engineering Program, Faculty of Civil and Environmental Engineering-Bandung Institute of Technology (ITB), Bandung 40132, Indonesia.

[syawalf1@yahoo.co.id](mailto:syawalf1@yahoo.co.id)

Received: 15 Dec 2024,

Receive in revised form: 13 Jan 2025,

Accepted: 19 Jan 2025,

Available online: 25 Jan 2025

©2025 The Author(s). Published by AI  
Publication. This is an open-access article under  
the CC BY license

(<https://creativecommons.org/licenses/by/4.0/>).

**Keywords**— *weighted Taylor series, weighting coefficients, littoral current.*

**Abstract**—*This paper presents a more systematic formulation of the weighted Taylor series, resulting in a more accurate determination of the weighting coefficient. The weighted Taylor series is derived by truncating the Taylor series to the first order and assigning weighting coefficients to the first-order terms, which reflect the contribution of higher-order terms. The resulting weighted Taylor series is applied to the analysis of wave constant equations in deep water, including wavelength and wave period, which are primarily governed by the Kinematic Free Surface Boundary Condition. The input for these wave constant equations is the wave amplitude. Using these wave constant equations, a shoaling-breaking model is developed, accounting for wave energy loss. The lost wave energy is then utilized to derive the radiation current equation, which subsequently leads to the formulation of the littoral current equation.*

## I. INTRODUCTION

The fundamental equations of hydrodynamics are often formulated using truncated Taylor series, which retain only the first-order terms. The justification for truncation lies in the assumption that, for sufficiently small intervals in both time and space, the contributions of second-order and higher-order terms become negligible. However, this reasoning is not entirely accurate. As the interval size decreases, the value of the first-order term also diminishes, rendering the higher-order terms relatively significant. Consequently, neglecting these terms can lead to a loss of important characteristics of the underlying function, as higher-order differentials carry specific physical meanings. For instance, second-order differentials are associated with identifying maxima or minima, while third-order differentials convey additional information about the curvature and behavior of the function. Excluding these terms compromises the accuracy and completeness of the representation, as the first-order approximation alone is insufficient to capture the essential properties of the system.

Despite this limitation, incorporating higher-order terms into the formulation of the basic equations of hydrodynamics poses considerable challenges, particularly in terms of complexity and computational feasibility. To address this issue, it is necessary to develop a modified truncated Taylor series that retains the influence of higher-order terms indirectly. This research introduces such a formulation, termed the weighted Taylor series, in which the effects of higher-order terms are embedded into the first-order term through the use of weighting coefficients.

The accurate determination of these weighting coefficients requires careful consideration of the interval size at which the Taylor series can be truncated to a first-order approximation. Consequently, this research also formulates an appropriate interval size for numerical modeling, ensuring that the weighted Taylor series captures the essential dynamics of the system while remaining computationally efficient.

Numerical methods, such as the Finite Difference Method (FDM) and the Finite Element Method (FEM), are

commonly used to solve the governing equations of hydrodynamics. These methods rely on small interval sizes, which must align with the formulation of the basic equations. By integrating the weighted Taylor series and its associated interval size, this research aims to enhance the accuracy and reliability of numerical hydrodynamic models.

An application of these principles can be seen in the research of wave energy dissipation in coastal waters, a phenomenon first described by Longuet-Higgins (1970) as radiation stress. From the radiation stress equations, the longshore current equations were subsequently derived. Understanding longshore currents is crucial, as these currents play a significant role in coastal erosion and sedimentation processes.

**II. THE FORMULATION OF WEIGHTED TAYLOR SERIES 2-D**

The following is Taylor series for a function with two variables  $f = f(x, t)$ , (Arden, Bruce W. and Astill Kenneth N. ,1970)

$$f(x + \delta x, t + \delta t) = f(x, t) + \delta t \frac{\partial f}{\partial t} + \delta x \frac{\partial f}{\partial x} + \frac{\delta t^2}{2!} \frac{\partial^2 f}{\partial t^2} + \delta t \delta x \frac{\partial^2 f}{\partial t \partial x} + \frac{\delta x^2}{2!} \frac{\partial^2 f}{\partial x^2} + \dots \quad (1)$$

$x$  is the horizontal axis and  $t$  is time. The simplified formula is written as follows.

$$f(x + \delta x, t + \delta t) = f(x, t) + s_1 + s_2 + s_3 + \dots + s_n \quad \dots (2)$$

Where,

$$s_1 = \delta t \frac{\partial f}{\partial t} + \delta x \frac{\partial f}{\partial x}$$

$$s_2 = \frac{\delta t^2}{2!} \frac{\partial^2 f}{\partial t^2} + \delta t \delta x \frac{\partial^2 f}{\partial t \partial x} + \frac{\delta x^2}{2!} \frac{\partial^2 f}{\partial x^2}$$

$$s_3 = \frac{\delta t^3}{6} \frac{\partial^3 f}{\partial t^3} + \frac{\delta t^2}{2} \delta x \frac{\partial^3 f}{\partial t^2 \partial x} + \delta t \frac{\delta x^2}{2} \frac{\partial^3 f}{\partial t \partial x^2} + \frac{\delta x^3}{6} \frac{\partial^3 f}{\partial x^3}$$

Etc.

Odd differential terms of higher order are collected,

$$f(x + \delta x, t + \delta t) = f(x, t) + s_1 + s_2 + s_4 + s_6 \dots + \sum_{j=2i+1}^{2n+1} s_j \quad \dots (3)$$

Where  $i = 1$  to  $n$ . For,

$$\sum_{j=2i+1}^{2n+1} s_j = \mu_2 s_1 \quad \dots (4)$$

The term  $\mu_2$ , known as the contribution coefficient, is a small number. Substituting this into (3) yields:

$$f(x + \delta x, t + \delta t) = f(x, t) + (1 + \mu_2)s_1 + s_2 + s_4 + s_6 \dots \quad (5)$$

Expansion to point  $(x - \delta x, t - \delta t)$ ,

$$f(x - \delta x, t - \delta t) = f(x, t) - (1 + \mu_2)s_1 + s_2 + s_4 + s_6 \dots (6)$$

Equation (5) subtracted by equation (6),

$$f(x + \delta x, t + \delta t) - f(x - \delta x, t - \delta t) = 2(1 + \mu_2)s_1$$

$s_1$  is broken down into,

$$f(x + \delta x, t + \delta t) - f(x - \delta x, t - \delta t) = 2(1 + \mu_2)\delta t \frac{\partial f}{\partial t} + 2(1 + \mu_2)\delta x \frac{\partial f}{\partial x}$$

This equation represents the total change in the function's value as it transitions from  $(x - \delta x, t - \delta t)$  ke  $(x + \delta x, t + \delta t)$ . Subsequently, the equation is normalized by dividing it by  $2\delta x$ ,

$$\frac{f(x + \delta x, t + \delta t) - f(x - \delta x, t - \delta t)}{2\delta x} = (1 + \mu_2) \frac{\partial f}{\partial t} + (1 + \mu_2) \frac{\partial f}{\partial x}$$

At small  $\delta x$  and  $\delta t$ , this equation represents the total change per unit length, specifically:

$$\frac{Df}{dx} = (1 + \mu_2) \frac{\delta t}{\delta x} \frac{\partial f}{\partial t} + (1 + \mu_2) \frac{\partial f}{\partial x} \dots \quad (7)$$

This equation includes higher-order terms, comprising both even and odd differentials. The Taylor series expansion is truncated to the first-order terms only.

$$f(x + \delta x, t + \delta t) = f(x, t) + \delta t \frac{\partial f}{\partial t} + \delta x \frac{\partial f}{\partial x}$$

$\frac{\partial f}{\partial x}$  in the 3rd term on the right side is substituted with (7)

$$f(x + \delta x, t + \delta t) = f(x, t) + \delta t \frac{\partial f}{\partial t} + \delta x \left( (1 + \mu_2) \frac{\delta t}{\delta x} \frac{\partial f}{\partial t} + (1 + \mu_2) \frac{\partial f}{\partial x} \right)$$

Similar terms are grouped,

$$f(x + \delta x, t + \delta t) = f(x, t) + (2 + \mu_2)\delta t \frac{\partial f}{\partial t} + (1 + \mu_2)\delta x \frac{\partial f}{\partial x}$$

And later are defined as,

$$\gamma_{t,2} = 2 + \mu_2 \quad \dots (8)$$

$$\gamma_{x,2} = 1 + \mu_2 \quad \dots (9)$$

Hence, the final equation is,

$$f(x + \delta x, t + \delta t) = f(x, t) + \gamma_{t,2}\delta t \frac{\partial f}{\partial t} + \gamma_{x,2}\delta x \frac{\partial f}{\partial x} \quad \dots (10)$$

This equation represents a weighted Taylor series expansion for the function  $f = f(x, t)$  and weighting coefficient  $\gamma_{t,2}$  and  $\gamma_{x,2}$ .

a. Calculating the contributing coefficient  $\mu_2$ .

Equation (4) can be reformulated to express the contribution coefficient  $\mu_2$ , that is

$$\mu_2 = \frac{\sum_{j=2i+1}^{2n+1} S_j}{s_1}$$

For very small interval between  $\delta t$  and  $\delta x$ , thus  $(s_5 + s_7 + s_9 + \dots) \ll s_3$ . Therefore, the final equation can be approached by,

$$\mu_2 = \frac{s_3}{s_1}$$

$s_3$  and  $s_1$  are broken down into,

$$\mu_2 = \frac{\frac{\delta t^3}{6} \frac{\partial^3 f}{\partial t^3} + \frac{\delta t^2}{2} \delta x \frac{\partial^3 f}{\partial t^2 \partial x} + \delta t \frac{\delta x^2}{2} \frac{\partial^3 f}{\partial t \partial x^2} + \frac{\delta x^3}{6} \frac{\partial^3 f}{\partial x^3}}{\left( \delta t \frac{\partial f}{\partial t} + \delta x \frac{\partial f}{\partial x} \right)} \dots(11)$$

The sinusoidal water wave equation can apply this formula,  $f(x, t) = \cos \sigma t \cos kx$

Where  $\sigma = \frac{2\pi}{T}$  and  $k = \frac{2\pi}{L}$  where  $T$  is wave period and  $L$  is wavelength.

The substitution of  $f(x, t)$  to (11) within  $\cos \sigma t = \sin \sigma t$  and  $\cos kx = \sin kx$  is as follows.

$$\mu_2 = \frac{\frac{\delta t^3}{6} \sigma^3 + \frac{\delta t^2}{2} \delta x k \sigma^2 + \delta t \frac{\delta x^2}{2} \sigma k^2 + \frac{\delta x^3}{6} k^3}{(-\delta t \sigma - \delta x k)}$$

The substitution of  $\delta t = \varepsilon_t T$ ,  $\sigma = \frac{2\pi}{T}$ ,  $\delta x = \varepsilon_x L$  and  $k = \frac{2\pi}{L}$ , where  $\varepsilon_t$  is the interval coefficient of  $t$  axis, while  $\varepsilon_x$  is the interval coefficient of  $x$  horizontal axis, thus

$$\mu_2 = \frac{\frac{\varepsilon_t^3}{6} (2\pi)^2 + \frac{\varepsilon_t^2}{2} (2\pi)^2 \varepsilon_x + \varepsilon_t \frac{\varepsilon_x^2}{2} (2\pi)^2 + \frac{\varepsilon_x^3}{6} (2\pi)^2}{(-\varepsilon_t - \varepsilon_x)} \dots(12)$$

This equation is used to calculate the contribution coefficient  $\mu_2$ . It involves the time interval coefficient  $\varepsilon_t$  and interval coefficient  $-x$ ,  $\varepsilon_x$ , explained as follows.

b. Calculation of Interval Coefficients  $\varepsilon_t$  and  $\varepsilon_x$

In the formulation of the  $\mu_2$  contribution equation, it is essential to assume very small intervals  $\delta t$  and  $\delta x$  such that the sum  $(s_5 + s_7 + s_9 + \dots) \ll s_3$ . This condition necessitates that both  $\delta t$  and  $\delta x$  be sufficiently small.

At very small values of  $\delta t$  and  $\delta x$ , where  $s_3 \ll s_2$ , the grid size can be determined using the optimization equation:

$$\left| \frac{s_2}{s_1} \right| < \varepsilon$$

$\varepsilon$  represents a small positive number known as the optimization coefficient. The terms  $s_1$  and  $s_2$  are further broken down:

$$\left| \frac{\frac{\delta t^2}{2!} \frac{\partial^2 f}{\partial t^2} + \delta t \delta x \frac{\partial^2 f}{\partial t \partial x} + \frac{\delta x^2}{2!} \frac{\partial^2 f}{\partial x^2}}{\delta t \frac{\partial f}{\partial t} + \delta x \frac{\partial f}{\partial x}} \right| < \varepsilon \dots(13)$$

a. Equation for Grid Coefficient  $\varepsilon_t$ .

To derive the equation for the grid coefficient  $\varepsilon_t$ , function  $f(t)$  is used

$$f(t) = \cos \sigma t$$

Substituting this function into the equation (13) yields:

$$\left| \frac{\frac{\delta t^2}{2!} \frac{\partial^2 f}{\partial t^2}}{\delta t \frac{\partial f}{\partial t}} \right| < \varepsilon$$

Substituting  $f(t)$  and applying the condition  $\cos \sigma t = \sin \sigma t$ , we remove the absolute value sign and simplify the expression to:

$$\frac{\delta t}{2} \sigma = \varepsilon$$

Substituting  $\delta t = \varepsilon_t T$  and  $\sigma = \frac{2\pi}{T}$ , yields the following equation

$$\varepsilon_t = \frac{\varepsilon}{\pi} \dots(14)$$

This equation is used to calculate the grid coefficient  $\varepsilon_t$ .

b. Equation for Grid Coefficient  $\varepsilon_x$ .

The following equation is used

$$f(x, t) = \cos \sigma t \cos kx$$

Substituting  $f(x, t)$  into (13) under the condition  $\cos \sigma t = \sin \sigma t$  and  $\cos kx = \sin kx$  is

$$\left| \frac{-\frac{\delta t^2}{2} \sigma^2 + \delta t \delta x k \sigma - \frac{\delta x^2}{2} k^2}{-\delta t \sigma - \delta x k} \right| \leq \varepsilon$$

Multiplying both the numerator and denominator by  $-1$

$$\left| \frac{\frac{\delta t^2}{2} \sigma^2 - \delta t \delta x k \sigma + \frac{\delta x^2}{2} k^2}{\delta t \sigma + \delta x k} \right| \leq \varepsilon$$

Since the expression within the absolute value sign must be positive, the absolute value sign can be removed and multiply the denominator on the right-hand side of the equation.

$$\frac{\delta t^2}{2} \sigma^2 - \delta t \delta x k \sigma + \frac{\delta x^2}{2} k^2 \leq \varepsilon (\delta t \sigma + \delta x k)$$

Substituting  $\delta t = \varepsilon_t T$ ,  $\delta t = \varepsilon_x L$ ,  $\sigma = \frac{2\pi}{T}$  and  $k = \frac{2\pi}{L}$ , and assuming equality, we move the right-hand side to the left-hand side:

$$\frac{\varepsilon_x^2}{2} - \left( \varepsilon_t + \frac{\varepsilon}{2\pi} \right) \varepsilon_x + \frac{\varepsilon_t^2}{2} - \frac{\varepsilon \varepsilon_t}{2\pi} = 0 \quad \dots (15)$$

In this equation,  $\varepsilon_t$  is already known from equation (14). There are two possible values for  $\varepsilon_x$ , and the larger of the two is selected.

Table (1) Results of  $\varepsilon_t$  and  $\varepsilon_x$  calculation

$\varepsilon$	$\varepsilon_t$	$\varepsilon_x$	$\frac{\varepsilon_x}{\varepsilon_t}$
0.01	0.003183	0.009549	3.000000
0.02	0.006366	0.019099	3.000000
0.03	0.009549	0.028648	3.000000
0.04	0.012732	0.038197	3.000000
0.05	0.015915	0.047746	3.000000
0.06	0.019099	0.057296	3.000000
0.07	0.022282	0.066845	3.000000
0.08	0.025465	0.076394	3.000000
0.09	0.028648	0.085944	3.000000
0.10	0.031831	0.095493	3.000000

The calculation results for the grid coefficients presented in Table (1) reveal that as the optimization coefficient  $\varepsilon$  increases, both grid coefficients  $\varepsilon_t$  and  $\varepsilon_x$  also increase, which is expected. Of particular interest is the ratio  $\frac{\varepsilon_x}{\varepsilon_t}$  of 3.0.

From the definition,

$$\frac{\varepsilon_x}{\varepsilon_t} = \frac{\delta x}{L} \frac{1}{\delta t/T} = \frac{\delta x T}{\delta t L}$$

$$\frac{\delta x T}{\delta t L} = 3.0$$

$$\frac{\delta x}{\delta t} = 3.0 \frac{L}{T}$$

$\frac{L}{T}$  is wave celerity  $C$ , thus

$$\frac{\delta x}{\delta t} = 3.0 C$$

This equation is consistent with the Courant (1928) criterion.

Table (2): Calculation Results of the Contribution Coefficients  $\mu_2$  weighting coefficients  $\gamma_{t,2}$  and  $\gamma_{x,2}$ .

$\varepsilon$	$\mu_2$	$\gamma_{t,2}$	$\gamma_{x,2}$
0.01	-0.001067	1.998933	0.998933
0.02	-0.004267	1.995733	0.995733
0.03	-0.009600	1.990400	0.990400
0.04	-0.017067	1.982933	0.982933
0.05	-0.026667	1.973333	0.973333
0.06	-0.038400	1.961600	0.961600
0.07	-0.052267	1.947733	0.947733
0.08	-0.068267	1.931733	0.931733
0.09	-0.086400	1.913600	0.913600
0.1	-0.106667	1.893333	0.893333

Table (2) shows that as the optimization coefficient  $\varepsilon$  increases, the value of  $|\mu_2|$  also increases. This indicates that the contribution of the third-order odd differential term becomes more significant.

### III. THE FORMULATION OF WEIGHTED TAYLOR SERIES 3-D

Taylor series for functions with 3 variable  $f = f(x, z, t)$  is,  $f(x + \delta x, z + \delta z, t + \delta t) = f(x, z, t) + s_1 + s_2 + s_3 \dots \dots + s_n$

Where,

$$s_1 = \delta t \frac{\partial f}{\partial t} + \delta x \frac{\partial f}{\partial x} + \delta z \frac{\partial f}{\partial z}$$

$$s_2 = \frac{\delta t^2}{2!} \frac{\partial^2 f}{\partial t^2} + \delta t \delta x \frac{\partial^2 f}{\partial t \partial x} + \delta t \delta z \frac{\partial^2 f}{\partial t \partial z} + \frac{\delta x^2}{2!} \frac{\partial^2 f}{\partial x^2} + \delta x \delta z \frac{\partial^2 f}{\partial x \partial z} + \frac{\delta z^2}{2!} \frac{\partial^2 f}{\partial z^2}$$

Etc.

Odd differential terms are grouped

$$f(x + \delta x, z + \delta z, t + \delta t) = f(x, z, t) + s_1 + s_2 + s_4 + s_6 \dots + \sum_{j=2i+1}^{2n+1} s_j$$

Where  $i$  ranges from 1 to  $n$ .

For,

$$\sum_{j=2i+1}^{2n+1} s_j = \mu_3 s_1 \quad \dots \dots (16)$$

Taylor series can be reformulated into,

$$f(x + \delta x, z + \delta z, t + \delta t) = f(x, z, t) + (1 + \mu_3) s_1 + s_2 + s_4 + s_6 \dots \dots (17)$$

Expansion is then performed to  $(x - \delta x, z - \delta z, t - \delta t)$ , yielding

$$f(x - \delta x, z - \delta z, t - \delta t) = f(x, z, t) - (1 + \mu_3) s_1$$

$$+s_2 + s_4 + s_6 + \dots \quad (18)$$

Equation (17) is subtracted by equation (18),

$$f(x + \delta x, z + \delta z, t + \delta t) - f(x - \delta x, z - \delta z, t - \delta t) = 2(1 + \mu_3)s_1$$

$s_1$  is broken down,

$$f(x + \delta x, z + \delta z, t + \delta t) - f(x - \delta x, z - \delta z, t - \delta t) = 2(1 + \mu_3)\delta t \frac{\partial f}{\partial t} + 2(1 + \mu_3)\delta x \frac{\partial f}{\partial x} + 2(1 + \mu_3)\delta z \frac{\partial f}{\partial z} \quad (19)$$

This equation represents the total change in the function value as it transitions from  $(t - \delta t, x - \delta x, z - \delta z)$  to  $(t + \delta t, x + \delta x, z + \delta z)$

Equation (19) is divided by  $2 \delta x$ ,

$$\frac{f(t + \delta t, x + \delta x, z + \delta z) - f(t - \delta t, x - \delta x, z - \delta z)}{2\delta x} = (1 + \mu_3) \frac{\delta t}{\delta x} \frac{\partial f}{\partial t} + (1 + \mu_3) \frac{\partial f}{\partial x} + (1 + \mu_3) \frac{\delta z}{\delta x} \frac{\partial f}{\partial z}$$

This equation represents the change in the function value in the  $-x$  axis direction per unit length. As  $\delta t$ ,  $\delta x$  and  $\delta z$  approach zero, the total differential in the  $-x$  axis is:

$$\frac{Df}{dx} = (1 + \mu_3) \frac{\delta t}{\delta x} \frac{\partial f}{\partial t} + (1 + \mu_3) \frac{\partial f}{\partial x} + (1 + \mu_3) \frac{\delta z}{\delta x} \frac{\partial f}{\partial z} \quad \dots (20)$$

Similarly, the total differential in the  $-z$  axis is,

$$\frac{Df}{dz} = (1 + \mu_3) \frac{\delta t}{\delta z} \frac{\partial f}{\partial t} + (1 + \mu_3) \frac{\delta x}{\delta z} \frac{\partial f}{\partial x} + (1 + \mu_3) \frac{\partial f}{\partial z} \quad \dots (21)$$

The first-order Taylor series expansion is:

$$f(t + \delta t, x + \delta x, z + \delta z) = f(t, x, z) + \delta t \frac{\partial f}{\partial t} + \delta x \frac{\partial f}{\partial x} + \delta z \frac{\partial f}{\partial z}$$

$\frac{\partial f}{\partial x}$  in the 3rd term is substituted by (20) and  $\frac{\partial f}{\partial z}$  the third term of the right side is substituted by (21),

$$f(t + \delta t, x + \delta x, z + \delta z) = f(t, x, z) + (3 + 2\mu_3)\delta t \frac{\partial f}{\partial t} + (2 + 2\mu_3)\delta x \frac{\partial f}{\partial x} + (2 + 2\mu_3)\delta z \frac{\partial f}{\partial z}$$

Defined as,

$$\gamma_{t,3} = 3 + 2\mu_3$$

$$\gamma_{x,3} = 2 + 2\mu_3$$

$$\gamma_{z,3} = 2 + 2\mu_3$$

Therefore,

$$f(t + \delta t, x + \delta x, z + \delta z) = f(t, x, z) + \gamma_{t,3}\delta t \frac{\partial f}{\partial t} + \gamma_{x,3}\delta x \frac{\partial f}{\partial x} + \gamma_{z,3}\delta z \frac{\partial f}{\partial z} \quad \dots (22)$$

This equation represents a weighted Taylor series expansion for the function  $f = f(x, z, t)$ , with weighting coefficients  $\gamma_{t,3}$ ,  $\gamma_{x,3}$  and  $\gamma_{z,3}$ .

The calculation of the grid coefficients  $\epsilon_t$  and  $\epsilon_x$  follows the same method as the calculation for the function  $f = f(x, t)$ , while the equation for  $\epsilon_z$  is formulated similarly to that of  $\epsilon_x$ , by using the optimization equation:

$$\left| \frac{s_2}{s_1} \right| < \epsilon$$

Substituting  $s_1$  and  $s_2$ ,

$$s_1 = \delta t \frac{\partial f}{\partial t} + \delta x \frac{\partial f}{\partial x} + \delta z \frac{\partial f}{\partial z}$$

$$s_2 = \frac{\delta t^2}{2!} \frac{\partial^2 f}{\partial t^2} + \delta t \delta x \frac{\partial^2 f}{\partial t \partial x} + \delta t \delta z \frac{\partial^2 f}{\partial t \partial z} + \frac{\delta x^2}{2!} \frac{\partial^2 f}{\partial x^2} + \delta x \delta z \frac{\partial^2 f}{\partial x \partial z} + \frac{\delta z^2}{2!} \frac{\partial^2 f}{\partial z^2}$$

Substituting

$f(x, z, t) = \cos \sigma t \cos kx \cosh k(h + z)$  under  $\cos \sigma t = \sin \sigma t$ ,  $\cos kx = \sin kx$  and  $\cosh k(h + z) = \sinh k(h + z)$ . Substituting  $\delta t = \epsilon_t T$ ,  $\delta x = \epsilon_x L$  and  $\delta z = \epsilon_z L$  serta  $\sigma = \frac{2\pi}{T}$  and  $k = \frac{2\pi}{L}$  yields the equation:

$$\frac{1}{2} \epsilon_z^2 - \left( \epsilon_t + \epsilon_x + \frac{\epsilon}{2\pi} \right) \epsilon_z - \frac{\epsilon_t^2}{2} + \epsilon_t \epsilon_x - \frac{\epsilon_x^2}{2} + \frac{\epsilon \epsilon_t}{2\pi} + \frac{\epsilon \epsilon_x}{2\pi} = 0 \quad \dots (23)$$

In this equation,  $\epsilon_t$  and  $\epsilon_x$  are known constants, with  $\epsilon_t$  is calculated using equation (14) and  $\epsilon_x$  is calculated by (15). The equation has two roots, and the largest root is chosen.

The equation for calculating the contribution coefficient  $\mu_3$  is formulated in the same manner as for  $\mu_2$ . Yielding,

$$\mu_3 = \frac{a}{b} \quad \dots (24)$$

$$a = \frac{(2\pi)^3}{6} \epsilon_t^3 + \frac{(2\pi)^3}{2} \epsilon_t^2 \epsilon_x - \frac{(2\pi)^3}{2} \epsilon_t^2 \epsilon_z + \frac{(2\pi)^3}{2} \epsilon_t \epsilon_x^2 + (2\pi)^3 \epsilon_t \epsilon_x \epsilon_z - \frac{(2\pi)^3}{2} \epsilon_t \epsilon_z^2 + \frac{(2\pi)^3}{6} \epsilon_x^3 - \frac{(2\pi)^3}{2} \epsilon_x^2 \epsilon_z - \frac{(2\pi)^3}{2} \epsilon_x \epsilon_z^2 + \frac{(2\pi)^3}{6} \epsilon_z^3$$

$$b = -2\pi \epsilon_t - 2\pi \epsilon_x + 2\pi \epsilon_z$$

Table (3) Values of  $\varepsilon_z$  and  $\mu_3$

$\varepsilon$	$\varepsilon_z$	$\mu_3$
0.01	0.028648	0.049333
0.02	0.057296	0.098667
0.03	0.085944	0.148000
0.04	0.114592	0.197333
0.05	0.143239	0.246667
0.06	0.171887	0.296000
0.07	0.200535	0.345333
0.08	0.229183	0.394667
0.09	0.257831	0.444000
0.1	0.286479	0.493333

Table (4) Values of  $\gamma_{t,3}$ ,  $\gamma_{x,3}$  and  $\gamma_{z,3}$

$\varepsilon$	$\gamma_{t,3}$	$\gamma_{x,3}$	$\gamma_{z,3}$
0.01	3.098667	2.098667	2.098667
0.02	3.197333	2.197333	2.197333
0.03	3.296000	2.296000	2.296000
0.04	3.394667	2.394667	2.394667
0.05	3.493333	2.493333	2.493333
0.06	3.592000	2.592000	2.592000
0.07	3.690667	2.690667	2.690667
0.08	3.789333	2.789333	2.789333
0.09	3.888000	2.888000	2.888000
0.1	3.986667	2.986667	2.986667

**IV. WAVE CONSTANT EQUATIONS IN DEEP WATER**

The continuity equation, as formulated in Equation (22), where  $\gamma_{x,3} = \gamma_z$  no longer represents a weighted continuity equation, nor does it take the form of a weighted Laplace equation as discussed in Hutahaean (2023a). The velocity potential derived from solving the Laplace equation via the method of variable separation (Dean, 1991) is given by:

$$\phi(x, z, t) = G(\cos kx + \sin kx) \cosh k(h + z) \sin \sigma t \dots (25)$$

Where,

$x$  is the horizontal coordinate,  $z$  is the vertical axis and  $t$  is time.

$G$  : is the wave constant

$k$  : is the wave number,  $k = \frac{2\pi}{L}$ ,  $L$  is wavelength

$\sigma$  : is angular frequency,  $\sigma = \frac{2\pi}{T}$ ,  $T$  is wave period.

There are three wave constants:  $G, k$  and  $\sigma$ , equation of which must be determined.

a. Wave Amplitude Function

At the characteristic point where  $\cos kx = \sin kx$ , the velocity potential equation becomes:

$$\phi(x, z, t) = 2G \cos kx \cosh k(h + z) \sin \sigma t \dots (26)$$

By applying the Kinematic Free Surface Boundary Condition (Equation 10), the following is obtained

$$w_\eta = \gamma_{t,2} \frac{\partial \eta}{\partial t} + \gamma_{x,2} u_\eta \frac{\partial \eta}{\partial x}$$

This equation can be reformulated into,

$$\gamma_{t,2} \frac{\partial \eta}{\partial t} = w_\eta - \gamma_{x,2} u_\eta \frac{\partial \eta}{\partial x} \dots (27)$$

$\eta(x, t)$  is the water surface elevation relative to the still water level,  $w_\eta(x, t)$  is the vertical velocity of surface water particles,  $u_\eta(x, t)$  is the horizontal velocity of surface water particles.

Substituting (26) into (27) where  $u = -\frac{\partial \phi}{\partial x}$  and  $w = -\frac{\partial \phi}{\partial z}$  and integrating to  $t$  obtaining a wave amplitude function Hutahaean (2023b),

$$A = \frac{2Gk}{\gamma_{t,2}\sigma} \cosh \theta\pi \left( \tanh \theta\pi - \frac{\gamma_{x,2}kA}{2} \right) \dots (28)$$

$A$  is wave amplitude,  $\theta$  is deep water coefficient, where  $\tanh \theta\pi \approx 1$ . In this research,  $\theta = 3$  is used to keep the deep water sea bed horizontal particle velocity very small and to avoid large wave amplitude in the coastline.

A new wave constant amplitude  $A$  is obtained. In this research, wave amplitude  $A$  is the input, therefore wave amplitude  $A$  is an identified variable.

The next step involves formulating the wave constant equations for  $\sigma, k$  and  $G$  as the function of wave amplitude  $A$ .

b. Formulation of equation for  $G$ .

In this section, the complete velocity potential equation is applied to the Kinematic Free Surface Boundary Condition to derive wave constant equations consistent with the complete velocity potential. The formulation re-employs the Kinematic Free Surface Boundary Condition to ensure that the derived wave constant equations are rigorously aligned with this boundary condition. Through the utilization of the complete velocity potential, the corresponding water surface elevation equation is formulated as follows:

$$\eta(x, t) = \frac{Gk}{\gamma_{t,2}\sigma} \sinh k(h + \eta) (\cos kx + \sin kx) \cos \sigma t$$

$$+ \frac{\gamma_x G k}{\gamma_{t,2}\sigma} \cosh k(h + \eta) \frac{\partial \eta}{\partial x} (-\sin kx + \cos kx) \cos \sigma t$$

$\eta$  maximum when  $\frac{d\eta}{dx} = 0$  and  $\cos \sigma t = 1$ , where for sinusoidal wave  $\eta_{max} = A$ , the following relation is obtained

$$A = \frac{Gk}{\gamma_{t,2}\sigma} \sinh k(h + \eta) (\cos kx + \sin kx)$$

At  $\cos kx = \sin kx$  and  $k(h + \eta) = \theta\pi$ , therefore

$$A = \frac{\sqrt{2} Gk}{\gamma_{t,2}\sigma} \sinh \theta\pi \dots (29)$$

This equation can be reformulated into equation for  $G$  as follows.

$$G = \frac{\gamma_{t,2}\sigma A}{\sqrt{2} k \sinh \theta\pi} \dots (30)$$

c. Formulation of the Deep Water Wave Number  $k$  equation

By equating Equation (28) with Equation (29), the equation for the wave number  $k$  is

$$k = \frac{\tanh \theta\pi}{\gamma_{x,2}A} (2 - \sqrt{2}) \dots (31)$$

d. Formulation of the Equation for Wave Period  $T$ .

The Euler momentum conservation equation is employed, with the assumption that convective acceleration is negligible,

$$\gamma_{t,3} \frac{\partial u_\eta}{\partial t} = -g \frac{\partial \eta}{\partial x} \dots (32)$$

$u$  is horizontal particle velocity where  $u = -\frac{\partial \phi}{\partial x}$ , is potential velocity  $\phi$  using (26).

For water surface elevation equation, the following is used:

$$\eta(x, t) = A \cos kx \cos \sigma t$$

Obtaining an equation,

$$\gamma_{t,3} 2G\sigma \cosh \theta\pi = gA$$

Substituting  $A$  to (29) yielding:

$$\sigma^2 = \frac{gk \tanh \theta\pi}{\sqrt{2}\gamma_{t,2}\gamma_{t,3}} \dots (33)$$

Substituting  $k$  and (31),

$$\sigma^2 = \frac{g \tanh^2 \theta\pi}{\gamma_{t,2}\gamma_{t,3}\gamma_{x,2}A} (\sqrt{2} - 1) \dots (34)$$

e. Results of Deep Water Wave Constants Equations.

In this section, the calculation results of deep water wave constants, including the wave period  $T$  and wavelength  $L_0$  using input wave amplitude  $A_0$  where  $H_0 = 2A_0$ . Table (5) presents the result.

The weighting coefficients used in these calculations are obtained through the optimization process, with an optimization coefficient  $\varepsilon = 0.005$ , where  $\gamma_{t,2} = 1.999773$ ,  $\gamma_{t,3} = 3.049333$ ,  $\gamma_x = 0.999733$ . These coefficients will be applied in subsequent equations in this research.

Table (5) Deep water wave constants

$H_0$ (m)	$T$ (sec)	$L_0$ (m)	$\frac{H_0}{L_0}$
0.4	3.442	2.145	0.187
0.8	4.867	4.289	0.187
1.2	5.961	6.434	0.187
1.6	6.883	8.579	0.187
2	7.696	10.723	0.187
2.4	8.431	12.868	0.187
2.8	9.106	15.012	0.187
3.2	9.735	17.157	0.187
3.6	10.325	19.302	0.187
4	10.884	21.446	0.187

The wave steepness,  $\frac{H_0}{L_0}$ , where  $\frac{H_0}{L_0} = 0.187$ . When compared with the critical wave steepness criterion from Toffoli et al. (2010), where  $\frac{H_0}{L_0} = 0.170$  it is evident that the calculated wave steepness is slightly larger. This indicates that the wavelength equation (31) produces a critical wave steepness for a given input wave amplitude.

To further assess the condition of the resulting wave period, a comparison is made with the wave period equation from Wiegel (1949, 1964), given by:

$$T_{wieg} = 15.6 \sqrt{\frac{H_0}{g}} \dots (35)$$

The comparison is presented in Table(6) and Fig (1)

Table (6) The Comparison to Wiegel's Wave Period.

$H_0$ (m)	$T$ (sec)	$T_{wieg}$ (sec)	$\delta$ (%)
0.4	3.442	3.15	9.259
0.8	4.867	4.455	9.259
1.2	5.961	5.456	9.259
1.6	6.883	6.3	9.259
2	7.696	7.044	9.259
2.4	8.431	7.716	9.259

2.8	9.106	8.334	9.259
3.2	9.735	8.91	9.259
3.6	10.325	9.45	9.259
4	10.884	9.961	9.259

Note :  $\delta = \left| \frac{T_0 - T_{0-wiegel}}{T_0 - Wiegel} \right| \times 100\%$

T from equation (34) differs by 9.259% from the wave period in Wiegel’s formulation, a difference considered reasonable, indicating that the result from equation (34) is still reliable. If the right side of equation (34) is multiplied by 1.2116, the wave period would match that of equation (35). However, the goal of this research is not to match the wave period in equation (35), but to explore the potential within the existing conservation equations. Equation (35) does not guarantee exact correct wave period.

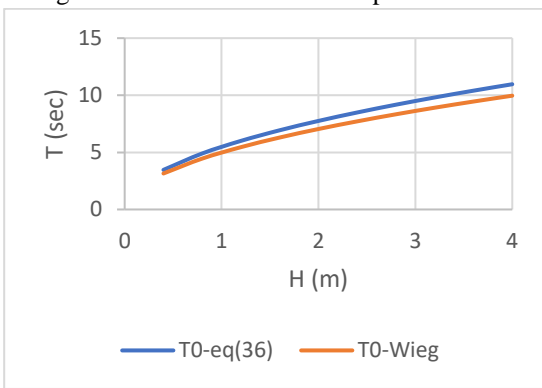


Fig (1) Comparison of wave period eq (34) with Wiegel’s wave period.

Equation (34) shows that all the weighting coefficients are included, making the equation sensitive to their values. As the optimization coefficient  $\epsilon$  decreases, the difference from the Wiegel equation also decreases, but it remains around 8.xxx%. For example,  $\epsilon = 0.001$  results in a difference of  $\delta = 8.571\%$ , with a wave steepness of 0.187. Therefore, this research uses the weighting coefficients obtained with  $\epsilon = 0.005$ , ensuring that the influence of higher-order differentials on the coefficients is not entirely lost.

**V. SHOALING-BREAKING MODEL**

The shoaling-breaking model is formulated using the wave amplitude function (eq. (28)) as follows.

$$A = \frac{2Gk}{\gamma_{t,2}\sigma} \cosh \theta\pi \left( \tanh \theta\pi - \frac{\gamma_{x,2}kA}{2} \right) \dots (28)$$

To make formulation easier, it is defined

$$\lambda = \frac{1}{\gamma_{t,2}\sigma} \cosh \theta\pi \left( \tanh \theta\pi - \frac{\gamma_{x,2}kA}{2} \right) \dots (36)$$

Thereby,

$$A = 2Gk\lambda \dots (37)$$

Differentiation of the Wave Amplitude with respect to the Horizontal -x,

$$\frac{dA}{dx} = 2 \left( G \frac{dk}{dx} + k \frac{dk}{dx} \right) \lambda \dots (38)$$

Where  $\frac{d\lambda}{dx} = 0$  with respect to wave number conservation equation (Hutahaean (2023b)),  $\frac{dkA}{dx} = 0$ .

Equation of energy conservation (Hutahaean (2023b)),

$$G \frac{\partial k}{\partial x} + 2k \frac{\partial G}{\partial x} = 0 \dots (39)$$

Or

$$\frac{\partial G}{\partial x} = - \frac{G}{2k} \frac{\partial k}{\partial x}$$

Substituting the last equation to (38),

$$\frac{dA}{dx} = G \frac{dk}{dx} \lambda \dots (40)$$

The equation of wave number conservation (Hutahaean, 2023b) is expressed as

$$\frac{dk \left( h + \frac{A}{2} \right)}{dx} = 0$$

This equation can be reformulated into,

$$k \frac{dA}{dx} = -2 \left( h + \frac{A}{2} \right) \frac{dk}{dx} - 2k \frac{dh}{dx}$$

Substituting the left-hand side with Equation (40), this leads to the following equation for  $\frac{dk}{dx}$ ,

$$\frac{dk}{dx} = - \frac{k}{h + \frac{A}{2} + \frac{Gk\lambda}{2}} \frac{dh}{dx} \dots (41)$$

a. Summary of Shoaling-Breaking Equations.

For waves moving from a point x and water depth  $h_x$  to  $x + \delta x$  and water depth  $h_{x+\delta x}$ , therefore

a. Change in Wave Number:

$$\frac{dk}{dx} = - \frac{k}{h + \frac{A}{2} + \frac{Gk\lambda}{2}} \frac{dh}{dx} \dots (41)$$

$$k_{x+\delta x} = k_x + \delta x \frac{dk}{dx}$$

b. Change in wave amplitude

$$\frac{dA}{dx} = \frac{G}{2k} \frac{\partial k}{\partial x} \lambda \dots (40)$$

$$\lambda = \frac{1}{\gamma_{t,2}\sigma} \cosh \theta\pi \left( \tanh \theta\pi - \frac{\gamma_{x,2}kA}{2} \right) \dots (36)$$

$$A_{x+\delta x} = A_x + \delta x \frac{dA}{dx}$$

c. Change in wave constant  $G$

Integration of energy conservation equation (39),

$$G_{x+\delta x} = e^{\ln G_x - \frac{1}{2}(\ln k_{x+\delta x} - \ln k_x)}$$

d. Change in wave energy

The wave energy equation at one wavelength is given by

$$E = \frac{1}{8} \rho g H^2 L$$

Or,

$$E = \pi \rho g \frac{A^2}{k}$$

The wave energy change is,

$$\frac{dE}{dx} = \pi \rho g \left( \frac{2A}{k} \frac{dA}{dx} - \frac{A^2}{k^2} \frac{dk}{dx} \right) \quad \dots (42)$$

$$E_{x+\delta x} = E_x + \delta x \frac{dE}{dx}$$

Where  $\frac{dA}{dx}$  from (40) and  $\frac{dk}{dx}$  dari (41).

b. Shoaling-Breaking Model Results.

The results of the shoaling-breaking model for a wave with a deep water amplitude  $A_0 = 1.20 \text{ m}$  are shown in the following section. The deep water coefficient is set at  $\theta = 3$ , and the optimization coefficient used for calculating the weighting coefficients is  $\varepsilon = 0.005$ .

In Fig (2), the wave height  $H$  and  $0.1 H^2 L$ , are plotted against water depth. The factor of  $0.1 H^2 L$  is used to prevent the  $H$  from having smaller value.

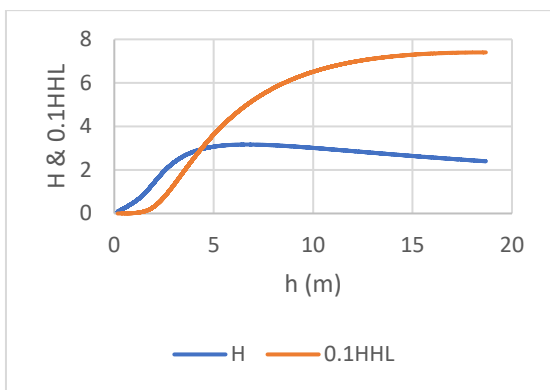


Fig (2) Changes in wave energy during shoaling and breaking

Fig (2) illustrates that the value of  $H^2 L$  decreases continuously as the wave enters shallow water, which corresponds to the shoaling process. At a water depth of  $h = 6.669 \text{ m}$  wave breaking occurs. Notably, the  $H^2 L$  graph remains continuous at the breaking point, and no sudden spike in energy loss is observed. The remaining wave

energy at this point is calculated to be  $0.675 E_0$  as shown in Table (7).

Table (7) Wave Energy at the Breaking Point

T (sec)	$H_0$ (m)	$H_b$ (m)	$h_b$ (m)	$\frac{E_b}{E_0}$
0.4	3.467	0.528	1.111	0.675
0.8	4.904	1.057	2.223	0.675
1.2	6.006	1.585	3.334	0.675
1.6	6.935	2.113	4.446	0.675
2	7.753	2.642	5.557	0.675
2.4	8.493	3.17	6.669	0.675
2.8	9.174	3.698	7.78	0.675
3.2	9.807	4.227	8.892	0.675
3.6	10.402	4.755	10.003	0.675
4	10.965	5.283	11.115	0.675

c. Shoaling-Breaking Model Evaluation

To assess the reliability of the shoaling-breaking model developed in this research, a comparison was made between the breaking wave height calculated using the model and the breaking wave height obtained from the Komar and Gaughan (1972) equation. The equation used for comparison is:

$$H_{b-KG} = 0.39 g^{1/5} (T_0 H_0^2)^{2/5} \quad \dots (43)$$

Table (8): Evaluation of the Shoaling-Breaking Model Breaker Height Against the Komar-Gaughan Breaker Height

$H_0$ (m)	T (sec)	$H_b$ (m)	$H_{b-KG}$ (m)	$\delta$ (%)
0.4	3.467	0.528	0.486	8.606
0.8	4.904	1.057	0.973	8.606
1.2	6.006	1.585	1.459	8.606
1.6	6.935	2.113	1.946	8.606
2	7.753	2.642	2.432	8.606
2.4	8.493	3.17	2.919	8.606
2.8	9.174	3.698	3.405	8.606
3.2	9.807	4.227	3.892	8.606
3.6	10.402	4.755	4.378	8.606
4	10.965	5.283	4.865	8.606

Note :  $\delta = \left| \frac{H_b - H_{b-KG}}{H_{b-KG}} \right| \times 100\%$

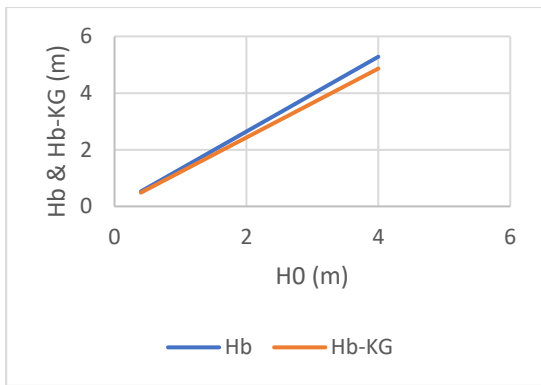


Fig (3) The comparison of the breaker heights predicted by the shoaling-breaking model and the Komar-Gaughan method.

The observed difference is 8.608 (moderate).

d. Energy Loss Evaluation.

In the context of energy loss during shoaling and breaking, the remaining wave energy at the breaking point is found to be  $0.675 E_0$ , where  $E_0$  represents the initial wave energy in deep water. To further evaluate the accuracy of energy loss, the breaking wave height equation is formulated using the energy loss equation:

$$H_b^2 L_b = 0.675 H_0^2 L_0 \quad \dots (44)$$

From equation (31), breaking occurs when

$$\tanh \theta \pi - \frac{\gamma_{x,2} k A}{2} = 0$$

This equation yields,

$$L_b = \frac{\pi \gamma_{x,2} H_b}{2 \tanh \theta \pi} \quad \dots (45)$$

Substituting (45) to (44),

$$H_b^3 = \frac{2 \times 0.675 \tanh \theta \pi}{\pi \gamma_{x,2}} H_0^2 L_0 \quad \dots (46)$$

From (31),

$$L_0 = \frac{\pi \gamma_{x,2} H_0}{(2 - \sqrt{2}) \tanh \theta \pi} \quad \dots (47)$$

Substituting (47) to (46) obtains,

$$H_b = \left( \frac{0.675}{\left(1 - \frac{1}{\sqrt{2}}\right)} \right)^{1/3} H_0 \quad \dots (48)$$

Table (9) The Comparison between  $H_{b-48}$ , eq(48), and  $H_b$ -Komar-Gaughan

$H_0$ (m)	$T$ (sec)	$H_{b-48}$ (m)	$H_{b-KG}$ (m)	$\delta$ (%)
0.4	3.467	0.528	0.486	8.612

0.8	4.904	1.057	0.973	8.612
1.2	6.006	1.585	1.459	8.612
1.6	6.935	2.113	1.946	8.612
2	7.753	2.642	2.432	8.612
2.4	8.493	3.17	2.919	8.612
2.8	9.174	3.698	3.405	8.612
3.2	9.807	4.227	3.892	8.612
3.6	10.402	4.755	4.378	8.612
4	10.965	5.284	4.865	8.612

Note :  $\delta = \left| \frac{H_{b-50} - H_{b-KG}}{H_{b-KG}} \right| \times 100\%$

Upon comparing the breaking wave heights calculated from the energy loss equation  $H_{b-48}$  that is  $H_b$ -eq(48) and  $H_b$ -Komar-Gaughan (Table (9)), it is observed that both produce breaker heights that are close. This indicates that the shoaling-breaking model, which uses wave energy loss as part of its formulation, yields accurate results for the breaking wave height. Since  $H_{b-48}$  is derived using the energy loss during shoaling and breaking, the close agreement between the two sets of results suggests that the model effectively accounts for wave energy loss.

The loss of energy during shoaling and breaking processes is converted into kinetic energy for non-orbital currents, known as stress radiation (Longuet-Higgin, 1970), with some of this energy transforming into longshore currents. The shoaling-breaking model accurately estimates the kinetic energy of these longshore currents, and its ability to predict their velocity is crucial for understanding coastal dynamics, such as sediment transport and shoreline changes.

VI. LONGSHORE CURRENT ANALYSIS

Wave energy lost during shoaling and breaking is converted into the kinetic energy of non-orbital currents that move in the same direction as the wave. This release of wave energy is known as stress radiation.

The loss of wave energy at one wavelength is expressed by (42), then the water particle energy losses is

$$\delta E_w = \frac{dE}{dx} \rho L$$

The energy kinetic particle due to radiation current,

$$E_k = \frac{V_k^2}{2g}$$

Then this equation applies,

$$\frac{V_R^2}{2g} = \left| \frac{dE}{dx} \right| \left| \frac{1}{\rho L} \right|$$

Substituting (42)

$$V_R^2 = \frac{2\pi g^2}{L} \left| \frac{2A dA}{k dx} - \frac{A^2 dk}{k^2 dx} \right| \dots (49)$$

$V_R$  is the total velocity of the radiation current. For waves that form an angle  $\alpha$  to the normal of the coast, the longshore current velocity is:

$$V_{Ls} = V_R \sin \alpha \dots (50)$$

An example of the radiation current velocity analysis  $V_R$  is shown in Figure (4), where the waves used have a deep-water wave height  $H_0 = 2.4 \text{ m}$ , with breaking occurring at a breaker depth of  $h_b = 6.669 \text{ m}$ .

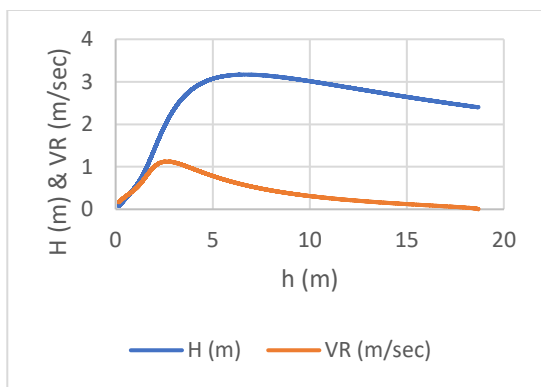


Fig (4) Stress radiation current velocity  $V_R$ .

Similar to the wave energy graph, this radiation current graph is continuous, with no spike at the breaking point. The highest velocity is 1.13 m/sec, occurring at a water depth of  $h = 2.65 \text{ m}$ , while at the breaker depth of  $h_b = 6.669 \text{ m}$ , velocity  $V_R = 0.57 \text{ m/sec}$ . Notably, the maximum velocity does not occur at the breaking point. As shown in Figure (4), the maximum velocity occurs at a depth where the wave height has decreased significantly.

Table (10) presents the radiation current velocities at different wave periods. It shows that the maximum current velocity does not occur at the breaking point, but rather at a shallower water depth than the breaker depth. For example, with a deep-water wave height  $H_0 = 2.0 \text{ m}$ ,  $V_R$  the radiation current velocity at the breaking point  $V_{R-b} = 0.52 \text{ m/sec}$  at a breaker depth of  $h_b = 5.56 \text{ m}$ , while the maximum velocity  $V_{max} = 1.03 \text{ m/sec}$ , occurs at a shallower water depth of  $h_{vmx} = 2.21 \text{ m}$ .

Table (10): Velocity  $V_R$  at breaking point  $V_{R-b}$  and maximum speed  $V_{max}$ .

$H_0$ (m)	$T$ (sec)	$V_{R-b}$ (m)	$h_b$ (m/s)	$V_{max}$ (m/s)	$h_{vmx}$ (m)
0.4	3.47	0.23	1.11	0.46	0.44
0.8	4.9	0.33	2.22	0.65	0.88
1.2	6.01	0.4	3.33	0.8	1.33
1.6	6.93	0.46	4.45	0.92	1.77
2	7.75	0.52	5.56	1.03	2.21
2.4	8.49	0.57	6.67	1.13	2.65
2.8	9.17	0.61	7.78	1.22	3.09
3.2	9.81	0.66	8.89	1.3	3.53
3.6	10.4	0.7	10	1.38	3.98
4	10.96	0.73	11.11	1.45	4.42

a. Results of Prior Research

The theory of stress radiation was first proposed by Longuet-Higgin (1970), which describes how wave energy, transferred through the orbital motion of water particles, is converted into non-orbital currents moving in the same direction as the wave. Based on this theory, the longshore current equation was formulated. Several researchers have developed longshore current equations based on Longuet-Higgins' theory, which are widely used in the field:

1. Komar (1976), modified Longuet Higgins

$$V_{Kom} = 2.7 \left( \frac{\gamma_b}{2} \sqrt{gH_b} \right) \sin \alpha_b \cos \alpha_b$$

Where  $\gamma_b = 0.78$

2. Galvin, C. (1987)

$$V_{Gal} = g m T \sin 2\alpha_b$$

$T$ : wave period

$m$ : bottom slope

Table (11) presents a comparison of the longshore current velocity model results at the breaking point  $V_{L-b}$  as derived from the model and the equations from Komar and Galvin, using an angle  $\alpha_b = 15^\circ$ , resulting in model  $V_{L-b}$  as the smallest among the three methods..

Table (11) Comparison longshore current velocity at breaking point.

$T$ (sec)	$H_b$ (m)	$V_{Kom}$ (m/sec)	$V_{Gal}$ (m/sec)	$V_{L-b}$ (m/sec)
3.47	0.53	0.6	0.17	0.06
4.9	1.06	0.85	0.24	0.09

6.01	1.58	1.04	0.29	0.1
6.93	2.11	1.2	0.34	0.12
7.75	2.64	1.34	0.38	0.13
8.49	3.17	1.47	0.42	0.15
9.17	3.7	1.59	0.45	0.16
9.81	4.23	1.7	0.48	0.17
10.4	4.75	1.8	0.51	0.18
10.96	5.28	1.9	0.54	0.19

Table (12) compares the longshore current velocities from Komar and Galvin with the maximum velocity from the model. As seen in the table, the model results are still the smallest, but they are quite close to the longshore current velocity from Galvin.

Table (12) Comparison with the maximum velocity.

$T$ (sec)	$H_b$ (m)	$V_{Kom}$ (m/sec)	$V_{Gal}$ (m/sec)	$V_{L-max}$ (m/sec)
3.47	0.53	0.6	0.17	0.12
4.9	1.06	0.85	0.24	0.17
6.01	1.58	1.04	0.29	0.21
6.93	2.11	1.2	0.34	0.24
7.75	2.64	1.34	0.38	0.27
8.49	3.17	1.47	0.42	0.29
9.17	3.7	1.59	0.45	0.31
9.81	4.23	1.7	0.48	0.34
10.4	4.75	1.8	0.51	0.36
10.96	5.28	1.9	0.54	0.38

However, velocities from the model and Galvin's equation occur at different water depths.

There is a significant difference between the model results and those from previous equations. The previous equations are applied to the breaker depth, whereas the maximum velocity in the model occurs at a shallower depth, not at the breaker depth.

Nevertheless, the analysis of breaker height and the remaining wave energy at the breaking point validates the accuracy of the wave energy release in the shoaling and breaking model, which in turn confirms the accuracy of the resulting longshore current.

The calculations in Table (12) are performed using a deep-water coefficient of  $\theta = 3.0$ . In Table (13), with a coefficient  $\theta = 1.95$ , where  $\frac{H_b}{h_b} \approx 0.78$ ,  $V_{L-max}$  is found

close to  $V_{Gal}$ , however these velocities occur at different water depths.  $V_{Gal}$  occurs at the breaker depth, while  $V_{L-max}$  occurs at a shallower water depth (see Table (10)).

Table (13) Comparison longshore current velocity at  $\theta = 1.95$ .

$T$ (sec)	$H_b$ (m)	$V_{Kom}$ (m/sec)	$V_{Gal}$ (m/sec)	$V_{L-max}$ (m/sec)
3.47	0.53	0.6	0.17	0.16
4.9	1.06	0.85	0.24	0.22
6.01	1.58	1.04	0.29	0.27
6.93	2.11	1.2	0.34	0.31
7.75	2.64	1.34	0.38	0.35
8.49	3.17	1.47	0.42	0.39
9.17	3.7	1.59	0.45	0.42
9.81	4.23	1.7	0.48	0.44
10.4	4.75	1.8	0.51	0.47
10.96	5.28	1.9	0.54	0.5

### VII. CONCLUSION

This research shows that the method used to formulate the weighting coefficient in the weighted Taylor series is more systematic and accurate compared to the previous approach by the same researcher. By applying the correct weighting coefficient, the resulting weighted Taylor series effectively represents the complete Taylor series.

The development of the shoaling-breaking model through the application of the weighted Taylor series yields accurate predictions for both the breaker height and the remaining energy at the breaking point. Therefore, it can be concluded that the shoaling-breaking model in this research successfully simulates the release of wave energy, or stress radiation, with high fidelity. Moreover, given the appropriate kinetic energy supply from the shoaling-breaking model, it can be concluded that the longshore current produced by the model is accurate.

The maximum longshore current velocity does not occur at the breaking point. Instead, it is observed at a shallower depth than the breaker depth, specifically at a depth where a significant reduction in wave energy occurs.

### REFERENCES

[1] Longuet Higgins, MS (1970). Longshore current generated by Obliquely Incident wave, 1. J.Geophysics. Res., 75, 6778-6789.

[2] Arden, Bruce W. and Astill Kenneth N. (1970). Numerical Algorithms : Origins and Applications. Philippines copyright (1970) by Addison-Wesley Publishing Company, Inc.

- [3] Courrant, R., Friedrichs, K., Lewy, H. (1928). Uber die Partiellen Differenzengleichungen der mathematischen Physik. *Mathematischen Annalen* (in German). 100 (1);32-74, Bibcode : 1928,MatAn. 100.32.c. doi: 10.1007/BF01448839, JFM 54.0486.01 MR 1512478.
- [4] Hutahaean, S. (2023a). Method for Determining Weighting Coefficients in Weighted Taylor Series Applied to Water Wave Modeling. *International Journal of Advance Engineering Research and Science (IJAERS)*. Vol. 10, Issue 12; Dec, 2023, pp 105-114. Article DOI: <https://dx.doi.org/10.22161/ijaers.1012.11>.
- [5] Dean, R.G., Dalrymple, R.A. (1991). *Water wave mechanics for engineers and scientists*. Advance Series on Ocean Engineering.2. Singapore: World Scientific. ISBN 978-981-02-0420-4. OCLC 22907242.
- [6] Hutahaean, S. (2023b). Water Wave Velocity Potential on Sloping Bottom in Water Wave Transformation Modeling . *International Journal of Advance Engineering Research and Science (IJAERS)*. Vol. 10, Issue 10; Oct, 2023, pp 149-157. Article DOI: <https://dx.doi.org/10.22161/ijaers.1010.15>.
- [7] Toffoli, A., Babanin, A., Onaroto, M. and Wased, T. (2010). Maximum steepness of oceanic waves : Field and laboratory experiments. *Geophysical Research Letters*. First published 09 March 2010. <https://doi.org/10.1029/2009GL.0441771>
- [8] Wiegel, R.L. (1949). An Analysis of Data from Wave Recorders on the Pacific Coast of the United States, *Trans. Am. Geophys. Union*, Vol.30, pp.700-704.
- [9] Komar, P.D. & Gaughan M.K. (1972). Airy Wave Theory and Breaker Height Prediction, *Coastal Engineering Proceedings*, 1 (13).
- [10] Komar, P.D (1976). *Beach processes and sedimentation* (Prentice Hall Inc. New Jersey), 430 pp.
- [11] Galvin, C.J. Eagleson, P.S.(1965). Experimental study of longshore current on a plane beach, (US Army Coastal Engineering Research Center, Washington D.C), 1965, pp.198. <https://apps.dtic.mil/sti/pdfs/ADA345211.pdf>

# Implementation of the K-Means Clustering Algorithm to Determine the Promotion Strategy of Institut Agama Kristen Negeri Tarutung

Frainskoy Rio Naibaho, Bambang TJ Hutagalung, Riden Anakampun

Institut Agama Kristen Negeri Tarutung, Indonesia

[frainskoy.rio.naibaho@gmail.com](mailto:frainskoy.rio.naibaho@gmail.com), [bambangtjh@gmail.com](mailto:bambangtjh@gmail.com), [riden.anakampun@gmail.com](mailto:riden.anakampun@gmail.com)

Received: 19 Dec 2024,

Receive in revised form: 21 Jan 2025,

Accepted: 25 Jan 2025,

Available online: 30 Jan 2025

©2025 The Author(s). Published by AI  
Publication. This is an open-access article under  
the CC BY license

(<https://creativecommons.org/licenses/by/4.0/>).

**Keywords**— *strategy, k-means clustering, and promotional*

**Abstract**—*This research aims to determine the strategy for recruiting new students at IAKN Tarutung. Currently, competition between state and private universities in accepting new students is increasingly competitive. This is proven by the decreasing trend of prospective students registering at IAKN Tarutung, especially in the Cultural and Religious Tourism study program (as the research sample). Based on data from active students in The Cultural and Religious Tourism Study Program, the K-Means algorithm can be implemented to assist decision-making in determining effective promotional targets for the following year. The results of the research show that data processing for students from the classes of 2021, 2022, and 2023 shows different trends based on Criterion 1 (high school or equivalent vocational school graduates), Criterion 2 (student achievement at their school of origin), and Criterion 3 (community economic ability). Based on data from Criterion 1, criterion 2, and criterion 3, it is stated that promotional strategies must continue to be carried out in all high schools or equivalent vocational schools (public and private) and provide scholarships for prospective Cultural and Religious Tourism study program who are outstanding or economically disadvantaged.*

## I. INTRODUCTION

The rapid development of information technology covers almost all sectors such as the economy, industry, education, and other areas of life (Rashid & Kausik, 2024; Roztocky et al., 2019). This results in the availability of extensive data that can store important information with several processes (Nasution et al., 2021; Plekhanov et al., 2023; Wang, 2024). The application of information technology in education can also produce abundant data, starting from learning process data and personal data of teachers and students (Jud et al., 2023). In a higher education institution, a large amount of data is stored as historical data, which continues to grow, such as student data (Ma, 2024; Plekhanov et al., 2023; Razavian et al., 2024).

The process of admitting new students to a university result in additional data collection every year and creates a large amount of data in the database (Nasution et al., 2021). Students who are undergoing the selection process for admission to a university usually provide profile data on campus. The stored data will be integrated into each faculty and related study program. The data will then be used for student administration purposes as part of the learning process during lectures at the university. IAKN Tarutung is one of the state universities under the auspices of the Ministry of Religion located in North Sumatra. IAKN Tarutung offers postgraduate programs and three faculties, namely FISHK, FIPK, and FIT. Each faculty has several study programs that can be chosen by students. Young

learners to obtain education develop their potential and channel their interests. The New Student Admissions activity at IAKN Tarutung is a routine activity held every year to recruit new students. IAKN Tarutung always improves the quality of facilities and infrastructure, teaching staff, education staff, administration, and other facilities and infrastructure to attract prospective new students. However, it is very unfortunate that information about each faculty and study program is not well distributed. Moreover, the emergence of many other universities in the North Sumatra region and Indonesia has created very tight competition for IAKN Tarutung in accepting new students.

Currently, the competition between state and private universities to accept new students is getting tighter (Jud et al., 2023). Some people spend a lot of money on promotional media and some offer various offers such as affordable tuition fees, promises of easy jobs after graduation, and so on (PrastYesbudi et al., 2024). Therefore, careful planning is needed in determining the scope of promotion to achieve the target of accepting new students each year and expectations to produce the best human resources to support quality national development in the future. postgraduate students (Haleem et al., 2022; Jud et al., 2023; Naibaho, 2019; PrastYesbudi et al., 2024).

The application of information technology in the field of promotion can help campuses manage data that can store valuable and useful information so that it has its own added value so that the desired goal is achieved in recruiting students with the best potential (Haleem et al., 2022; Wahyudi & Arroufu, 2022). (United Kingdom: 2020). Promotion is the key to success for a university that wants to introduce its campus environment to attract the attention of prospective applicants (Bengnga & Ishak, 2018; Haleem et al., 2022; Wahyudi & Arroufu, 2022).

Promotion requires precise planning so that all promotional objectives can be achieved so that competition also increases in each region with the dissemination of targeted information (Gómez-Olmedo et al., 2024; R. Kumar et al., 2025). The large collection of student data obtained by generating big data will be an opportunity to find information from many groups based on data characteristics on campus. (Firat & Gungor, 2009; S. Kumar et al., 2021; Nasution et al., 2021; Saltz, 2021), Many student data sets are formed so that effective and efficient campus promotion goals can be determined.

One of the causes of the decline in the number of students in higher education is the inappropriate planning of promotional strategies that will have an impact on the fluctuation of the number of new students (Abbas et al., 2019; Dwivedi et al., 2021; Valero & Van Reenen, 2019). This large amount of data can be processed using data

mining science. Data mining is designed to explore data to find consistent patterns by applying the patterns found to new subgroups (Handoko et al., 2020; Li et al., 2025; Peng et al., 2024; Shu & Ye, 2023).

Data collection for new student admissions can be done using the K-Means clustering method, which groups data into several groups based on data similarities, while data that has different characteristics will be grouped into other clusters that have the same similarities (Darmansah & Wardani, 2021; Hu & Su, 2008; Park et al., 2025). K-Means clustering has the advantage of being able to create large data sets quickly and efficiently (Bang & Jhun, 2014; Fuss et al., 2016) to help decision-makers determine effective promotion goals for the coming year (Bengnga & Ishak, 2018).

To meet expectations regarding the number of new students accepted each year, this study was conducted to analyze and process data on new student admissions for 2021-2023 at IAKN Tarutung to obtain information that can help determine promotion goals in the following year. The data attributes that will be used in this study focus on the type of school of origin (Senior High School, Vocational School, Or Equivalent), The Success/Failure of Education, and the economic situation of the student's family, which should help and provide information to the PMB team. conducting promotions in various schools in Indonesia, especially in the North Sumatra region. Processing these data attributes will produce several groupings to determine job promotion targets at IAKN Tarutung.

## II. RESEARCH METHODOLOGY

The method used in this study is an applied method, namely the researcher applied the Data Mining method with the K-Means Clustering algorithm to the data of students of the Cultural and Religious Tourism study program from 2020 to 2023 at the State Christian Institute to be analyzed and grouped according to regional distribution and according to school of origin based on the cumulative achievement index during the first two semesters, namely one grade and second grade. To carry out the K-Means Clustering process, of course, requires a lot of data and according to what is needed, in this study, the researcher used data from students of the Cultural and Religious Tourism study program from 2020 to 2023 at the State Christian Institute (IAKN) Tarutung. Data collection at IAKN Tarutung is sufficient by attaching a research permit letter from IAKN Tarutung and attaching a research proposal to the academic section of IAKN Tarutung. After receiving a reply from IAKN Tarutung, the data can be taken to the student data section by copying the data according to the needs that have been written in the proposal. For the coding process of various

commands and functions needed to build an application with the K-Means Clustering algorithm, Microsoft Visual Studio 2010 was used. The first stage carried out by the researcher was to create a web application system design using the DFD method. (Data Flow Diagram) and ERD (Entity Relationship Diagram). The DFD method is a system design method that explains the flow and process information in the system being built, while the ERD method is a system design method that describes the database design model of the system being built. The following is the system design.

### III. RESULT AND DISCUSSION

#### A. Initial Data

Student criteria data consists of three aspects, namely:

1. Type of secondary school of origin (Senior High School, Vocational School, or equivalent), hereinafter referred to as Criteria K1.
2. The student achievements while at high school or equivalent (student achievements include ever having ranked in the top 10 or received other academic awards), hereinafter referred to as Criteria K2.
3. The economic situation of the student's family (the economic capacity of the student's family), hereinafter referred to as the K3 Criteria.

Table 3.1 Performance Weighting 1

No	Type of Secondary School	Score
1	Senior High School	9
2	Vocational School Equivalent	8

Table 3.2 Performance Weighting 2

No	Student achievement at school	Score
1	Achievement	9
2	Underachievement	8

Table 3.3 Performance Weighting 3

No	The economic situation of students	Score
1	Capable	9
2	Less capable	8

1. **Student data for the Cultural and Religious Tourism study program consists of three batches 2021, 2022, and 2023. Data on Cultural and Religious Tourism Study program, 2021 intake**

Table 3.4 Data for Cultural and Religious Tourism Study Program, 2021 intake before Weighting

No	Name of Students	Criteria 1	Criteria 2	Criteria 3
		Type of School of Origin	Achievement	Economic Conditions
1	Yunvinus Molama	Senior High School	No	Less Fortunate
2	Melkisedek Wuwute	Senior High School	No	Less Fortunate
3	Fifin Murnikmat Lase	Vocational School	Yes	Less Fortunate
4	Gebri Margaretha Verbauli	Senior High School	Yes	Capable
5	Meilani Lida Siahaan	Senior High School	Yes	Capable
6	Evi Agustina Harianja	Vocational School	No	Capable
7	Juliana Marbun	Senior High School	No	Capable
8	Nelli Oktavisari Silitonga	Vocational School	Yes	Less Fortunate
9	Severoni Lase	Senior High School	No	Less Fortunate
10	Yestin Harefa	Vocational School	No	Capable
11	Naomi Angel Veronika Hutagalung	Senior High School	No	Capable
12	Kristiawan Ndraha	Senior High School	Yes	Less Fortunate
13	Melista br.Marbun Lumban Gaol	Senior High School	Yes	Capable
14	Mira Silitonga	Senior High School	Yes	Capable
15	Pernando Panjaitan	Senior High School	Yes	Capable
16	Putra Rata Harefa	Senior High School	Yes	Capable
17	Cari Nosta Adil Laoli	Senior High School	No	Less Fortunate
18	Elisabeth Oktavia Sihombing	Senior High School	Yes	Capable

19	Ezra Angelita Simanjuntak	Vocational School	No	Capable
20	Gladys Sitanggang	Senior High School	Yes	Capable
21	HelmaYesna Hutasoit	Senior High School	No	Capable
22	Ensiklira Silaban	Senior High School	Yes	Capable
23	Jonathan Mark Manullang	Vocational School	No	Less Fortunate
24	Jupita Sianturi	Senior High School	No	Less Fortunate
25	Paian Jonatan Nababan	Senior High School	No	Capable
26	Romasi Ernawati.S	Senior High School	No	Capable
27	Sebastinus Gulo	Senior High School	No	Less Fortunate
28	Eska Romauli Simamora	Senior High School	Yes	Capable
29	Fairy Sinaga	Vocational School	No	Capable
30	Putri Ayu Andriani Simanjuntak	Senior High School	Yes	Capable
31	Christien	Senior High School	Yes	Capable
32	Dini Resavita Hariandja	Vocational School	No	Capable
33	Esra Silali	Senior High School	No	Capable
34	Ifo Siska Sigalingging	Senior High School	Yes	Less Fortunate
35	Repalita Gulo	Vocational School	No	Capable
36	Putri Sapta Maria Silitonga	Senior High School	No	Capable
37	Santa TiaSenior High School	Senior High School	Yes	Less Fortunate
38	Sanovida Tamba	Senior High School	Yes	Capable
39	Pontianus Rekaman Halawa	Vocational School	No	Capable

**2. The data for the Cultural and Religious Tourism study program from the 2021 intake after weighting is shown in Table 3.5 below**

*Table 3.5 Data for Cultural and Religious Tourism study program, 2021 intake after*

No	Name	Criteria 1	Criteria 2	Criteria 3
		Type of School of Origin	Achievement	Economic Conditions
1	Yunvinus Molama	9	8	8
2	Melkisedek Wuwute	9	8	8
3	Fifin Murnikmat Lase	8	9	8
4	Gebri Margaretha Verbauli Hutagalung	9	9	9
5	Meilani Lida Siahaan	9	9	9
6	Evi Agustina Harianja	8	8	9
7	Juliana Marbun	9	8	9
8	Nelli Oktavisari Silitonga	8	9	8
9	Severoni Lase	9	8	8
10	Yestin Harefa	8	8	9
11	Naomi Angel Veronika Hutagalung	9	8	9
12	Kristiawan Ndraha	9	9	8
13	Melista br.Marbun Lumban Gaol	9	9	9
14	Mira Silitonga	9	9	9
15	Pernando Panjaitan	9	9	9
16	Putra Rata Harefa	9	9	9
17	Cari Nosta Adil Laoli	9	8	8
18	Elisabeth Oktavia Sihombing	9	9	9
19	Ezra Angelita Simanjuntak	8	8	9
20	Gladys Sitanggang	9	9	9
21	Helmayana Hutasoit	9	8	9
22	Ensiklira Silaban	9	9	9
23	Jonathan Mark Manullang	8	8	8

24	Jupita Sianturi	9	8	8
25	Paian Jonatan Nababan	9	8	9
26	Romasi Ernawati.S	9	8	9
27	Sebastinus Gulo	9	8	8
28	Eska Romauli Simamora	9	9	9
29	Fairy Sinaga	8	8	9
30	Putri Ayu Andriani Simanjuntak	9	9	9
31	Christien	9	9	9
32	Dini Resavita Hariandja	8	8	9
33	Esra Silali	9	8	9
34	Ifo Siska Sigalingging	9	9	8
35	Repalita Gulo	8	8	9
36	Putri Sapta Maria Silitonga	9	8	9
37	Santa TiaSenior High School Tambunan	9	9	8
38	Sanovida Tamba	9	9	9
39	Pontianus Rekaman Halawa	8	8	9

**3. Data on Cultural and Religious Tourism Study Program, class of 2022, Data on Cultural Religious Tourism Study Program for the 2022 intake before weighting is shown in Table 3.6 below.**

*Table 3.6 Data for the Cultural and Religious Tourism study program, class of 2022 before weighting*

No	Name	Criteria 1	Criteria 2	Criteria 3
		Type of School Origin	Achievement	Economic Conditions
1	Noak Yasai	Senior High School	No	Less Fortunate
2	Selfianus Pahabol	Senior High School	No	Less Fortunate
3	Iman Peris Toansiba	Senior High School	No	Less Fortunate
4	Imerlina Laia	Senior High School	Yes	Less Fortunate
5	Melisa Manurung	Senior High School	Yes	Less Fortunate
6	Gabby Ribkamawaty Siburian	Senior High School	Yes	Less Fortunate
7	Pebrianto Nababan	Senior High School	No	Less Fortunate
8	Trinitas Harefa	Senior High School	Yes	Less Fortunate
9	Gabriel Evandio Hutabarat	Vocational School	Yes	Less Fortunate
10	Heri Santoso Simanjuntak	Senior High School	Yes	Less Fortunate
11	Zefanya Simalango	Senior High School	Yes	Capable
12	Alvin Juliyanto Lase	Senior High School	Yes	Less Fortunate
13	Dita Larissa	Senior High School	Yes	Less Fortunate
14	Pernando Panjaitan	Vocational School	No	Less Fortunate
15	Apri Twenty Sirait	Senior High School	Yes	Less Fortunate
16	Garry Anderson Nainggolan	Senior High School	Yes	Capable
17	Joel Fernandes Gultom	Vocational School	No	Capable
18	Yonathan Pusran Hutajulu	Senior High School	No	Capable
19	Chalvin Christian Sihite	Vocational School	No	Capable
20	Dewi Sartika Sari Sinamo	Senior High School	No	Capable
21	Ebenezer Nianggolan	Vocational School	No	Capable
22	Erwand Daniel Sihotang	Senior High School	No	Capable
23	Eyendri Hondo	Senior High School	Yes	Capable
24	Guna Ernawati Sinamo	Vocational School	No	Capable
25	Mariska Sihite	Senior High School	Yes	Capable
26	Sofy Anisa Sri Asina Nababan	Senior High School	No	Capable
27	Ardin Jultriman Mendrofa	Senior High School	Yes	Capable
28	Milawati Pasaribu	Senior High School	Yes	Capable
29	Rohani Andika Sari Hutabalian	Vocational School	No	Capable
30	Rona Sumantri Lumbantungkup	Senior High School	No	Capable

31	Siska Mariana Hutagalung	Senior High School	No	Less Fortunate
32	Tessalonika Hutapea	Senior High School	Yes	Capable
33	Sondang Paulina Pasaribu	Senior High School	Yes	Capable
34	Suardin Zega	Senior High School	Yes	Capable
35	Yossi Pratiwi Pardosi	Vocational School	Yes	Capable
36	Wantri Novita Tampubolon	Senior High School	Yes	Capable

**4. Data on the Cultural and Religious Tourism study program class of 2022 after weighting is shown in Table 3.7 below.**

*Table 3.7 Data Cultural and Religious Tourism study program class of 2022 after weighting*

No	Name	Criteria 1	Criteria 2	Criteria 3
		Type of School of Origin	Achievement	Economic Conditions
1	Noak Yasai	9	8	8
2	Selfianus Pahabol	9	8	8
3	Iman Peris Toansiba	9	8	8
4	Imerlina Laia	8	9	8
5	Melisa Manurung	9	9	8
6	Gabby Ribkamawaty Siburian	9	9	8
7	Pebrianto Nababan	9	8	8
8	Trinitas Harefa	8	9	8
9	Gabriel Evandio Hutabarat	8	9	8
10	Heri Santoso Simanjuntak	9	9	8
11	Zefanya Simalango	9	9	9
12	Alvin Juliyanto Lase	9	9	8
13	Dita Larissa	9	9	8
14	Pernando Panjaitan	8	8	8
15	Apri Twenty Sirait	9	9	8
16	Garry Anderson Nainggolan	9	9	9
17	Joel Fernandes Gultom	8	8	9
18	Yonathan Pusran Hutajulu	9	8	9
19	Chalvin Christian Sihite	8	8	9
20	Dewi Sartika Sari Sinamo	9	8	9
21	Ebenezer Nianggolan	8	8	9
22	Erwand Daniel Sihotang	9	8	9
23	Eyendri Hondo	9	9	9
24	Guna Ernawati Sinamo	8	8	9
25	Mariska Sihite	9	9	9
26	Sofy Anisa Sri Asina Nababan	9	8	9
27	Ardin Jultriman Mendrofa	9	9	9
28	Milawati Pasaribu	9	9	9
29	Rohani Andika Sari Hutabalian	8	8	9
30	Rona Sumantri Lumbantungkup	8	8	9
31	Siska Mariana Hutagalung	9	8	8
32	Tessalonika Hutapea	9	9	9
33	Sondang Paulina Pasaribu	9	9	9
34	Suardin Zega	9	9	9
35	Yossi Pratiwi Pardosi	8	9	9
36	Wantri Novita Tampubolon	9	9	

**5. Data on the Cultural and Religious Tourism study program for the 2023 intake before weighting is:**

*Table 3.8 Data Cultural and Religious Tourism study program, class of 2023 before weighing*

No	Name	Criteria 1	Criteria 2	Criteria 3
		Type of School Origin	Achievement	Economic Conditions
1	Dinda Nesa Gamalie Br Silitonga	Senior High School	Yes	Capable
2	Josep Harianja	Senior High School	Yes	Capable
3	Efra Zerika Sitio	Vocational School	Yes	Less Fortunate
4	Ardi Yesnto Halawa	Senior High School	No	Capable
5	Puspa Wahyu Pratiwi	Senior High School	Yes	Less Fortunate
6	Rivan Nababan	Vocational School	Yes	Less Fortunate
7	Josua Simatupang	Senior High School	No	Capable
8	Dian Febrian Firmanto	Senior High School	Yes	Less Fortunate
9	Niar Elizabeth Geofani Panjaitan	Vocational School	Yes	Less Fortunate
10	Esra Yesnti A Siahaan	Senior High School	No	Capable
11	Adelina Angelica Sibagariang	Senior High School	Yes	Capable
12	Yoni Pransiska Simanjuntak	Vocational School	Yes	Less Fortunate
13	Masriara Lubis	Senior High School	Yes	Less Fortunate
14	Aldo Sampetua Tambunan	Senior High School	Yes	Less Fortunate
15	Andre David Ario Lumban Gaol	Vocational School	No	Capable
16	Indah Sari	Senior High School	Yes	Capable
17	Johannes Parera	Vocational School	No	Capable
18	Rotua Br Purba	Senior High School	Yes	Less Fortunate
19	Mery Grecelyta Sianipar	Vocational School	Yes	Less Fortunate
20	Winda Lovika Putri Silalahi	Senior High School	No	Capable
21	Indah Amelia V. Simanullang	Senior High School	No	Capable
22	Arina Tiurma Manalu	Senior High School	Yes	Less Fortunate
23	Hiyos Fiter Sababalat	Senior High School	Yes	Less Fortunate
24	Rugun Panggabean	Vocational School	Yes	Less Fortunate
25	Elisabet Sitompul	Senior High School	Yes	Less Fortunate
26	Isak Lumbantobing	Vocational School	Yes	Capable
27	Pria Sitompul	Senior High School	No	Capable
28	Savana Pane	Senior High School	No	Capable
29	Ricardo Sagala	Senior High School	Yes	Capable
30	Sadar Fernando Siahaan	Senior High School	No	Capable
31	Rona Sari Ayu Simamora	Senior High School	Yes	Less Fortunate
32	Nahael Marudut Amin Mungkur	Senior High School	No	Capable
33	Ida Natalria Tumangger	Senior High School	No	Capable
34	Weimi Erinda Berutu	Vocational School	Yes	Less Fortunate
35	Desinta Riana Tumangger	Senior High School	Yes	Less Fortunate

**6. The data for the Cultural and Religious Tourism study program for the 2023 intake after weighting is shown in Table 3.9 below.**

*Table 3.9 Data Cultural and Religious Tourism study program, class of 2023 after weighting*

No	Name	Criteria 1	Criteria 2	Criteria 3
		Type of School of Origin	Achievement	Economic Conditions
1	Dinda Nesa Gamalie Br Silitonga	9	9	9
2	Josep Harianja	9	9	9
3	Efra Zerika Sitio	8	9	8
4	Ardi Yanto Halawa	9	8	9
5	Puspa Wahyu Pratiwi	9	9	8

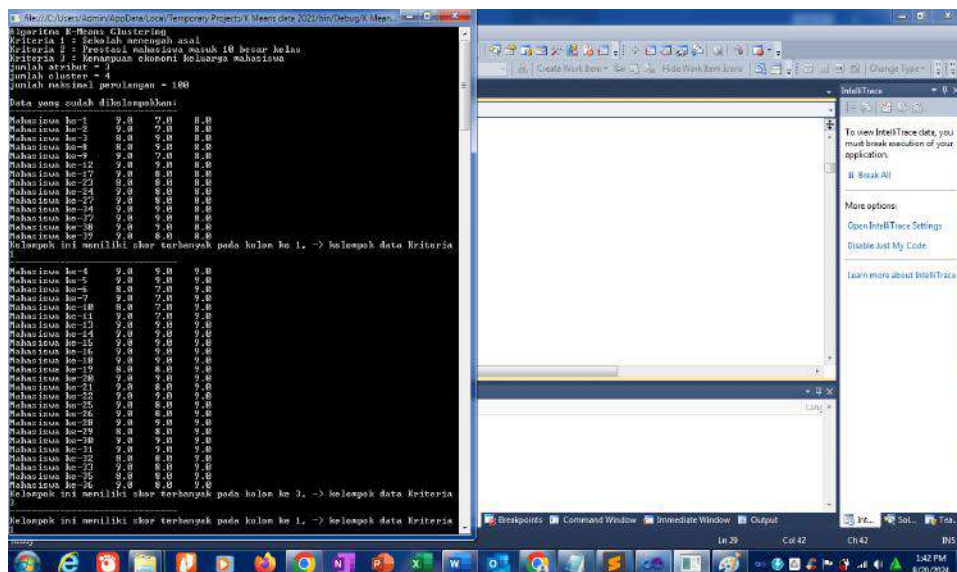
6	Rivan Nababan	8	9	8
7	Josua Simatupang	9	8	9
8	Dian Febrian Firmanto	9	9	8
9	Niar Elizabeth Geofani Panjaitan	8	9	8
10	Esrayanti A Siahaan	9	8	9
11	Adelina Angelica Sibagariang	9	9	9
12	Yoni Pransiska Simanjuntak	8	9	8
13	Masriara Lubis	9	9	8
14	Aldo Sampetua Tambunan	9	9	8
15	Andre David Ario Lumban Gaol	8	8	9
16	Indah Sari	9	9	9
17	Johannes Parera	8	8	9
18	Rotua Br Purba	9	9	8
19	Mery Grecelyta Sianipar	8	9	8
20	Winda Lovika Putri Silalahi	9	8	9
21	Indah Amelia V. Simanullang	9	8	9
22	Arina Tiurma Manalu	9	9	8
23	Hiyos Fiter Sababalat	9	9	8
24	Rugun Panggabean	8	9	8
25	Elisabet Sitompul	9	9	8
26	Isak Lumbantobing	8	9	9
27	Pria Sitompul	9	8	9
28	Savana Pane	9	8	9
29	Ricardo Sagala	9	9	9
30	Sadar Fernando Siahaan	9	8	9
31	Rona Sari Ayu Simamora	9	9	8
32	Nahael Marudut Amin Mungkur	9	8	9
33	Ida Natalria Tumangger	9	8	9
34	Weimi Erinda Berutu	8	9	8
35	Desinta Riana Tumangger	9	9	8

**B. Testing**

The following are the results of testing data on the Cultural and Religious Tourism study program from the 2021, 2022, and 2023 intakes using the K-Means

Clustering algorithm using Microsoft Visual Studio 2010.

1. The results of the 2021 intake of Cultural and Religious Tourism study program data testing can be seen in Figure 3.1. the following



Based on Figure 3.1, it is shown that from 100 tests (iterations) conducted, only two groups can be formed. The first group based on Criteria 1 (school of origin of Senior high School equivalent) consists of 14 students or equivalent to 35.89%. Then, the second group based on Criteria 3 (student economic ability) consists of 25 people or equivalent to 64.10%.

The results of the data testing of the Cultural and Religious Tourism Study Program in the year 2022 showed that from 100 tests (iterations) carried out, three groups could be formed. The first group was based on Criteria 3 (student economic ability) of 15 people or equivalent to 41.66%. Then the second group was based on Criteria 1 (school of origin of SMA or equivalent vocational school) of 15 students or equivalent to 41.66%. Then, the third group was also based on Criteria 1 of 6 people or equivalent to 16.66%.

The results of the data testing of the Cultural and Religious Tourism study program in the year 2023 showed that from 100 tests (iterations) carried out, three groups could be formed. The first group was based on Criteria 2 (student achievement while at school) of 17 people or equivalent to 48.57%. Then the second group was based on Criteria 3 of 11 students or equivalent to 31.42%. Then, the third group was also based on Criteria 2 again of 7 people or equivalent to 20%.

#### IV. CONCLUSION

Based on the results of the research that has been conducted, the following are the conclusions that can be obtained, among others.

1. Based on the data testing of the Cultural and Religious Tourism Study Program, class of 2021, can only form two groups. The first group based on Criteria 1 (school of origin of Senior high School or equivalent) as many as 14 students or equivalent to 35.89%. Then, the second group based on Criteria 3 (student economic ability) as many as 25 people or equivalent to 64.10%. This shows that the majority of students who register for the study program are dominated by the economic ability of the student's family.
2. Based on the data testing of the Cultural and Religious Tourism Study Program, the class of 2022 formed three groups. The first group is based on Criteria 3 (student economic ability) as many as 15 people or equivalent to 41.66%. Then the second group based on Criteria 1 (school of origin of Senior

high school or equivalent) as many as 15 students or equivalent to 41.66%. Then, the third group is also based on Criteria 1 as many as 6 people or equivalent to 16.66%. The results show that students who register for the Cultural and Religious Tourism Study Program are based on the same dominance of Criteria 1 and Criteria 3.

3. Based on the data testing, students in the 2023 Cultural and Religious Tourism Study Program formed three groups. The first group is based on Criteria 2 (student achievement while at school) as many as 17 people or equivalent to 48.57%. Then the second group is based on Criteria 3 as many as 11 students or equivalent to 31.42%. Then, the third group is also based on Criteria 2 again as many as 7 people or equivalent to 20%. The results show that the majority of students in the Cultural and Religious Tourism Study Program are based on Criteria 2 (achievement while at their original school).
4. The data testing of students in the 2021, 2022, and 2023 classes, shows different trends based on Criteria 1 (high school or equivalent vocational high school graduates), Criteria 2 (student achievement while at their original school), and Criteria 3 (community economic ability).
5. Promotion strategies must continue to be implemented in all high schools or equivalent vocational schools, providing scholarships for prospective Cultural and Religious Tourism Study Program who excel or are economically disadvantaged.

#### REFERENCES

- [1] Abbas, J., Aman, J., Nurunnabi, M., & Bano, S. (2019). The Impact of Social Media on Learning Behavior for Sustainable Education: Evidence of Students from Selected Universities in Pakistan. *Sustainability*, 11(6), 1683. <https://doi.org/10.3390/su11061683>
- [2] Bang, S., & Jhun, M. (2014). Weighted Support Vector Machine Using K-Means Clustering. *Communications in Statistics - Simulation and Computation*, 43(10), 2307–2324. <https://doi.org/10.1080/03610918.2012.762388>
- [3] Bengnga, A., & Ishak, R. (2018). Prediksi Jumlah Mahasiswa Registrasi Per Semester Menggunakan Linier Regresi Pada Universitas Ichsan Gorontalo. *ILKOM Jurnal Ilmiah*, 10(2), 136–143. <https://doi.org/10.33096/ilkom.v10i2.274.136-143>
- [4] Darmansah, D. D., & Wardani, N. W. (2021). Analisis Pesebaran Penularan Virus Corona di Provinsi Jawa Tengah Menggunakan Metode K-Means Clustering. *JATISI (Jurnal Teknik Informatika Dan Sistem Informasi)*, 8(1), 105–117. <https://doi.org/10.35957/jatisi.v8i1.590>

- [5] Dwivedi, Y. K., Ismagilova, E., Hughes, D. L., Carlson, J., Filieri, R., Jacobson, J., Jain, V., Karjaluo, H., Kefi, H., Krishen, A. S., Kumar, V., Rahman, M. M., Raman, R., Rauschnabel, P. A., Rowley, J., Salo, J., Tran, G. A., & Wang, Y. (2021). Setting the future of digital and social media marketing research: Perspectives and research propositions. *International Journal of Information Management*, 59, 102168. <https://doi.org/10.1016/j.ijinfomgt.2020.102168>
- [6] Firat, M., & Gungor, M. (2009). Generalized Regression Neural Networks and Feed Forward Neural Networks for prediction of scour depth around bridge piers. *Advances in Engineering Software*, 40(8), 731–737. <https://doi.org/10.1016/j.advengsoft.2008.12.001>
- [7] Fuss, C. E., Berg, A. A., & Lindsay, J. B. (2016). DEM Fusion using a modified k-means clustering algorithm. *International Journal of Digital Earth*, 9(12), 1242–1255. <https://doi.org/10.1080/17538947.2016.1208685>
- [8] Gómez-Olmedo, A. M., Eizaguirre Diéguez, M., & Vicente Pascual, J. A. (2024). Redefining success in innovative crowdfunding projects: Empirical evidence of effective mindful consumption promotion in Kickstarter. *Journal of Innovation & Knowledge*, 9(4), 100558. <https://doi.org/10.1016/j.jik.2024.100558>
- [9] Haleem, A., Javaid, M., Asim Qadri, M., Pratap Singh, R., & Suman, R. (2022). Artificial intelligence (AI) applications for marketing: A literature-based study. *International Journal of Intelligent Networks*, 3, 119–132. <https://doi.org/10.1016/j.ijin.2022.08.005>
- [10] Handoko, S., Fauziah, F., & Handayani, E. T. E. (2020). IMPLEMENTASI DATA MINING UNTUK MENENTUKAN TINGKAT PENJUALAN PAKET DATA TELKOMSEL MENGGUNAKAN METODE K-MEANS CLUSTERING. *Jurnal Ilmiah Teknologi Dan Rekayasa*, 25(1), 76–88. <https://doi.org/10.35760/tr.2020.v25i1.2677>
- [11] Hu, Y.-C., & Su, B.-H. (2008). Accelerated k-means clustering algorithm for colour image quantization. *The Imaging Science Journal*, 56(1), 29–40. <https://doi.org/10.1179/174313107X176298>
- [12] Jud, J., Hirt, C. N., Rosenthal, A., & Karlen, Y. (2023). Teachers' motivation: Exploring the success expectancies, values, and costs of the promotion of self-regulated learning. *Teaching and Teacher Education*, 127, 104093. <https://doi.org/10.1016/j.tate.2023.104093>
- [13] Kumar, R., Mukherjee, S., & Bose, I. (2025). Metaverse advertising and promotional effectiveness: The route from immersion to joy. *Decision Support Systems*, 189, 114386. <https://doi.org/10.1016/j.dss.2024.114386>
- [14] Kumar, S., Kar, A. K., & Ilavarasan, P. V. (2021). Applications of text mining in services management: A systematic literature review. *International Journal of Information Management Data Insights*, 1(1), 100008. <https://doi.org/10.1016/j.ijime.2021.100008>
- [15] Li, Y., Yin, H., Dong, F., Cheng, W., Zhuang, N., Xie, D., & Di, W. (2025). The key to green water-preserved mining: Prediction and integration of mining rock failure height by big data fusion simulation algorithm. *Process Safety and Environmental Protection*, 193, 1015–1035. <https://doi.org/10.1016/j.psep.2024.11.096>
- [16] Ma, Y. (2024). Simulation and Implementation of Intelligent Network Technology System Based on Big Data. *Procedia Computer Science*, 247, 545–552. <https://doi.org/10.1016/j.procs.2024.10.065>
- [17] Naibaho, F. R. (2019). Sistem Pendukung Keputusan Dalam Penentuan Dosen Terbaik Di IAKN Tarutung Dengan Menggunakan Kombinasi Metode Likert dan Metode VIKOR. In *Seminar Nasional Sains & Teknologi Informasi (SENSASI)* (Vol. 2, Issue Tantangan & Peluang di Bidang Pendidikan untuk Menghadapi Era Disrupsi pada Teknologi RI 4.0). <http://seminar-id.com/prosiding/index.php/sensasi/article/view/335>
- [18] Nasution, M. K. M., Sitompul, O. S., Elveny, M., & Syah, R. (2021). Data science: A Review towards the Big Data Problems. *Journal of Physics: Conference Series*, 1898(1), 012006. <https://doi.org/10.1088/1742-6596/1898/1/012006>
- [19] Park, B., Park, C., Hong, S., & Choi, H. (2025). Sparse kernel k-means clustering. *Journal of Applied Statistics*, 52(1), 158–182. <https://doi.org/10.1080/02664763.2024.2362266>
- [20] Peng, C., Chen, J., Wan, S., & Xu, G. (2024). A Quarterly High RFM Mining Algorithm for Big Data Management. *Computers, Materials & Continua*, 80(3), 4341–4360. <https://doi.org/10.32604/cmc.2024.054109>
- [21] Plekhanov, D., Franke, H., & Netland, T. H. (2023). Digital transformation: A review and research agenda. *European Management Journal*, 41(6), 821–844. <https://doi.org/10.1016/j.emj.2022.09.007>
- [22] Prastyabudi, W. A., Alifah, A. N., & Nurdin, A. (2024). Segmenting the Higher Education Market: An Analysis of Admissions Data Using K-Means Clustering. *Procedia Computer Science*, 234, 96–105. <https://doi.org/10.1016/j.procs.2024.02.156>
- [23] Rashid, A. Bin, & Kausik, M. A. K. (2024). AI revolutionizing industries worldwide: A comprehensive overview of its diverse applications. *Hybrid Advances*, 7, 100277. <https://doi.org/10.1016/j.hybadv.2024.100277>
- [24] Razavian, B., Hamed, S. M., Fayyaz, M., Ghasemi, P., Ozkul, S., & Tirkolaei, E. B. (2024). Addressing barriers to big data implementation in sustainable smart cities: Improved zero-sum grey game and grey best-worst method. *Journal of Innovation & Knowledge*, 9(4), 100593. <https://doi.org/10.1016/j.jik.2024.100593>
- [25] Roztocki, N., Soja, P., & Weistroffer, H. R. (2019). The role of information and communication technologies in socio-economic development: towards a multi-dimensional framework. *Information Technology for Development*, 25(2), 171–183. <https://doi.org/10.1080/02681102.2019.1596654>
- [26] Saltz, J. S. (2021). CRISP-DM for Data Science: Strengths, Weaknesses, and Potential Next Steps. *2021 IEEE International Conference on Big Data (Big Data)*, 2337–2344. <https://doi.org/10.1109/BigData52589.2021.9671634>
- [27] Shu, X., & Ye, Y. (2023). Knowledge Discovery: Methods from data mining and machine learning. *Social Science Research*, 110, 102817. <https://doi.org/10.1016/j.ssresearch.2022.102817>
- [28] Valero, A., & Van Reenen, J. (2019). The economic impact of universities: Evidence from across the globe. *Economics of Education Review*, 68, 53–67. <https://doi.org/10.1016/j.econedurev.2018.09.001>

- [29] Wahyudi, T., & Arroufu, D. S. (2022). Implementation of Data Mining Prediction Delivery Time Using Linear Regression Algorithm. *Journal of Applied Engineering and Technological Science (JAETS)*, 4(1), 84–92. <https://doi.org/10.37385/jaets.v4i1.918>
- [30] Wang, L. (2024). Enhancing tourism management through big data: Design and implementation of an integrated information system. *Heliyon*, 10(20), e38256. <https://doi.org/10.1016/j.heliyon.2024.e38256>

## Dengue Hospitalizations in the state of Pará over the last decade: An ecological study

## Internações por Dengue no estado do Pará na última década: Um estudo ecológico

Vando Delgado de Souza Santos<sup>1</sup>, Bianca Abreu Pantoja<sup>2</sup>, Matheus Bassalo Aflalo<sup>2</sup>, Ana Luísa Damasceno Rodrigues<sup>2</sup>, Eduardo de Pinho Domingues<sup>2</sup>, Henrique Fayad Pinheiro<sup>2</sup>, Fábio Costa de Vasconcelos<sup>3</sup>, William Robert Souza<sup>3</sup>, Marcos Gabriel Barbosa Castello Branco<sup>4</sup>, Maria Gabriela da Rocha Florêncio<sup>4</sup>, Dara Estrela Santos Esteves<sup>4</sup>, Valnilson Dias Reis<sup>4</sup>, Ana Olívia Semblano Monteiro<sup>4</sup>, Alcilene Monteiro Lima<sup>4</sup>, Marivaldo de Moraes e Silva<sup>4</sup>, Beatriz Colares Coelho de Souza<sup>4</sup>, Francisco Miguel da Silva Freitas<sup>4</sup>, Larissa Araújo Queiroz<sup>5</sup>, Társis da Silva Sousa<sup>5</sup>, Carlos Vinicius Carrera do Nascimento<sup>5</sup>, Leonardo Barbosa Duarte<sup>5</sup>, Brenda do Socorro Preuss Cardoso<sup>6</sup>, Verena Sousa Reis<sup>1</sup>, Kaylana de Silva Leite<sup>1</sup>, Rayza Gregório Lima<sup>1</sup>, Ayla Luiza Preuss Erbes<sup>1</sup>, Sebastiana Brandão da Costa<sup>1</sup>, Isis Bruna Vasques Carvalho<sup>1</sup>, Rafaella Casanova Ataíde dos Santos<sup>1</sup>, Diego Romani da Costa<sup>1</sup>, Nicole Morais Dillon<sup>1</sup>, Filipe Santos da Silva<sup>1</sup>, Ayanne Castro de Miranda<sup>1</sup>, Eduardo Alberto Rodrigues Tiago<sup>1</sup>

<sup>1</sup>Universidade Federal do Pará, Brasil

<sup>2</sup>Centro Universitário do Pará, Brasil

<sup>3</sup>Universidade da Amazônia, Brasil

<sup>4</sup>Centro Universitário Metropolitano da Amazônia, Brasil

<sup>5</sup>Universidade do Estado do Pará, Brazil

<sup>6</sup>Universidade Federal Rural da Amazônia, Brazil

Received: 18 Dec 2024,

Receive in revised form: 22 Jan 2025,

Accepted: 26 Jan 2025,

Available online: 30 Jan 2025

©2025 The Author(s). Published by AI  
Publication. This is an open-access article  
under the CC BY license

(<https://creativecommons.org/licenses/by/4.0/>).

**Keywords**— *Dengue; Epidemiology; Public Health.*

**Abstract**— *Introduction: Dengue is an arboviral disease transmitted by the mosquito *Aedes aegypti* and represents a public health problem in tropical and subtropical countries, especially in regions with limited access to healthcare services. However, the literature lacks studies on dengue-related hospitalizations in Pará, which could support more effective health policies for controlling and reducing the disease in the state. Objectives: To evaluate the temporal trend and compare dengue hospitalizations in Pará with other states in the Northern Region, outlining the epidemiological profile. Methods: This is a descriptive ecological epidemiological study using data from the Hospital Information System (SIH) from 2014 to 2023, referring to hospitalizations due to dengue (ICD C32.1). The analyzed variables included year and month of care, number of hospitalizations, hospitalization rate per 100,000 inhabitants, sex, age, and type of care. Statistical analysis*

**Palavras-chave—** Dengue; Epidemiologia; Saúde Pública.

was performed using Simple Linear Regression, the Kruskal-Wallis test, and Dunn's post-hoc test, using Statistics Kingdom software. Results: A total of 13,956 hospitalizations for dengue were recorded in Pará during the study period. A reduction trend of 2.88 hospitalizations per year was observed ( $p < 0.005$ ,  $BI = -2.88$ , 95% CI [-4.62, -1.14],  $R = -0.80$ ). The Kruskal-Wallis test, followed by Dunn's post-hoc test, showed that Pará did not present a significantly different hospitalization rate compared to the other states. In the epidemiological profile, females had a higher number of hospitalizations ( $n=7,201$ ) compared to males ( $n=6,755$ ). The adult hospitalization rate was 4.7 times higher than that of the elderly and 1.6 times higher than that of children and adolescents. Additionally, 92.9% of hospitalizations occurred on an emergency basis. Conclusion: Pará has shown a reduction in hospitalizations due to dengue over the years. Women and adults are the most affected, with the majority of hospitalizations occurring on an emergency basis. The results suggest that this decrease may be due to more effective preventive strategies, underreporting of cases, or reduced exposure to risk factors among the population of Pará. Future studies are needed to confirm these hypotheses and guide more targeted interventions.

**Resumo—** Introdução: A dengue é uma arbovirose transmitida pelo mosquito *Aedes aegypti* e representa um problema de saúde pública em países tropicais e subtropicais, especialmente em regiões com acesso limitado a serviços de saúde. No entanto, a literatura carece de estudos sobre internações relacionadas à dengue no Pará, que poderiam subsidiar políticas de saúde mais eficazes para o controle e redução da doença no estado. Objetivos: Avaliar a tendência temporal e comparar as internações por dengue no Pará com outros estados da Região Norte, traçando o perfil epidemiológico. Métodos: Trata-se de um estudo epidemiológico ecológico descritivo utilizando dados do Sistema de Informações Hospitalares (SIH) de 2014 a 2023, referentes às internações por dengue (CID C32.1). As variáveis analisadas incluíram ano e mês de atendimento, número de internações, taxa de internação por 100 mil habitantes, sexo, idade e tipo de atendimento. A análise estatística foi realizada por meio de regressão linear simples, teste de Kruskal-Wallis e teste post-hoc de Dunn, por meio do software Statistics Kingdom. Resultados: Foram registradas 13.956 internações por dengue no Pará no período do estudo. Observou-se tendência de redução de 2,88 internações por ano ( $p < 0,005$ ,  $BI = -2,88$ , IC 95% [-4,62, -1,14],  $R = -0,80$ ). O teste de Kruskal-Wallis, seguido do teste post-hoc de Dunn, mostrou que o Pará não apresentou taxa de internação significativamente diferente em comparação aos demais estados. No perfil epidemiológico, o sexo feminino apresentou maior número de internações ( $n=7.201$ ) em relação ao masculino ( $n=6.755$ ). A taxa de internação de adultos foi 4,7 vezes maior que a de idosos e 1,6 vezes maior que a de crianças e adolescentes. Além disso, 92,9% das internações ocorreram em caráter emergencial. Conclusão: O Pará apresentou redução nas internações por dengue ao longo dos anos. Mulheres e adultos são os mais afetados, com a maioria das hospitalizações ocorrendo em caráter emergencial. Os resultados sugerem que essa diminuição pode ser decorrente de estratégias preventivas mais eficazes, da subnotificação de casos ou da redução da exposição a fatores de risco da população paraense. Estudos futuros são necessários para confirmar estas hipóteses e orientar intervenções mais direcionadas.

## I. INTRODUÇÃO

A dengue é uma das doenças endêmicas mais relevantes no Brasil, causada pelo vírus transmitido pelo mosquito *Aedes aegypti*. Ela se divide em quatro sorotipos virais (DENV-1, DENV-2, DENV-3 e DENV-4). Embora a doença tenha sido registrada pela primeira vez no Brasil no final do século XIX, só em 1981 foi possível identificar e isolar seus sorotipos (Ratto et al., 2024). Desde então, a dengue se espalhou por todo o país, tornando-se um problema persistente de saúde pública (Chaves et al., 2018).

A classificação da dengue é organizada em três estágios. No primeiro, dengue sem sinais de alerta, os sintomas iniciais incluem febre alta (39–40 °C), acompanhada de cefaléia, dores musculares e articulares, e dor atrás dos olhos. Outros sintomas possíveis são erupções na pele, perda de apetite, náuseas e vômitos, que normalmente melhoram após o terceiro dia (Oneda et al., 2021).

Em alguns casos, após a febre ceder, os pacientes podem evoluir para a dengue com sinais de alerta, caracterizada por dores abdominais intensas, vômitos persistentes, e outros sinais mais graves, como derrame pleural ou pericárdico, aumento do fígado, sangramentos nas mucosas, e alterações no hematócrito (Silva et al., 2019). Esses sinais devem ser avaliados cuidadosamente, pois indicam o risco de progressão para o estágio mais severo da doença, a dengue grave, que pode levar a choque, hemorragias extensas, falência de órgãos e até óbito (Ratto et al., 2024).

O diagnóstico da dengue é feito em laboratório por meio de sorologia e testes de antígenos virais (Lima et al., 1998). No entanto, para casos suspeitos sem sinais de sangramento, a Organização Mundial da Saúde (OMS) recomenda o uso do teste do torniquete como medida preliminar (Chaves et al., 2018). A principal forma de prevenção da dengue é o controle do mosquito vetor, *A. aegypti*, que ainda representa um grande desafio para a saúde pública no Brasil (Ratto et al., 2024).

A dengue persiste como um grave problema de saúde pública em países tropicais e subtropicais, especialmente na região Norte do Brasil. No Pará, fatores como o clima quente e úmido, infraestrutura limitada e falta de acesso adequado a serviços de saúde contribuem para a proliferação do vetor e para o aumento dos casos graves da doença, que demandam hospitalização (Chaves et al., 2018). Esse cenário é intensificado durante o período chuvoso, de janeiro a junho, quando a transmissão e as internações por dengue atingem picos preocupantes (Silva et al., 2019).

O impacto econômico da dengue no sistema de saúde é significativo. O Sistema Único de Saúde (SUS) enfrenta grandes desafios para atender ao crescente número de pacientes com dengue grave, o que implica em custos

elevados e na necessidade de leitos hospitalares especializados (Ratto et al., 2024). Estudos que analisam a distribuição geográfica e sazonal das internações podem oferecer subsídios para a formulação de políticas públicas mais eficazes e voltadas para as necessidades regionais.

## II. METODOLOGIA

Trata-se de um estudo observacional, subtipo descritivo, de cunho epidemiológico realizado a partir de dados secundários obtidos no Departamento de Informática do Sistema Único de Saúde (DATASUS) em relação ao perfil de pacientes internados por dengue clássica no estado do Pará, no período de janeiro de 2014 a dezembro de 2023. No presente trabalho, foram considerados os valores absolutos de internações e a taxa de internação por 100.000 habitantes no estado de interesse e nos estados da região norte, para fins comparativos.

Subsequentemente, as variáveis “sexo”, “faixa etária”, “cor/raça” foram correlacionadas com as informações de óbitos pré-selecionadas para a definição de um perfil de mortalidade na região. Dados complementares como o caráter de atendimento (urgência e eletivo) e o regime de atendimento (rede pública ou privada) desses pacientes também foram incluídos no estudo. Com o intuito de simplificar a análise e apresentação de dados referentes à faixa etária, a mesma foi padronizada em 3 grupos: pediátrica (0 a 19 anos), adulta (20 a 59 anos) e geriátrica (acima de 60 anos).

Por fim, os dados obtidos foram organizados em planilhas usando o programa Microsoft Excel 2016, posteriormente, foram elaborados gráficos utilizando os recursos do mesmo programa para otimizar a apresentação dos resultados. Definiu-se o modelo gráfico em linha para a demonstração dos dados ao longo dos anos considerados, enquanto o gráfico em porções (“em pizza”) expõe os valores cumulativos da série histórica considerada.

Vale ressaltar que por se tratarem de dados secundários e públicos, a pesquisa não precisou ser submetida à análise e aprovação do comitê de ética, de modo que encontra-se em conformidade com a Resolução 466/2012, a qual regula a pesquisa com seres humanos no país.

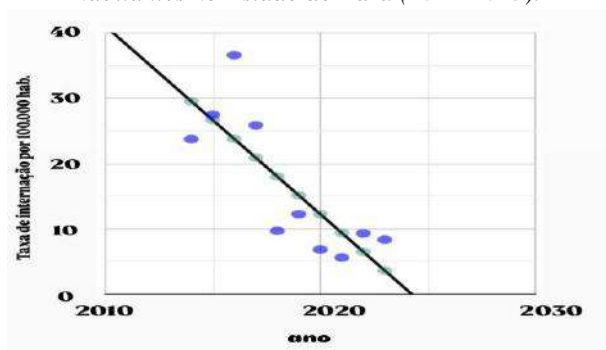
## III. RESULTADOS

Durante o período avaliado, foi registrado um total de 13.956 internações hospitalares relacionadas à Dengue no estado do Pará. Os dados indicam uma tendência estatisticamente significativa de redução no número de internações ao longo dos anos, com uma diminuição média de 2,88 internações por ano ( $p < 0,005$ ), como mostra o gráfico 1. Essa tendência foi reforçada pela análise do

coeficiente B1, que apresentou um valor de -2,88, com um intervalo de confiança de 95% variando entre -4,62 e -1,14, além de uma forte correlação negativa ( $R = -0,80$ ). Esses resultados sugerem que, apesar do número ainda expressivo de hospitalizações, houve uma leve melhoria na gestão e no controle da doença no período estudado.

Quando analisado o perfil epidemiológico das internações, constatou-se que o sexo feminino foi responsável pela maior parcela dos casos, com 7.201 internações (51,6%), em comparação ao sexo masculino, que registrou 6.755 internações (48,4%). Essa diferença, ainda que não muito acentuada, pode refletir fatores biológicos, comportamentais ou mesmo de acesso aos serviços de saúde, que requerem estudos mais aprofundados para uma compreensão detalhada.

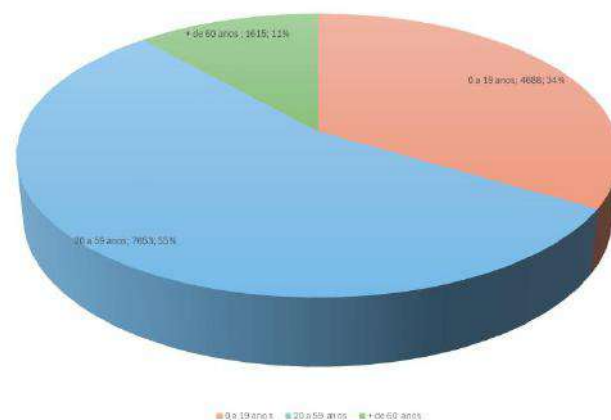
Gráfico 1: Taxa de internação por dengue por 100.000 habitantes no Estado do Pará (2014-2023).



Fonte: Autores, 2024.

A análise etária revelou um padrão interessante no que diz respeito à taxa de internação, destacando que os adultos apresentaram um risco de hospitalização consideravelmente maior em relação a outros grupos etários. A taxa de internação em adultos foi 4,7 vezes superior à observada em idosos, grupo que, apesar de mais vulnerável às formas graves de dengue, teve um menor número absoluto de hospitalizações. Em relação às crianças e adolescentes, os adultos apresentaram uma taxa de internação 1,6 vezes maior, evidenciando que esse grupo foi particularmente afetado pela doença no período analisado (gráfico 2). Esses achados podem estar associados a diferenças no padrão de exposição ao mosquito transmissor, na resposta imunológica ou mesmo no acesso e utilização dos serviços de saúde.

Gráfico 2: Distribuição por faixa etária do número de internações por dengue no Estado do Pará (2014-2023).



Fonte: Autores, 2024.

Outro dado relevante obtido na análise foi a natureza predominantemente urgente das internações. Do total de hospitalizações registradas, impressionantes 92,9% ocorreram em caráter de urgência, o que reflete a gravidade clínica dos casos de dengue e reforça a importância de intervenções rápidas e eficazes no manejo da doença. Esse dado também aponta para possíveis lacunas na identificação precoce dos casos e na oferta de atendimento ambulatorial eficaz, o que pode estar contribuindo para o agravamento da doença e, conseqüentemente, para a necessidade de hospitalização.

Esses achados epidemiológicos sublinham a necessidade de estratégias mais eficazes de controle e prevenção da dengue, com atenção especial às populações mais afetadas, como os adultos e as mulheres, além de um foco maior na redução dos casos que evoluem para internação de urgência. A análise dos dados também ressalta a importância de políticas públicas que promovam a educação em saúde, o fortalecimento da vigilância epidemiológica e o combate ao vetor transmissor da dengue, especialmente em áreas mais vulneráveis do estado.

#### IV. DISCUSSÃO

Campanhas de educação em saúde têm mostrado ser uma estratégia essencial no combate à dengue. Programas como o Programa Saúde na Escola (PSE) e o trabalho dos Agentes Comunitários de Saúde (ACS) visam informar a população sobre a importância de eliminar criadouros do mosquito e adotar práticas de proteção pessoal, como o uso de repelentes e telas nas janelas. Embora essas campanhas tragam resultados positivos, sua efetividade pode ser limitada em áreas onde as condições socioeconômicas dificultam a adoção de medidas preventivas, reforçando a necessidade de um fortalecimento contínuo e abrangente nas políticas de combate à dengue.

Nesse sentido, observa-se que há tendência anual de redução do número de internações por dengue, o que se deve às políticas públicas e campanhas de prevenção que abrangem a população como um todo. Porém, faz-se necessário dar maior auxílio às populações que vivem em situações inadequadas de moradia, abastecimento de água e coleta de lixo, onde esses determinantes sociais contribuem para o aumento do risco de incidência dos casos de dengue. Para isso, a utilização de indicadores de condição de vida têm sido indicados, por alguns autores, para determinar critérios de alocação de verbas nas políticas públicas de saúde (Chaves et al., 2018).

Além disso, foi observado que houve o sexo feminino representa maior número de internações em comparação ao sexo masculino, o que pode ser justificado pelo fato de que as mulheres procuram mais por atendimentos de saúde do que os homens, o que se reflete nas notificações (Lima et al., 1998). Ademais, outros estudos mostram que o mosquito tem característica domiciliar, o que se assemelha ao comportamento feminino, visto que as mulheres permanecem mais tempo em casa do que os homens. Em concordância com isso, as mulheres negras e pardas são a maioria em situação de moradia vulnerável, que são os locais de maior foco da dengue (Vega, 2019).

Em relação à faixa etária onde houve maior incidência, observa-se que esta é a população economicamente ativa do país, logo, esses indivíduos estão propensos a se afastarem do trabalho devido à doença, principalmente aquelas que se expõe a áreas de maior proliferação do vetor. Nesse contexto, identificar os indivíduos mais vulneráveis à infecção e intervir, até onde for possível, é uma forma de prevenção da doença e controle de recursos (Silva et al., 2019).

Estudos mostram que o tipo de dengue em que há maior números de internações em caráter de urgência é a dengue grave, visto que, mesmo no início do quadro, a hospitalização imediata é essencial, devido a rápida evolução e agravamento do quadro clínico da doença, o que torna o número de casos de dengue grave coerente com número de internações. Por outro lado, o número de casos de dengue com sinais de alarme não é proporcional ao número de internações, já que, o tratamento desses casos é ambulatorial (Ratto et al., 2019).

## V. CONCLUSÃO

O estado do Pará tem apresentado, ao longo dos anos, uma redução significativa nas taxas de internações hospitalares relacionadas à dengue. Essa tendência vem sendo observada de forma contínua, refletindo um possível avanço no enfrentamento dessa arbovirose, que historicamente representa um grave problema de saúde pública no Brasil.

Análises epidemiológicas indicam que os grupos mais acometidos por essa enfermidade são predominantemente compostos por mulheres e adultos, caracterizando um perfil demográfico específico de maior vulnerabilidade. Além disso, a maioria das internações ocorre em caráter de urgência, o que evidencia a gravidade clínica associada às formas mais severas da doença, como a dengue com sinais de alarme ou a dengue grave.

A diminuição das internações pode ser atribuída a diferentes fatores, incluindo a implementação de estratégias preventivas mais eficazes, como o fortalecimento das ações de controle do *Aedes aegypti*, vetor responsável pela transmissão da doença. Adicionalmente, a hipótese de subnotificação de casos não pode ser descartada, considerando as dificuldades logísticas e estruturais enfrentadas em diversas regiões, sobretudo em áreas de difícil acesso. Outro aspecto que merece atenção é a possível redução da exposição da população a fatores de risco, seja por mudanças ambientais, climáticas ou de comportamento, que podem ter contribuído para a redução da incidência de casos mais graves.

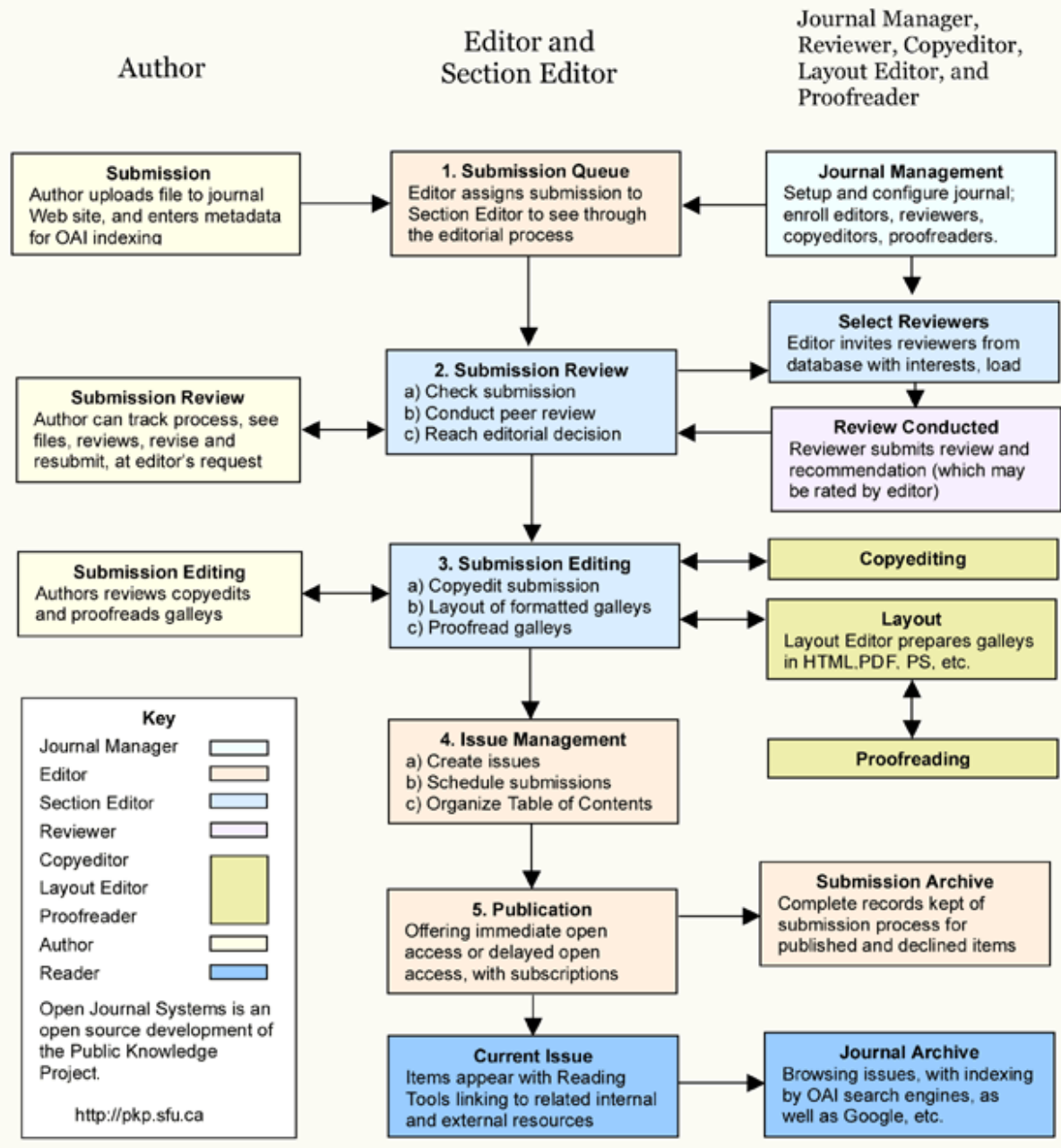
No entanto, é fundamental reconhecer que essas inferências são preliminares e requerem validação por meio de estudos mais aprofundados. A condução de novas investigações científicas, com metodologias robustas e abrangentes, será essencial para confirmar essas hipóteses e compreender, de forma mais detalhada, os determinantes dessa redução. Essas análises poderão subsidiar o desenvolvimento de intervenções ainda mais direcionadas, visando à manutenção e ao aprimoramento das estratégias de controle e prevenção da dengue na população paraense e em outras regiões com características semelhantes.

## REFERENCES

- [1] Chaves, E. C., Costa, S. V., Flores, R. L. dos R., & Bernardes, A. C. (2018). Condições de vida populacional e incidência de dengue no estado do Pará, Brasil. *Pará Research Medical Journal*, 2(1-4). <https://doi.org/10.4322/prmj.2018.002>
- [2] Lima, M. M., Marzochi, K., Gadelha, P., Almeida, A. B. de S., & Benchimol, J. L. (1998). Dengue no Brasil. *História, Ciências, Saúde-Manguinhos*, 5(1), 27-48. <https://doi.org/10.1590/S0104-59701998000100012>
- [3] Oneda, R. M., Basso, S. R., Frasson, L. R., Mottecy, N. M., Saraiva, L., & Bassani, C. (2021). Epidemiological profile of dengue in Brazil between the years 2014 and 2019. *Revista da Associação Médica Brasileira*, 67(5), 731-735. <https://doi.org/10.1590/1806-9282.20210121>
- [4] Ratto, A. C. P., Silva, I. L. A., Ferreira, L. M., & do Ó, M. M. (2024). Análise dos custos e internações da dengue com sinais de alarme e dengue grave no Brasil entre os anos de 2013 e 2023. *Brazilian Journal of Integrative Health Sciences*, 24(1), 959-974.

- [5] Silva, M. R., Oliveira, J. P., Santos, F. T., & Almeida, R. T. (2019). Prevalência de dengue clássica e dengue hemorrágica no Brasil, entre 2011 e 2015. *Acervo Saúde*, 11(1), 123-132. <https://acervomais.com.br/index.php/saude/article/view/753/372>

# OJS Editorial and Publishing Process



~JJAERS Workflow~

## Important links:

### Paper Submission Link:

<https://ijaers.com/submit-paper/>

### Editorial Team:

<https://ijaers.com/editorial-board/>

### Peer Review Process:

<https://ijaers.com/peer-review-process/>

### Publication Ethics:

<https://ijaers.com/publication-ethics-and-publication-malpractice-statement/>

### Author Guidelines:

<https://ijaers.com/instruction-to-author/>

### Reviewer Guidelines:

<https://ijaers.com/review-guidelines/>

---

## Journal Indexed and Abstracted in:

- Qualis-CAPES (A2)-Brazil
- Normatiza (Under Review- Ref.020191511)
- NAAS Score: 3.18
- Bielefeld Academic Search Engine(BASE)
- Aalborg University Library (Denmark)
- WorldCat: The World's Largest Library Catalog
- Semantic Scholar
- J-Gate
- Open J-Gate
- CORE-The world's largest collection of open access research papers
- JURN
- Microsoft Academic Search
- Google Scholar
- Kopernio - powered by Web of Science
- Pol-Index
- PBN(Polish Scholarly Bibliography) Nauka Polaska
- Scilit, MDPI AG (Basel, Switzerland)
- Tyndale University College & Seminary
- Indiana Library WorldCat
- CrossRef DOI-10.22161/ijaers
- Neliti - Indonesia's Research Repository
- Journal TOC
- WIKI-CFP
- Scinapse- Academic Search Engine
- Mendeley-Reference Management Software & Researcher Network
- Dimensions.ai: Re-imagining discovery and access to research
- Index Copernicus Value(ICV): 81.49
- Citeseerx
- Massachusetts Institute of Technology (USA)
- Simpson University (USA)
- University of Louisville (USA)
- Biola University (USA)
- IE Library (Spain)
- Mount Saint Vincent University Library ( Halifax, Nova Scotia Canada)
- University Of Arizona (USA)
- INDIANA UNIVERSITY-PURDUE UNIVERSITY INDIANAPOLIS (USA)
- Roderic Bowen Library and Archives (United Kingdom)
- University Library of Skövde (Sweden)
- Indiana University East (campuslibrary (USA))
- Tilburg University (The Netherlands)
- Williams College (USA)
- University of Connecticut (USA)
- Brandeis University (USA)
- Tufts University (USA)
- Boston University (USA)
- McGill University (Canada)
- Northeastern University (USA)
- BibSonomy-The blue social bookmark and publication sharing system
- Slide Share
- Academia
- Archive
- Scribd
- ISRJIF
- Cite Factor
- SJIF-InnoSpace
- ISSUU
- Research Bib
- infobaseindex
- I2OR
- DRJI journal-repository



### AI Publication

International Journal of Advanced Engineering Research and Science (IJAERS)

104/108, Sector-10, Pratap Nagar, Jaipur, India